ON NUMERICAL METHODS FOR DIRECT AND INVERSE PROBLEMS IN ELECTROMAGNETISM

Viera Zemanová

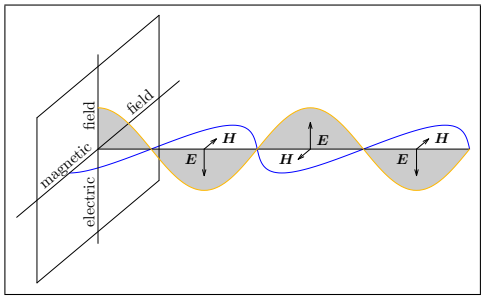

Promotor: Marián Slodička

September 18, 2009

Ghent University
Faculty of Engineering
Department of Mathematical Analysis
Research Group for Numerical Analysis
and Mathematical Modelling

Thesis submitted to Ghent University
in candidature for the degree
of Doctor of Philosophy
in mathematics

To my parents and all I like.

Acknowledgments

When I take a look back at my first lesson of functional analysis I see an enthusiastic and zealous professor standing in front of his class, speaking about the Sobolev Spaces. These Spaces were something so natural to him. He was able to see them all over around. He proved each statement, inconceivable for the students, with so much elegance and without any special effort. Every one of us wanted to have this ability! Professor Jozef Kačur, thank you for showing me the beauty of real mathematics and for the first real touch with it.

My sincere thanks go also to my promotor, professor Marián Slodička, for his help during all these years, for his inspiring ideas and helpful advices whenever I knocked on his office door. I appreciate that so much.

I would like to thank to professor Roger Van Keer, the head of our department, for providing me awesome conditions to do my research.

I cannot forget to dedicate my special thanks to my amazing colleagues: Stephane, Hendrik, Lode and Wouter, who helped me with my integration into the social and sport life and thanks to whom I really enjoyed my stay in Belgium. I find your interest and ambition to learn some basics in Slovak (very handy language for you, by the way;)) cute and sympathetic.

Hendrik - Zlatko, my reviewer, thank you for being tolerant enough to stand your talkative and sometimes a bit crazy office mate. Edi, my well-skilled colleague and friend, many thanks for your mathematical advisory services opened especially for me 24/7 and for the tea sessions in Galglaan's kitchen that I will miss so much. Thank you, Janko, longstanding fellow for being here. I value your willingness to help me with everything you could. Gunnar, thanks to you I discovered Belgium, this cycling paradise, from another point of view. Thank

you for each kilometer. To Jana, thank you for tearing me out the world of mathematics whenever we had fun together.

To my dear Slovak "mini"-community, Tonka, Valdo, Cimo, Mirka, Ibi and Jožko and to my friends spread all over the world. Fortunately the long distance did not have any negative effect on our friendship.

Potoční, with you I have always felt like being with a family. I am very grateful for this feeling.

Last but not least, to my parents and to the rest of my family for all that love and support you are giving me.

My research has been supported by the following projects:

- IUAP/V project sponsored by Belspo *Computational electromagnetics for electrical power applications and interactions with information technology devices* (promoters: Willy Legros, Ronnie Belmans, Jan Melkebeek, Roger Van Keer, Francis Piriou),
- BOF/GOA project of Ghent University *Magnetic non destructive evaluation of ferromagnetic materials supported by numerical micromagnetic methods* (promoters: Luc Dupré, Marián Slodička),
- FWO project *Numerical methods for inverse low frequency electromagnetic problems* (promoters: Luc Dupré, Marián Slodička, Roger Van Keer).

I appreciate I could be present at several mathematical schools and international meetings where I have met the top talents from mathematical world. Knowing these people and having discussions with them is something that money cannot buy.

Viera Zemanová

Contents

Chapter 1

Introduction

This thesis is devoted to the study of processes in the propagation of electromagnetic fields. We do not aim at one particular problem, actually very different kinds of topics are analyzed here. We deal with direct problems as well as with inverse ones, low frequency electromagnetism is discussed and consequently the wave propagation problem in high frequency domain is studied.

Study of electromagnetic materials and their behavior is of a huge interest for the technological world. Its importance originates from the increasing requirements for high performance devices as motors, transformers, radars, ... To improve the character of electromagnets, new models, accurate numerical schemes and their rigorous analysis are needed to be worked out. Some numerical techniques and approaches on how to model and design electrical machines and devices are for example analyzed in the books of Sadiku and Hameyer-Belmans [49, 76].

The properties and behavior of electric and magnetic fields are described by a set of four partial differential equations, namely Maxwell's equations.

1.1 Maxwell's equations

"To anyone who is motivated by anything beyond the most narrowly practical, it is worthwhile to understand Maxwell's equations simply for the good of his soul." J.R.Pierce

The equations accounting for the facts that a compass needle points north, that light bends when it enters water, that your car starts when you turn the ignition key, ...
Maxwell's equations in all their glory:

$$\nabla \cdot \boldsymbol{D} = \rho \qquad \text{Gauss's electric law,} \tag{1.1}$$

$$\nabla \cdot \boldsymbol{B} = 0 \qquad \text{Gauss's magnetic law,} \tag{1.2}$$

$$\nabla \times \boldsymbol{E} = -\partial_t \boldsymbol{B} \qquad \text{Faraday's law,} \tag{1.3}$$

$$\nabla \times \boldsymbol{H} = \boldsymbol{J} + \partial_t \boldsymbol{D} \qquad \text{Ampère - Maxwell's law.} \tag{1.4}$$

In case of a time-varying field when the electric and magnetic field exist simultaneously, the following physical quantities are involved:

$\boldsymbol{H}$ magnetic field intensity ($A\ m^{-1}$);

$\boldsymbol{E}$ electric flux intensity ($V\ m^{-1}$);

$\boldsymbol{B}$ magnetic flux density (magnetic induction) ($Wb\ m^{-2}$);

$\boldsymbol{D}$ electric flux density ($C\ m^{-2}$);

$\boldsymbol{J}$ electric current density ($A\ m^{-2}$);

ρ electric charge density ($C\ m^{-3}$).

These four partial differential equations summarize the experimental results of Coulomb, Ampère, Gauss and Faraday. They got their name after J. C. Maxwell who, as the first one, wrote them down in 1864 and fixed them up so that they made mathematical sense. He introduced the idea of *displacement current*, which generalizes Ampère law and makes it valid in "all situations". This detection allowed him to foresee the physical phenomenon of propagation of electromagnetic waves. *Maxwell's great discovery was that light is an electromagnetic wave whose speed can be measured by making purely electric and magnetic measurements.*

The first equation describes that the flux of the vector $\boldsymbol{D}$ is not conservative, i.e. there is a difference between the electric fluxes entering and leaving the volume. The sign for the net charge is included in the symbol itself: if ρ is positive, the net flux is outward; if ρ is negative, the net flux is inward.

Gauss's law for magnetism states that isolated magnetic poles do not exist. Magnetic flux is conservative, i.e. the same amount of magnetic flux is entering and leaving the volume.

Equation (1.3) implies that by changing a magnetic field an electric field is produced.

The last equation was Maxwell's great achievement. He realized that Ampère's law in original state

$$\nabla \times \boldsymbol{H} = \boldsymbol{J} \tag{1.5}$$

"misses something". He discovered that there are at least two ways of setting up a magnetic field: by means of a current and by means of changing electric field. In general, we must allow for both principles.
To try out Maxwell's scheme (1.4), we want the flux of the right hand side to be well defined, in other words, we want its divergence to be zero. The divergence of the left hand side is automatically zero using the well-known identity $\nabla \cdot (\nabla \times .) = 0$ and therefore the divergence of the right hand side of (1.4) has to vanish as well, i.e.

$$0 = \nabla \cdot \boldsymbol{J} + \partial_t (\nabla \cdot \boldsymbol{D}). \tag{1.6}$$

Substituting (1.1) into the latter equality we arrive at

$$0 = \nabla \cdot \boldsymbol{J} + \partial_t \rho. \tag{1.7}$$

Thus, an important consequence of Maxwell's law (1.4) is conservation of charge.[1] Further, we invented that by adding $\partial_t \boldsymbol{D}$ (called displacement current) into Ampère's law, a symmetric relation between magnetic and electric field holds, i.e. changing an electric field accordingly induces a magnetic field. The reason why the displacement current was not included in the equations earlier is that it is not detectable in all circumstances. The electric induction of magnetic fields is observable only if the electric field oscillates fast, that is when the electromagnetic radiation is important. The high–frequency electromagnetism case is discussed in the second part of my thesis.

For a more exhausting review on Maxwell's equations we refer a reader to [15, 65, 79].

1.2 Steady state, eddy current problem

The first part of the thesis is devoted to low-frequency electromagnetism. In this case, when electromagnetic radiation is unimportant, the displacement current

[1] Ampère's law itself was not consistent with the conservation law as the condition $\nabla \cdot \boldsymbol{J} = 0$ holds only for stationary currents.

can be safely neglected. Maxwell's equations are then linked by the so-called constitutive laws for linear and isotropic media:

$$\boldsymbol{J} = \boldsymbol{J}_a + \sigma \boldsymbol{E}, \tag{1.8}$$
$$\boldsymbol{D} = \varepsilon \boldsymbol{E}, \tag{1.9}$$
$$\boldsymbol{B} = \mu \boldsymbol{H}. \tag{1.10}$$

In addition to these we define the following scalar functions describing the properties of the media

ε electric permittivity (Fm^{-1}),

μ magnetic permeability (Hm^{-1}),

σ electric conductivity (Sm^{-1}).

The magnetic permeability and the electric permittivity are moreover positive and bounded. In anisotropic materials, where the material properties depend on the direction of the field, ε and μ are 3 x 3 positive–definite matrix functions of the position. The conductivity of the medium can be zero, when speaking about insulators. Further, $\boldsymbol{J}_a$ is the *applied current density* and $\sigma\boldsymbol{E}$ represents the *induced current density.*

Using the constitutive laws (1.8)-(1.10), Maxwell's equations (1.1)–(1.4) with negligible displacement current term take the form of

$$\nabla \cdot (\varepsilon \boldsymbol{E}) = \rho, \tag{1.11}$$
$$\nabla \cdot (\mu \boldsymbol{H}) = 0, \tag{1.12}$$
$$\nabla \times \boldsymbol{E} = -\mu \partial_t \boldsymbol{H}, \tag{1.13}$$
$$\nabla \times \boldsymbol{H} = \boldsymbol{J}_a + \sigma \boldsymbol{E}. \tag{1.14}$$

The first equation can be considered as a definition for ρ and can be left out. Relation (1.12) is a direct consequence of (1.13), it does not need to be included into the system as well. We end up with "Maxwell's model of memory-less linear materials" which consists of the remaining two equations (1.13) and (1.14).

To cut down the number of unknowns the first order Maxwell's system is reduced to a single parabolic equation expressed either in terms of the magnetic field $\boldsymbol{H}$ or the electric field $\boldsymbol{E}$. The choice is usually determined by the boundary conditions. The analysis of both systems is fully analogous. Focusing on the electric field formulation one gets

$$\sigma \partial_t \boldsymbol{E} + \nabla \times (\mu^{-1} \nabla \times \boldsymbol{E}) = -\partial_t \boldsymbol{J}_a. \tag{1.15}$$

In addition, the eddy current formulation in terms of the magnetic field reads

$$\mu\partial_t \boldsymbol{H} + \nabla \times (\sigma^{-1}\nabla \times \boldsymbol{H}) = \nabla \times (\sigma^{-1}\boldsymbol{J}_a). \tag{1.16}$$

The $\boldsymbol{E}$–formulation (1.15) is used more often in the literature. One of the reasons is that it can be applied also when $\sigma = 0$. Throughout the thesis we do not consider the case of insulating regions. Consequently, we acquire the existence of a unique weak solution to (1.15) or (1.16) in appropriate spaces.

For a more detailed description of the eddy current model see [51, 78]. Finite element approximations for eddy current problems are proposed in [3, 50].

1.3 Boundary conditions

Any differential problem must be supplemented with certain conditions. If they are given at a time point from which the evolution of the process starts, we call them *initial values*. Since Maxwell's equations do not hold at the interface between different materials (e.g. copper–air), also *boundary conditions* (BCs) must be given. Physically, these conditions express the properties of the material surrounding the computing domain Ω through the fields on $\partial\Omega$. It is expected that the BCs allow for the existence of a unique solution in Ω.

Let us consider the case of two media with various electric and magnetic properties occupying two regions separated by the surface S as is depicted in Figure 1.1. The vector $\boldsymbol{\nu}$ denotes outward unit normal to Region 2. For $\nabla \times \boldsymbol{E}$ in (1.15) to be well defined, the vector $\boldsymbol{\nu} \times \boldsymbol{E}$ has to be continuous across S. We write,

$$\boldsymbol{\nu} \times (\boldsymbol{E}_1 - \boldsymbol{E}_2) = \boldsymbol{0} \qquad \text{on } S. \tag{1.17}$$

Here, $\boldsymbol{E}_1$ denotes the limiting value of $\boldsymbol{E}$ approaching S from Region 1, $\boldsymbol{E}_2$ is the limit of electric field from the other region.

Moreover, the continuity of the normal components of $\mu\boldsymbol{H}$ across S is expressed in the following way

$$\boldsymbol{\nu} \cdot (\mu_1\boldsymbol{H}_1 - \mu_2\boldsymbol{H}_2) = 0. \tag{1.18}$$

The continuity conditions (1.17) and (1.18) hold for any electromagnetic field. But we cannot assume the analogue of (1.17) for magnetic fields. In general, we have

$$\boldsymbol{\nu} \times (\boldsymbol{H}_1 - \boldsymbol{H}_2) = \boldsymbol{J}_S, \tag{1.19}$$

where $\boldsymbol{J}_S$ is the surface current density.

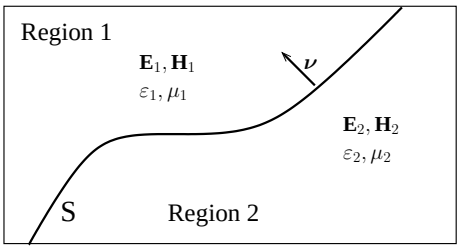

Figure 1.1: Geometry of the surface and subdomains in discussion of interface boundary conditions.

The presence of singularities in the charge density ρ may cause jumps in the normal component of $\varepsilon \boldsymbol{E}$

$$\boldsymbol{\nu} \cdot (\varepsilon_1 \boldsymbol{E}_1 - \varepsilon_2 \boldsymbol{E}_2) = \rho_S, \tag{1.20}$$

where ρ_S represents the surface charge density.

It is required that the tangential component of $\boldsymbol{E}$ and the normal component of $\boldsymbol{B}$ are continuous while crossing S. On the other hand, if ρ_S and $\boldsymbol{J}_S$ are different from zero, the tangential component of $\boldsymbol{H}$ and the normal component of $\boldsymbol{D}$ jump across the material boundary.

Now, let us focus on some physical interpretations of BCs. For instance, suppose that the material in Region 1 is a perfect conductor, i.e. $\sigma_1 \to \infty$. From Ohm's law (1.8) one can heuristically see that if the current density $\boldsymbol{J}$ remains bounded then the electric field vanishes, $\boldsymbol{E}_1 \to \mathbf{0}$. We arrive at the *perfect conducting boundary condition* for $\boldsymbol{E}_2$,

$$\boldsymbol{E}_2 \times \boldsymbol{\nu} = \mathbf{0}. \tag{1.21}$$

Another type of a homogeneous BC reads

$$\nabla \times \boldsymbol{E}_2 \times \boldsymbol{\nu} = \mathbf{0}. \tag{1.22}$$

In general, BC of the first type (1.21) and of the second type (1.22) could be non-homogeneous. Then, one considers

$$\boldsymbol{E}_2 \times \boldsymbol{\nu} = \boldsymbol{G}_1 \tag{1.23}$$

or

$$\nabla \times \boldsymbol{E}_2 \times \boldsymbol{\nu} = \boldsymbol{G}_2. \tag{1.24}$$

The boundary condition (1.24) describes the temporal variations of an external magnetic field. The conditions mentioned above can be prescribed for an electric field $\boldsymbol{E}$ as well as for a magnetic field $\boldsymbol{H}$.

Further, to depict the relation between the flux and the potential, the BC of the third type is used as will be discussed in the next subsection. Throughout the thesis this condition defines either imperfectly conducting or absorbing character of the domain's boundary.

1.3.1 Boundary condition of third type

If the material on one side of the boundary, e.g. in Region 2, is a non-perfect conductor but allows the field to penetrate a small distance, *imperfectly conducting boundary condition* reads

$$\boldsymbol{H}_2 \times \boldsymbol{\nu} + \lambda(\boldsymbol{E}_2 \times \boldsymbol{\nu}) \times \boldsymbol{\nu} = \boldsymbol{0}, \tag{1.25}$$

where the impedance λ is a positive function of the position on the surface, see [30, 31]. In the first part of the thesis related to low–frequency electromagnetism we consider an imperfectly conducting BC written in a reversed order, namely

$$\boldsymbol{\nu} \times \boldsymbol{E_2} - \boldsymbol{\nu} \times \lambda\left(\boldsymbol{H_2} \times \boldsymbol{\nu}\right) = \boldsymbol{0}. \tag{1.26}$$

The condition of this type is known as Silver-Müller BC. When $\lambda(\boldsymbol{x}) = \boldsymbol{x}$, the BCs (1.25), (1.26) represent the classical Silver-Müller condition (see [22, 40]). It is a first order approximation to the so-called "transparent" BC, i.e. no energy loss is observed on the boundary. It can be found in the literature under other names as well such as Leontovich or impedance BC, see [37, 58, 61, 62]. For more information about the Silver-Müller BC we highly recommend the book of Müller [66].

In Chapters 7 and 8 a numerical method to approximate the scattering problem posed on an unbounded domain has been developed. Thus, an auxiliary boundary with Silver-Müller absorbing boundary condition is introduced sufficiently far from the scatterer. A condition prescribed at an artificial boundary to simulate the solution in an open domain is said to be *absorbing* if

$$(\boldsymbol{E} \times \boldsymbol{H}) \cdot \boldsymbol{\nu} \geq 0, \tag{1.27}$$

see, e.g. [37, §7.12]. The authors use various synonyms for absorbing BC, e.g. dissipative, scattering or reflecting BC.

If equality holds in (1.27), the boundary is called *conservative*. If the vector fields $\boldsymbol{E}$ and $\boldsymbol{H}$ satisfy the stronger condition

$$(\boldsymbol{E} \times \boldsymbol{H}) \cdot \boldsymbol{\nu} \geq C \left(\|\boldsymbol{E} \times \boldsymbol{\nu}\|^2 + \|\boldsymbol{H} \times \boldsymbol{\nu}\|^2 \right) \tag{1.28}$$

then the boundary is said to be *strictly absorbing*.

The general BC with the absorbing character considered along the time-dependent problem is given by a hereditary model of the following form (see [37]),

$$\boldsymbol{E} \times \boldsymbol{\nu} = \eta_0(\boldsymbol{x}) \boldsymbol{H} \times \boldsymbol{\nu} \times \boldsymbol{\nu} + \int_0^\infty \eta(\boldsymbol{x}, u) \boldsymbol{H}(\boldsymbol{x}, t-u) \times \boldsymbol{\nu} \times \boldsymbol{\nu} du \quad u \in \mathbb{R}^+. \tag{1.29}$$

The BC (1.29) satisfies the definition (1.28) of a strictly absorbing boundary condition. For the proof see [37, §7.13]. We come back to this condition in the second part of the thesis.

An accurate prescription for absorbing BC depends on various aspects, e.g. quality of the material, definition of the problem setting, ... Thus, for instance, for time-harmonic problem the tangential electric field and tangential magnetic field are related by

$$\boldsymbol{E}(\boldsymbol{x}, \omega) \times \boldsymbol{\nu} = \lambda(\boldsymbol{x}, \omega) \boldsymbol{H}(\boldsymbol{x}, \omega) \times \boldsymbol{\nu} \times \boldsymbol{\nu}, \tag{1.30}$$

where λ is an appropriate, possibly complex, scalar and ω is an angular frequency. Because λ depends on ω, the relation (1.30) cannot be transferred to arbitrary time-dependent fields. Fabrizio and Morro showed in [38] that the (1.29) is a generalization of (1.30) to time-dependent fields.

There are many approaches for obtaining absorbing BCs. The question is whether they are better than the mentioned Silver-Müller one. Webb and Kanellopoulos [95] have derived a family of operators of increasing order. The lowest operator is exactly the Silver-Müller condition. The higher order operators require an extra regularity what seems difficult to fulfill in general applications. Furthermore, Grote and Keller [44, 45] construct BC of an arbitrary order by the analysis of the series expansion. The major criticism of their work is that the auxiliary domain has to be spherical. An alternative approach, proposed by Mur [67], uses absorbing BC appropriate for the Helmholtz equation on each component of scattered field. This approach is difficult to implement.

BCs arise naturally from the variational formulation of Maxwell's equations. For more information on this topic, see [5].

1.4 Overview of the thesis

The thesis is divided into three parts: direct problems in low–frequency electromagnetism, direct problems in high–frequency electromagnetism and inverse problems in low–frequency electromagnetism.

Direct problems in low–frequency electromagnetism

In the first part we aimed at a time dependent eddy current equation for the magnetic field $\boldsymbol{H}$ when a non–perfect contact of two different materials is considered on the boundary.

Firstly, in Chapter 5, we consider a boundary value problem (4.5) with a nonlinear vector function $\boldsymbol{G}$ defined by (4.3). Thus, the monotone and non-Lipschitz continuous nonlinearity on the boundary is considered. We establish the existence and uniqueness of a weak solution, design the non-linear time discrete approximation scheme based on the backward Euler method and prove the convergence of the approximations to a weak solution on the basis of Minty-Browder's trick [36]. Finally, the linear dependence of the error of the approximation on the length of the time step is derived. The proposed scheme stays nonlinear.

The numerical results of Chapter 5 will be presented at the international conference on Mathematical Modeling and Computational Physics 2009 in Dubna. Theoretical results are summarized in the paper [83] published in Journal of Computational and Applied Mathematics.

Chapter 6 is based on the article [98] submitted to the Journal of Mathematical Analysis and Applications. Here we focus on the linearization and the full discretization of the previous problem setting (4.5). In this case, we consider the power law (4.4) which implies that the nonlinear vector function $\boldsymbol{G}$ is Lipschitz continuous. This property improves the error estimates for the time discretization. Linearization is performed using the well-known fixed-point principle, whereas for discretization in space Whitney's edge elements (Section 6.2.2) are employed. First, we prove the well-posedness of the proposed method. Then, we show the convergence of the approximations to a weak solution and finally we derive the error estimates depending on the choice of the discretization parameters. Based on our numerical results we regard the method as fast, robust and stable.

Most of the theoretical and numerical results have been presented at the ICNAAM 2008 conference and are summarized in the proceedings of this conference, see [97].

Direct problems in high–frequency electromagnetism

The high-frequency domain (Chapter 7) includes the study of electromagnetic waves and propagation of energy through matter. These problems are mostly posed on an unbounded domain. Since 1977, the method of Artificial Boundary Condition (ABC) has been widely used for wave problems.

In Chapter 8 we use the one of the simplest ABCs, called Silver-Müller condition with a dissipative character. Here, the boundary condition of a linear nature is assumed. The way we are dealing with the ABC is motivated by the work of H. Barucq [7], where the theory of propagation of electromagnetic waves in unbounded domain is elaborated in two dimensions. This work stimulated us to extend the mentioned problem to three dimensions. At the NumAn 2008 conference, a detailed analysis of the proposed problem, i.e. the well-posedness, the time discretization based on the backward Euler method, the long-time stability results for the time discrete approximate solution and the error estimate for the time discrete scheme have been presented.

Significant results appeared already in the proceedings of the conference, see [82]. The whole article [84] is submitted to the journal Applied Numerical Mathematics.

Inverse problems in low–frequency electromagnetism

The third part of the thesis is devoted to the inverse problems in low-frequency electromagnetism. In Chapter 9 we introduce the principle of inverse problems and consequently, in the following chapter, we aim at the material characteristic determination.

In the specific problem discussed in Chapter 10, the missing material constant turns out to be a measure for the electromagnetic losses. The time-discretization scheme is applied to the proposed problem. We introduce a side condition which guarantees uniqueness of a solution. Furthermore, we investigate the character of the loss function. Thanks to its continuity, decreasing character and asymptotic nature the existence of the solution can be proved.

Some results of this chapter have been presented at the international conference ACOMEN 2008 ([99]). The whole paper [100] will appear in the Journal of Computational and Applied Mathematics.

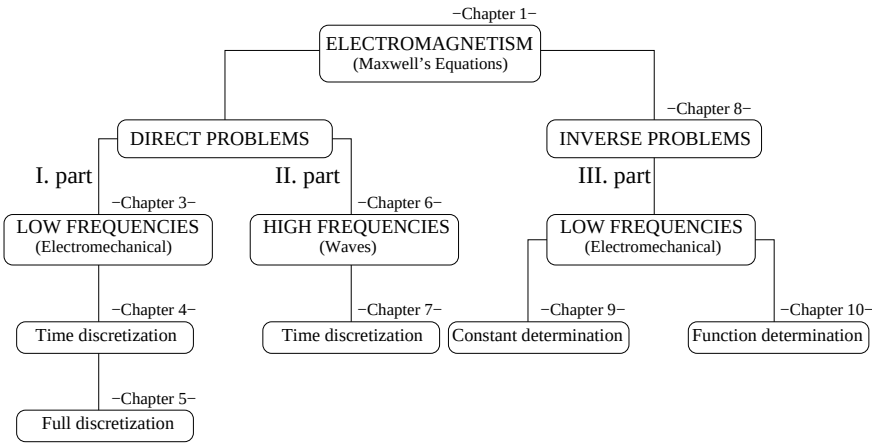

Figure 1.2: Overview of the thesis

Numerical experiments

The end of each chapter is devoted to numerical examples confirming the theoretical results. All the computations are performed using The Finite Element Toolbox ALBERT developed in 2000 by a team of German mathematicians [77]. For approximation of electric and magnetic fields the Whitney elements implemented by Baňas [9] and Cimrák [24] are used. Whitney's finite elements are discussed in Section 6.2.

In the experiments, we consider the computational domain occupied by ferromagnetic material to be a unit cube in $\mathbb{R}^3$. This domain is split into a tetrahedral mesh. Throughout the thesis we prove either theoretically or numerically, that the finer the mesh, the more exact our approximation is. The basic mesh consists of 6 tetrahedra. The refinement process, in our case non-adaptive, is based on the bisection method, see [57]. By each refinement, the number of tetrahedra increases exponentially, i.e. $n_r = 2^3 n_{r-1}$, where n_{r-1} represents the number of tetrahedra of the previous refinement. The concept how the discretization parameter h decreases in consequence of refining, and meanwhile the number of tetrahedra and related number of degrees of freedom (DOF) increase, can be seen in Table 1.1.

n° ref.	h	n° tetrahedra	n° tetr. on Γ	n° DOF
0	$\sqrt{3}$	6	6	19
1	$\sqrt{3}/2$	48	48	98
2	$\sqrt{3}/4$	384	336	604
3	$\sqrt{3}/8$	3 072	1 776	4 184
4	$\sqrt{3}/16$	24 576	8 112	31 024
5	$\sqrt{3}/32$	196 608	34 608	238 688

Table 1.1: The influence of refining on the character of the used tetrahedral mesh. In numerical experiments maximum fivefold mesh refinement is used. The more refinements are applied, the more the discretization parameter h tends to zero and the more tetrahedra are used. We monitor the number of tetrahedra on the boundary Γ and the number of degrees of freedom (DOF) as well.

Solving the time dependent problems, the computations are realized on time interval [0,1].

For all numerical experiments computers with Intel Pentium IV 630 processor clocked at 3GHz with 1GB RAM memory were used.

Chapter 2

Nederlandse samenvatting

In dit proefschrift worden verschillende processen besproken aangaande de golfpropagatie van elektromagnetische velden. We concentreren ons niet op slechts één specifiek probleem, maar beschouwen verschillende onderwerpen. Dit betekent dat we zowel directe als inverse problemen bestuderen en zowel laagfrequent als hoogfrequent elektromagnetisme beschouwen.

De studie van elektromagnetische materialen en hun gedrag is van groot belang in onze technologische wereld. Om de karakteristieken van zulke materialen te verbeteren, is het van cruciaal belang om nieuwe modellen en accurate numerieke schema's te ontwikkelen.

De eigenschappen van elektrische en magnetische velden worden beschreven door een stelsel van vier partiële differentiaalvergelijkingen, de zogenaamde Maxwell vergelijkingen. Deze vergelijkingen worden gegeven in (1.1) - (1.4), met $\boldsymbol{H}$ het magnetisch veld, $\boldsymbol{E}$ het elektrisch veld, $\boldsymbol{B}$ de magnetische inductie, $\boldsymbol{D}$ de diëlektrische verplaatsing en $\boldsymbol{J}$ de elektrische stroomdichtheid.

De theorie van de Maxwell-vergelijkingen wordt besproken in Hoofdstuk 1. In Hoofdstuk 3 wordt een kort overzicht gegeven van de nodige definities, symbolen en functieruimten nodig voor de variationele analyse van de zwakke formulering van deze vergelijkingen.

Verder bestaat dit proefschrift uit drie grote delen, namelijk: directe problemen in laagfrequent elektromagnetisme, directe problemen in hoogfrequent elektromagnetisme en inverse problemen in laagfrequent elektromagnetisme.

Directe problemen in laagfrequent elektromagnetisme

Het overgrote deel van elektromagnetische toestellen, zoals motoren, relaisschakelingen en transformatoren, wordt beschreven in het laagfrequente domein (zie Hoofdstuk 4). Al deze toestellen werken bij stroomfrequenties lager dan enkele tientallen kHz. Strikt genomen kan elke toepassing waarbij de diëlektrische verplaatsing $\boldsymbol{D}$ verwaarloosd kan worden, een laagfrequente toepassing genoemd worden. In dat geval, corresponderend met een zogenaamde "steady-state" (zie Sectie 1.2), kunnen we in het algemeen het elektrisch veld $\boldsymbol{E}$ en het magnetisch veld $\boldsymbol{H}$ als onafhankelijke grootheden beschouwen.

In het eerste deel bestuderen we een tijdsafhankelijke "eddy current" vergelijking voor het magnetisch veld $\boldsymbol{H}$ met een niet-lineaire randvoorwaarde die een veralgemening is van de klassieke Silver-Müller voorwaarde (zie [22, 37, 40, 58, 61]) voor niet-perfecte geleiders. Het stelsel wordt dan gegeven door

$$\begin{aligned} \partial_t \boldsymbol{H} + \nabla \times \nabla \times \boldsymbol{H} &= \boldsymbol{0} && \text{in } \Omega, \\ \boldsymbol{\nu} \times \nabla \times \boldsymbol{H} &= \boldsymbol{\nu} \times \boldsymbol{G}\left(\boldsymbol{H} \times \boldsymbol{\nu}\right) && \text{op } \Gamma. \end{aligned} \tag{2.1}$$

In Hoofdstuk 5 bekijken we eerst een niet-perfecte randvoorwaarde uitgedrukt door de vectorfunctie

$$\boldsymbol{G}(\boldsymbol{H} \times \boldsymbol{\nu}) = \boldsymbol{\nu} \times \left(|\boldsymbol{H} \times \boldsymbol{\nu}|^{\alpha-1} \boldsymbol{H} \times \boldsymbol{\nu} \right)$$

met $\alpha \in (0, 1]$. Op die manier wordt het monotone, niet-Lipschitz continue en niet-lineaire karakter van de rand in rekening gebracht. Verder bekomen we existentie en uniciteit van een zwakke oplossing in een geschikte functieruimte onder minimale regulariteitseisen op de rand en voor de beginvoorwaarden. We ontwerpen een niet-lineair tijdsdiscreet approximatieschema gebaseerd op Rothe's methode. De convergentie van deze approximatie naar de zwakke oplossing wordt bewezen door gebruik te maken van Minty-Browder's techniek (zie [36]). Deze steunt op de monotoniciteit van de niet-lineaire operator. Dit bewijs is tevens het hoofdresultaat van dit hoofdstuk. Tot slot wordt de foutafschatting voor de tijdsdiscretisatie bepaald. Deze fout blijkt lineair afhankelijk te zijn van de tijdsvariabele. Het hoofdstuk wordt afgesloten met een aantal numerieke experimenten, die de efficiëntie van de beschreven methode bevestigen. In deze experimenten gebruiken we de Newton methode voor het oplossen van niet-lineaire steady-state partiële differentiaalvergelijkingen.

De numerieke resultaten van dit hoofdstuk zullen gepresenteerd worden op de internationale conferentie Mathematical Modeling and Computational Physics

2009 in Dubna. De theoretische resultaten werden gepubliceerd, [83].

Hoofdstuk 6 is gebaseerd op een artikel dat reeds opgestuurd werd voor publicatie, [98]. Hier richten we onze aandacht op de linearisatie en de volledige discretisatie van het voorgaande probleem (2.1). In dit geval wordt de niet-lineaire relatie tussen het magnetische en het elektrische veld op de grens licht aangepast. Bovendien wordt de niet-lineaire vector $\boldsymbol{G}$ nu Lipschitz-continu verondersteld door de machtswet (4.4). Dit laat toe om de foutafschatting voor de tijdsdiscretisatie, gebaseerd op de methode van Rothe, te verbeteren. Meer bepaald vinden we dat de tijdsdiscretisatiefout kwadratisch afhangt van de lengte van de tijdsstap. De linearisatie wordt uitgevoerd met behulp van het "fixed-point" principe, terwijl voor de ruimtediscretisatie gebruik gemaakt wordt van Whitney elementen (zie [65]). Eerst tonen we de welgesteldheid van de voorgestelde methode aan. Vervolgens bewijzen we de convergentie van de methode en leiden we foutafschattingen af die afhangen van de keuze van de discretisatieparameters: lengte van de tijdsstap, grid-verfijning en het stopcriterium tussen de iteraties in één tijdsstap.

We bestuderen de afhankelijkheid van de relatieve fout van onze methode ten opzichte van elke parameter, namelijk α, η, τ en h op een aantal numerieke voorbeelden. De convergentiesnelheid beantwoordt aan onze verwachtingen en is in een aantal gevallen zelfs beter. A priori zou men verwachten dat een linearisatieschema gebaseerd op een "fixed-point" principe traag is, maar onze numerieke resultaten doen ons besluiten dat de methode snel, robuust en stabiel is.

Wat betreft de interne iteraties, daalt de relatieve fout initiëel snel om vervolgens relatief constant te blijven. De reden hiervoor is dat in het begin de linearisatiefout dominant is, maar bij toenemend aantal iteraties gedomineerd wordt door de discretisatiefout. We concluderen dat hoe kleiner het grid, des te kleiner de relatieve fout. Hierbij dient evenwel opgemerkt te worden dat de griddiameter binnen redelijke grenzen gekozen dient te worden om een excessieve toename in computertijd en geheugengebruik te vermijden.

Het merendeel van de theoretische en numerieke resultaten uit dit hoofdstuk werden gepresenteerd op de conferentie ICNAAM 2008 en werden samengevat in een proceedingsbijdrage, [97].

Directe problemen in hoogfrequent elektromagnetisme

Tot het hoogfrequentiedomein (zie Hoofdstuk 7) behoren de studie van elektromagnetische golven en de voortplanting van energie door materie. Dergelijke

problemen worden meestal op onbegrensde gebieden geformuleerd. Numerieke methoden voor de oplossing van uitwendige problemen hebben in het verleden speciale aandacht gekregen. Sinds het pionierswerk van Engquist en Majda (zie [35]) in 1977 werd de methode van de "Artificial Boundary Condition" (ABC) veelvoudig toegepast om golfproblemen op te lossen. Deze methode introduceert een artificiële grens in het beschouwde onbegrensde gebied om het computationeel domein te beperken. Een ABC wordt dan opgelegd als de relatie die de sporen van de golf op de fictieve grens verbindt en de voortplanting van de golf door het oppervlak (van het computationeel domein naar het uitwendige) modelleert.

In Hoofdstuk 8 gebruiken we één van de eenvoudigste ABCs, namelijk de Silver-Müller randvoorwaarde met dissipatief karakter. Er wordt verder verondersteld dat deze randvoorwaarde lineair is. De moeilijkheid van het probleem ligt in het feit dat het volledige Maxwell stelsel beschouwd moet worden en dat bij hoge frequenties de elektrische en magnetische velden onderling afhankelijk zijn. In dit proefschrift behandelen we de ABC steunend op het werk van H. Barucq (zie [7]), waar de voortplanting van elektromagnetische golven in twee dimensies over een onbegrensd domein besproken wordt. We zijn erin geslaagd om het vermelde probleem te veralgemenen naar drie dimensies. Een gedetaileerde analyse werd gepresenteerd op de NumAn 2008 conferentie, met name de welgesteldheid, de tijdsdiscretisatie steunend op de achterwaartse Euler methode en de lange-tijd stabiliteit voor de benaderde oplossing en de foutafschatting. Deze fout blijkt lineair afhankelijk te zijn van de keuze van de tijdsstap τ.

Een deel van deze resultaten werd gepubliceerd in een proceedingsbijdrage (zie [82]). Verder werd een volledig artikel opgestuurd voor publicatie, zie [84].

Inverse problemen in laagfrequent elektromagnetisme

Het derde en laatste deel van dit proefschrift is gewijd aan de studie van inverse problemen in laagfrequent elektromagnetisme. In Hoofdstuk 9 introduceren we het principe van inverse problemen en vervolgens richten we ons in Hoofdstuk 10 op de bepaling van materiaalkarakteristieken.

Het bepalen van ongekende materiaaleigenschappen of geometrische data vormt een interessant onderzoeksthema binnen het elektromagnetisme, met duidelijke praktische relevantie. Aangezien er steeds strengere eisen gesteld worden aan hoogperformante toestellen, is het essentieel voor het ontwerp van elektromagnetische elementen dat bv. elektromagnetische verliezen, de permeabiliteit

en de elektrische conductiviteit accuraat bepaald kunnen worden.

In het specifieke probleem behandeld in Hoofdstuk 10, is de te bepalen materiaalkarakteristiek een maat voor de elektromagnetische verliezen.

Na het geven van een wiskundige formulering van het probleem en van de definitie van elektromagnetische verliezen passen we een tijdsdiscretisatie-schema toe op het probleem, zoals gewoonlijk gebaseerd op de achterwaartse Euler methode. In Sectie 10.3 introduceren we een specifieke randvoorwaarde die later gebruikt wordt om de uniciteit van de oplossing te garanderen. Vervolgens onderzoeken we het karakter van de verliesfunctie. Steunend op de continuïteit, dalend karakter en asymptotische aard van deze functie kunnen we het bestaan van de oplossing bewijzen. Zoals gewoonlijk wordt de laatste sectie gewijd aan een aantal numerieke experimenten.

Een aantal van de resultaten uit dit hoofdstuk werden gepresenteerd op de ACOMEN 2008 conferentie (zie [99]). Verdere resultaten werden gepubliceerd in [100].

Berekeningen

Het einde van elk hoofdstuk is gewijd aan numerieke voorbeelden die de theoretische resultaten bevestigen. Al deze berekeningen werden uitgevoerd met behulp van het pakket 'The Finite Element Toolbox ALBERT' ontwikkeld in 2000 door een team van Duitse wiskundigen (zie [77]). Voor de benadering van elektrische en magnetische velden werd gebruik gemaakt van Witney elementen, zoals geïmplementeerd door Baňas [9] en Cimrák [24].

In de experimenten beschouwen we telkens de eenheidskubus in $\mathbb{R}^3$ als computationeel domein.

Chapter 3

Functional analysis

This chapter is a brief overview of main definitions, symbols and spaces. Its goal is to provide a sufficient background for understanding variational analysis of weak formulations of Maxwell's equations. For a summary we also refer to the book Function spaces written by Kufner, John and Fučík [59].

3.1 Basic knowledge

Throughout this thesis we consider an open bounded domain $\Omega \subset \mathbb{R}^3$ with a Lipschitz continuous boundary $\partial\Omega$, usually denoted by Γ. A key property of this type of domain is that it has a well-defined unit outward normal vector $\boldsymbol{\nu}$ at almost every point on Γ.

There are many criteria for smoothness of mathematical functions. The most basic criterion may be continuity. The space of all continuous functions defined on Ω is denoted by $C(\Omega)$. A function is said to be of class $C^k(\Omega)$ if its derivatives up to the order k exist and are continuous. The function is said to be of class $C^\infty(\Omega)$, or smooth, if it has derivatives of all orders. $C_0^k(\Omega)$ is defined as the set of functions belonging to $C^k(\Omega)$ with a compact support in Ω. The last subset of $C^k(\Omega)$ which has to be mentioned, namely $C^k(\overline{\Omega})$, includes functions with bounded and uniformly continuous derivatives up to the order k in $\overline{\Omega}$.

Any normed vector space X has a corresponding dual vector space X^* that consists of all continuous linear functionals defined on X. A norm of a contin-

uous linear functional f is defined by

$$\|f\|_{X^*} = \sup_{x \in X} \frac{|f(x)|}{\|x\|_X}.$$

This turns the dual X^* into a normed vector space, a Banach space.

Let J be a canonical mapping from a Banach space X into its second dual X^{**}. A Banach space X is said to be *reflexive* if $J(X) = X^{**}$.
To become more familiar with the topic of functional analysis we refer to the book of Rudin [75].

So far we talked about functions of a real variable and their appropriate spaces. We now turn to an analysis of vector functions. To distinguish the notation, the vector functions are in **bold**. Throughout the thesis we work with vector functions of a vector variable in $\mathbb{R}^3$.

The Lebesgue spaces $\mathbf{L}_p(\Omega)$ for $p \geq 1$, see [29], are named after the famous french mathematician Henri Lebesgue. They form an important class of examples of Banach spaces and are defined as follows:

$$\mathbf{L}_p(\Omega) = \left\{ \boldsymbol{u} \in \Omega \to \mathbb{R}^3; \|\boldsymbol{u}\|_p = \left(\int_\Omega |\boldsymbol{u}(\boldsymbol{x})|^p \, \mathrm{d}\boldsymbol{x} \right)^{1/p} < \infty \right\}.$$

In words, $\mathbf{L}_p(\Omega)$ is the set of all measurable functions whose absolute value raised to the p-th power has a finite Lebesgue integral. A special case arises when $p = 2$ (it is basic example of a Hilbert space) and we will use a simpler notation $\|\cdot\|$ instead of $\|\cdot\|_2$.

A Hilbert space ([47, 48]) is a vector space on which a scalar product is defined. The scalar product between two real vectors $\boldsymbol{u}, \boldsymbol{v} \in \mathbb{R}^n$ is denoted by $\boldsymbol{u} \cdot \boldsymbol{v}$. The notation $(\boldsymbol{u}, \boldsymbol{v})$ is used for the scalar product in the $\mathbf{L}_2(\Omega)$ space

$$(\boldsymbol{u}, \boldsymbol{v}) = \int_\Omega \boldsymbol{u} \cdot \boldsymbol{v}. \tag{3.1}$$

The $\mathbf{L}_2(\Omega)$-inner product on the boundary Γ is written as $(\boldsymbol{u}, \boldsymbol{v})_\Gamma = \displaystyle\int_\Gamma \boldsymbol{u} \cdot \boldsymbol{v}$.

A similar notation $\langle \boldsymbol{u}, \boldsymbol{v} \rangle$ is used for the duality relation, i.e. $\boldsymbol{u} \in \boldsymbol{U}$ and $\boldsymbol{v} \in \boldsymbol{U}^*$. The Lebesgue spaces $\mathbf{L}_p(\Omega)$ and $\mathbf{L}_q(\Omega)$ are dual to each other if their exponents $p, q > 1$ are dual (conjugate) to each other, i.e. if $1/p + 1/q = 1$.

When $1 < p < \infty$, the space $\mathbf{L}_p(\Omega)$ is reflexive.

Remark 3.1 *The relation (3.1) can be interpreted either as a scalar product or as a duality relation.*

We now proceed to the properties of mappings used in the theory of monotone operators. We come back to this theory in Chapter 5 when proving the existence and uniqueness of a weak solution to the boundary value problem.

By *Lipschitz continuity* of a mapping $\boldsymbol{F} : \boldsymbol{X} \to \boldsymbol{Y}$ we mean that there exists a constant $C \geq 0$ such that the inequality

$$\|\boldsymbol{F}(\boldsymbol{x}) - \boldsymbol{F}(\boldsymbol{y})\|_{\mathbf{Y}} \leq C \|\boldsymbol{x} - \boldsymbol{y}\|_{\mathbf{X}}$$

holds for all $\boldsymbol{x}, \boldsymbol{y}$ in the definition domain of the mapping $\boldsymbol{F}$.

Let $\boldsymbol{X}$ be a real normed space. Then the mapping $\boldsymbol{F} : \boldsymbol{X} \to \boldsymbol{X}^*$ is said to be *monotone* if

$$\langle \boldsymbol{F}(\boldsymbol{x}) - \boldsymbol{F}(\boldsymbol{y}), \boldsymbol{x} - \boldsymbol{y} \rangle \geq 0 \tag{3.2}$$

for all $\boldsymbol{x}, \boldsymbol{y}$ from the definition domain of the mapping $\boldsymbol{F}$. If the equality in (3.2) holds only for $\boldsymbol{x} = \boldsymbol{y}$, then $\boldsymbol{F}$ is said to be *strictly monotone*.

The same mapping $\boldsymbol{F} : \boldsymbol{X} \to \boldsymbol{X}^*$ is said to be *coercive* if

$$\langle \boldsymbol{F}(\boldsymbol{x}), \boldsymbol{x} \rangle \geq c(\|\boldsymbol{x}\|_{\mathbf{X}}) \|\boldsymbol{x}\|_{\mathbf{X}} ,$$

where $c(t)$ for $t \geq 0$ is a real–valued function such that $c(t) \to \infty$ as $t \to \infty$.

Coercivity is also one of the properties of bilinear forms. A bilinear form $a : \boldsymbol{X} \times \boldsymbol{X} \to \mathbb{R}$ is said to be *coercive* or $\boldsymbol{X}$*-elliptic* if there exists a constant $C > 0$ such that

$$a(\boldsymbol{x}, \boldsymbol{x}) \geq C \|\boldsymbol{x}\|^2_{\mathbf{X}} \qquad \forall \boldsymbol{x} \in \boldsymbol{X}.$$

Another concept we have to be familiar with is that of the convergence. Let $\{\boldsymbol{x}_n\}$ be a sequence in a normed linear space $\boldsymbol{X}$. Then the sequence $\{\boldsymbol{x}_n\}$ converges to $\boldsymbol{x} \in \boldsymbol{X}$

- ▷ *strongly*: $\boldsymbol{x}_n \to \boldsymbol{x}$ if $\lim\limits_{n\to\infty} \|\boldsymbol{x}_n - \boldsymbol{x}\|_{\mathbf{X}} = 0$;
- ▷ *weakly*: $\boldsymbol{x}_n \rightharpoonup \boldsymbol{x}$ if $\lim\limits_{n\to\infty} \phi(\boldsymbol{x}_n) = \phi(\boldsymbol{x}) \quad \forall \phi \in \boldsymbol{X}^*$.

3.2 Sobolev spaces

We have already mentioned that continuity is the basic criterion of a function smoothness. A stronger notion of smoothness is that of differentiability and an even stronger is that the derivative also be continuous. Differentiable functions are important in many areas, and in differential equations in particular. But it has been observed in the 20th century that the spaces $\mathbf{C}^1, \mathbf{C}^2$, etc. are not

exactly the right spaces to study solutions of differential equations. The reason is that the classical solution of differential equation does not always exist, so we have to look for the variational one. The variational theory builds on Sobolev spaces. Thus, we conclude that Sobolev spaces are a necessary replacement for the spaces of continuous functions in which one looks for solutions of partial differential equations.

In this chapter we summarize some basic results concerning Sobolev spaces. The basic references for this material are the books of Adams [1] and Girault and Raviart [42].

Let $\mathbf{C}_0^\infty(\Omega)^*$ denote the dual space to $\mathbf{C}_0^\infty(\Omega)$, often called the space of distributions on Ω.
Let $\boldsymbol{\alpha} = (\alpha_1, \dots, \alpha_N) \in \mathbb{N}^N$ and set

$$|\boldsymbol{\alpha}| = \sum_{i=1}^{N} \alpha_i.$$

The distributional derivative $\partial^{\boldsymbol{\alpha}} \boldsymbol{u} \in \mathbf{C}_0^\infty(\Omega)^*$ of a function $\boldsymbol{u} \in \mathbf{C}_0^\infty(\Omega)^*$ is defined by

$$\langle \partial^{\boldsymbol{\alpha}} \boldsymbol{u}, \boldsymbol{\phi} \rangle = (-1)^{|\boldsymbol{\alpha}|} \langle \boldsymbol{u}, \partial^{\boldsymbol{\alpha}} \boldsymbol{\phi} \rangle \qquad \forall \boldsymbol{\phi} \in \mathbf{C}_0^\infty(\Omega).$$

In the case of an $|\boldsymbol{\alpha}|$–times differentiable distribution $\boldsymbol{u}$, the derivative $\partial^{\boldsymbol{\alpha}} \boldsymbol{u}$ coincides with the usual notation

$$\frac{\partial^{\boldsymbol{\alpha}} \boldsymbol{u}}{\partial \boldsymbol{x}^{\boldsymbol{\alpha}}} = \frac{\partial^{|\boldsymbol{\alpha}|} \boldsymbol{u}}{\partial x_1^{\alpha_1} \dots \partial x_N^{\alpha_N}}.$$

We are now ready to introduce the fundamental Sobolev space for each integer $k \geq 0$ and real $p : 1 \leq p \leq \infty$

$$\mathbf{W}^{k,p}(\Omega) = \{\boldsymbol{v} \in \mathbf{L}_p(\Omega) \,|\, \partial^{\boldsymbol{\alpha}} \boldsymbol{v} \in \mathbf{L}_p(\Omega) \text{ for all } |\boldsymbol{\alpha}| \leq k\}, \tag{3.3}$$

which is a Banach space if it is equipped with the norm

$$\|\boldsymbol{v}\|_{\mathbf{W}^{k,p}(\Omega)} = \left(\sum_{|\boldsymbol{\alpha}| \leq k} \int_\Omega |\partial^{\boldsymbol{\alpha}} \boldsymbol{v}|^p \right)^{1/p}. \tag{3.4}$$

In other words, it is the space of functions defined almost everywhere in Ω having distributional derivatives in $\mathbf{L}_p(\Omega)$ up to the order k.

The space $\mathbf{W}^{k,p}(\Omega)$ is separable for $1 \leq p < \infty$ and reflexive for $1 < p < \infty$. Sobolev spaces with $p = 2$ are especially important because they form a Hilbert space; we use a special notation $\mathbf{H}^k(\Omega)$ in this case.

The following theorem states that functions from the Sobolev space $\mathbf{W}^{k,p}(\Omega)$ are more regular than functions from the Lebesgue space $\mathbf{L}_q(\Omega)$ (see [69] for the proof).

Theorem 3.1 *If $kp \leq 3$ then $\mathbf{W}^{k,p}(\Omega) \subset \mathbf{L}_q(\Omega)$ for $1/q = 1/p - k/3$ and there exists a constant C such that*

$$\|\boldsymbol{u}\|_{\mathbf{L}_q(\Omega)} \leq C \, \|\boldsymbol{u}\|_{\mathbf{W}^{k,p}(\Omega)} \qquad \forall \boldsymbol{u} \in \mathbf{W}^{k,p}(\Omega).$$

The analysis of Maxwell's equations is a bit more complicated. When speaking about the regularity of the solution, it is necessary to use Sobolev spaces of fractional order. In a few words we go into these spaces in the following subsections.

3.2.1 The space $\mathbf{H}(\mathrm{div};\Omega)$

In this section we state some results concerning the Hilbert space of vector functions with square–integrable divergence denoted by

$$\mathbf{H}(\mathrm{div};\Omega) = \{\boldsymbol{u} \in \mathbf{L}_2(\Omega); \nabla \cdot \boldsymbol{u} \in \mathrm{L}_2(\Omega)\} \tag{3.5}$$

and equipped with the graph norm

$$\|\boldsymbol{u}\|_{\mathbf{H}(\mathrm{div};\Omega)} = \left(\|\boldsymbol{u}\|^2_{\mathbf{L}_2(\Omega)} + \|\nabla \cdot \boldsymbol{u}\|^2_{\mathrm{L}_2(\Omega)} \right)^{1/2}. \tag{3.6}$$

To ensure continuity conditions across interfaces between dissimilar materials, it is necessary to check if functions in $\mathbf{H}(\mathrm{div};\Omega)$ have a well–defined normal component on Γ. For a function $\boldsymbol{v} \in \mathbf{C}^\infty(\overline{\Omega})$ the normal trace operator is defined as

$$\gamma_n(\boldsymbol{v}) = \boldsymbol{v}\,|_\Gamma \cdot \boldsymbol{\nu}. \tag{3.7}$$

The following theorem, see [42], shows that this continuity condition is satisfied.

Theorem 3.2 *Let $\Omega \subset \mathbb{R}^3$ be a bounded Lipschitz domain with unit outward normal $\boldsymbol{\nu}$. Then*

(1) the mapping γ_n defined by (3.7) can be extended by continuity to a continuous linear map γ_n from $\mathbf{H}(\mathrm{div};\Omega)$ onto $\mathbf{H}^{-1/2}(\Gamma)$;

(2) the following Green's theorem holds for functions $\boldsymbol{v} \in \mathbf{H}(\mathrm{div};\Omega)$ and test functions $\phi \in \mathrm{H}^1(\Omega)$:

$$(\boldsymbol{v}, \nabla\phi) + (\nabla \cdot \boldsymbol{v}, \phi) = \langle \phi, \gamma_n(\boldsymbol{v}) \rangle_\Gamma. \tag{3.8}$$

3.2.2 The space $\mathbf{H}(\mathbf{curl}\,;\Omega)$

Now, we focus on the space of central importance for Maxwell's equations. It corresponds to the space of finite–energy solutions:

$$\mathbf{H}(\mathbf{curl}\,;\Omega) = \{\boldsymbol{u} \in \mathbf{L}_2(\Omega); \nabla \times \boldsymbol{u} \in \mathbf{L}_2(\Omega)\}. \tag{3.9}$$

This space of vector functions with $\mathbf{L}_2(\Omega)$ integrable *curl* operator are associated with the graph norm

$$\|\boldsymbol{u}\|_{\mathbf{H}(\mathbf{curl}\,;\Omega)} = \left(\|\boldsymbol{u}\|^2_{\mathbf{L}_2(\Omega)} + \|\nabla \times \boldsymbol{u}\|^2_{\mathbf{L}_2(\Omega)}\right)^{1/2}. \tag{3.10}$$

Further, we introduce the subspace $\mathbf{H}_0(\mathbf{curl}\,;\Omega)$ = closure of $\mathbf{C}_0^\infty(\Omega)$ in norm (3.10). The following Lemma 3.1 gives an alternative characterization of functions in $\mathbf{H}_0(\mathbf{curl}\,;\Omega)$, for proof see [42].

Lemma 3.1 *Let $\Omega \subset \mathbb{R}^3$ be a bounded Lipschitz domain and let $\boldsymbol{u} \in \mathbf{H}(\mathbf{curl}\,;\Omega)$ be such that for every $\boldsymbol{\phi} \in \mathbf{C}^\infty(\overline{\Omega})$*

$$(\nabla \times \boldsymbol{u}, \boldsymbol{\phi}) - (\boldsymbol{u}, \nabla \times \boldsymbol{\phi}) = 0.$$

Then $\boldsymbol{u} \in \mathbf{H}_0(\mathbf{curl}\,;\Omega)$.

In order to use $\mathbf{H}(\mathbf{curl}\,;\Omega)$ as the energy space for Maxwell's equations, it has to be verified that functions in this space have a well–defined tangential trace [2, 16–18]. For any smooth vector function $\boldsymbol{v} \in \mathbf{C}^\infty(\overline{\Omega})$ there are two traces defined by

$$\begin{aligned} \gamma_t(\boldsymbol{v}) &= \boldsymbol{\nu} \times \boldsymbol{v}\,|_\Gamma, \\ \gamma_T(\boldsymbol{v}) &= (\boldsymbol{\nu} \times \boldsymbol{v}\,|_\Gamma) \times \boldsymbol{\nu}. \end{aligned} \tag{3.11}$$

The trace γ_t gives rise to the following theorem.

Theorem 3.3 *Let $\Omega \subset \mathbb{R}^3$ be a bounded Lipschitz domain. Then*

(1) the trace mapping γ_t can be extended by continuity to a continuous linear map from $\mathbf{H}(\mathbf{curl}\,;\Omega)$ into $\mathbf{H}^{-1/2}(\Gamma)$;

(2) the following Green's theorem holds for any $\boldsymbol{v} \in \mathbf{H}(\mathbf{curl}\,;\Omega)$ and any test function $\boldsymbol{\phi} \in \mathbf{H}^1(\Omega)$:

$$(\nabla \times \boldsymbol{v}, \boldsymbol{\phi}) - (\boldsymbol{v}, \nabla \times \boldsymbol{\phi}) = \langle \gamma_t(\boldsymbol{v}), \boldsymbol{\phi}\rangle_\Gamma. \tag{3.12}$$

Remark 3.2 *The map γ_t is not surjective.*

A similar result for the mapping γ_T is not valid for Lipschitz domains, because even when $\boldsymbol{v} \in \mathbf{H}^1(\Omega)$, γ_t is not regular enough. Therefore, we follow the idea of [20] to define the trace space $Y(\Gamma)$:

$$Y(\Gamma) := \left\{ \boldsymbol{f} \in \mathbf{H}^{-1/2}(\Gamma) \;\middle|\; \exists\, \boldsymbol{v} \in \mathbf{H}(\mathbf{curl}\,;\Omega) \text{ with } \gamma_t(\boldsymbol{v}) = \boldsymbol{f} \right\},$$

with norm

$$\|\boldsymbol{f}\|_{Y(\Gamma)} = \inf_{\boldsymbol{v}\in\mathbf{H}(\mathbf{curl}\,;\Omega);\gamma_t(\boldsymbol{v})=\boldsymbol{f}} \|\boldsymbol{v}\|_{\mathbf{H}(\mathbf{curl}\,;\Omega)}\,.$$

We then have the following result.

Theorem 3.4 *The space $Y(\Gamma)$ is a Hilbert space. Then*

(1) the trace mapping $\gamma_t : \mathbf{H}(\mathbf{curl}\,;\Omega) \to Y(\Gamma)$ is surjective;
the map $\gamma_T : \mathbf{H}(\mathbf{curl}\,;\Omega) \to Y(\Gamma)^*$ is well-defined;

(2) for any $\boldsymbol{v} \in \mathbf{H}(\mathbf{curl}\,;\Omega)$ and $\boldsymbol{\phi} \in \mathbf{H}(\mathbf{curl}\,;\Omega)$ one has

$$(\nabla \times \boldsymbol{v}, \boldsymbol{\phi}) - (\boldsymbol{v}, \nabla \times \boldsymbol{\phi}) = \langle \gamma_t(\boldsymbol{\phi}), \gamma_T(\boldsymbol{v}) \rangle_\Gamma. \tag{3.13}$$

The definition of the trace space $Y(\Gamma)$ is not easy to use as one cannot judge whether $\boldsymbol{f}$ belongs to $Y(\Gamma)$ unless one constructs its extension to the whole Ω and tests if this extension belongs to $\mathbf{H}(\mathbf{curl}\,;\Omega)$.

For more exhaustive information about trace spaces, see [16–18].

Remark 3.3 *For a Lipschitz domain it is known that γ_T is surjective. The proof can be found in [18].*

Part I

Direct problems in low-frequency electromagnetism

Chapter 4

Problem formulation

The low-frequency domain includes the major part of electromagnetic devices like motors, relays and transformers. These are all applications at power frequencies below a few tens of kHz. Strictly speaking, any application in which displacement currents can be neglected is a low-frequency application. This case corresponds to a steady state (see Section 1.2), and we can, in general, study electric fields and magnetic fields as separate quantities.

We consider an open bounded domain $\Omega \subset \mathbb{R}^3$ with a Lipschitz boundary Γ occupied by a ferromagnetic material. The electromagnetic field in Ω is described by the vector fields $\boldsymbol{B}$- the magnetic induction, $\boldsymbol{H}$- the magnetic field, and $\boldsymbol{E}$- the electric field as was introduced in the first chapter. Further, we assume linear magnetic materials, governed by the constitutive law (1.10)

$$\boldsymbol{B} = \mu_0 \boldsymbol{H}.$$

The scalar μ_0 denotes the magnetic permeability of free space. The whole domain Ω is assumed to be conductive, i.e. $\sigma > 0$.

We deal with the steady state eddy current problem already derived in Section 1.2, i.e.

$$\begin{aligned} \nabla \times \boldsymbol{H} &= \boldsymbol{J}_a + \sigma \boldsymbol{E}, \\ \partial_t \boldsymbol{B} + \nabla \times \boldsymbol{E} &= \boldsymbol{0}. \end{aligned} \tag{4.1}$$

The system (4.1) is accompanied with a non-linear boundary condition between the normal components of $\boldsymbol{H}$ and $\boldsymbol{E}$, corresponding to a non-perfect

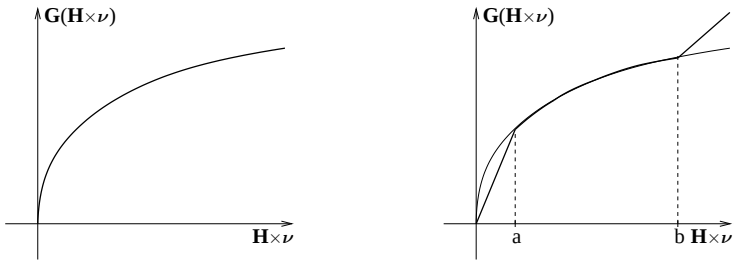

(a) power law (4.3)

(b) modified power law (4.4), also called Lipschitz continuous case

Figure 4.1: The sketch of the dependence of the vector function $\boldsymbol{G}$ on the normal component of the magnetic field $\boldsymbol{H}$ used in our model to illustrate a non-perfect contact of two materials on the boundary.

contact of different materials at the boundary. In other words, the material on one side of the boundary does not allow the field to penetrate without loosing energy. This can be described in terms of an absorbing boundary condition, see (1.27). For a non-perfect contact see relations (1.25) and (1.26). Simplified, we consider the following power law non-linearity

$$\boldsymbol{\nu} \times \boldsymbol{E} = \boldsymbol{\nu} \times \boldsymbol{G}\left(\boldsymbol{H} \times \boldsymbol{\nu}\right). \tag{4.2}$$

The aim of this part of the thesis is to analyze two different forms of the nonlinear vector field $\boldsymbol{G}$ following from the power law (4.2).

Firstly, we consider a non-perfect boundary condition expressed by the vector function

$$\boldsymbol{G}\left(\boldsymbol{H} \times \boldsymbol{\nu}\right) = \left|\boldsymbol{H} \times \boldsymbol{\nu}\right|^{\alpha-1} \boldsymbol{H} \times \boldsymbol{\nu} \qquad \alpha \in (0,1] \tag{4.3}$$

depicted in Figure 4.1(a). Notice that (4.2) leads to the following dissipation of energy on the boundary

$$\left(\boldsymbol{E} \times \boldsymbol{H}\right) \cdot \boldsymbol{\nu} = \boldsymbol{G}\left(\boldsymbol{H} \times \boldsymbol{\nu}\right) \cdot \left(\boldsymbol{H} \times \boldsymbol{\nu}\right) = \left|\boldsymbol{H} \times \boldsymbol{\nu}\right|^{\alpha+1}.$$

The derivation of the magnetic field in the zero region is unbounded, therefore we associate the power law (4.3) with the degenerate case. That is, the behavior of the conductor is unpredictable for very small values of $\boldsymbol{H}$.

In order to guarantee an appropriate mathematical behavior of the problem, the nonlinearity $\boldsymbol{G}$ is slightly modified, namely:

$$\boldsymbol{G}(\boldsymbol{H}\times\boldsymbol{\nu}) = \begin{cases} a^{\alpha-1}\boldsymbol{H}\times\boldsymbol{\nu} & 0 \le |\boldsymbol{H}\times\boldsymbol{\nu}| < a, \\ |\boldsymbol{H}\times\boldsymbol{\nu}|^{\alpha-1}\boldsymbol{H}\times\boldsymbol{\nu} & a \le |\boldsymbol{H}\times\boldsymbol{\nu}| \le b, \\ b^{\alpha-1}\boldsymbol{H}\times\boldsymbol{\nu} & b < |\boldsymbol{H}\times\boldsymbol{\nu}| \end{cases} \tag{4.4}$$

for some fixed positive constants $0 < a < b$, see Figure 4.1(b). The definition (4.4) assures that the newly defined vector field is Lipschitz continuous. The proof of this important analytical property can be found in Chapter 6 and it is also the reason why we refer to this modified problem as to the Lipschitz continuous case.

One can also consider a more general function $\boldsymbol{G}$, which is continuous, monotone and coercive in appropriate spaces. Then, as would be expected, the analysis of the problem is more difficult.

A non-linear degenerate BC (4.3) is considered for the generalization of the classical Silver-Müller condition, see Section 1.3.1.

For ease of the exposition, we set $\mu_0 = \sigma = 1$ and $\boldsymbol{J}_a = \boldsymbol{0}$, in order to focus on the non-linearity in the problem setting.

By employing the constitutive law (1.10) and after eliminating the electric field from the system of Maxwell's equations (4.1) we arrive at the boundary value problem in terms of the magnetic field only

$$\begin{aligned} \partial_t\boldsymbol{H} + \nabla\times\nabla\times\boldsymbol{H} &= \boldsymbol{0} && \text{in } \Omega, \\ \boldsymbol{\nu}\times\nabla\times\boldsymbol{H} &= \boldsymbol{\nu}\times\boldsymbol{G}\left(\boldsymbol{H}\times\boldsymbol{\nu}\right) && \text{on } \Gamma. \end{aligned} \tag{4.5}$$

Hence, the variational formulation of (4.5) together with initial condition reads as follows:
Find $\boldsymbol{H}(t) \in \boldsymbol{V}$, such that

$$\begin{aligned} (\partial_t\boldsymbol{H},\boldsymbol{\varphi}) + (\nabla\times\boldsymbol{H},\nabla\times\boldsymbol{\varphi}) + (\boldsymbol{G}(\boldsymbol{H}\times\boldsymbol{\nu}),\boldsymbol{\varphi}\times\boldsymbol{\nu})_\Gamma &= 0, \\ \boldsymbol{H}(0) &= \boldsymbol{H}_0 \end{aligned} \tag{4.6}$$

holds for any $\boldsymbol{\varphi} \in \boldsymbol{V}$ and for almost every $t \in (0,T)$.

Depending on the choice of the power law nonlinearity, $\boldsymbol{V}$ denotes an appropriate space of functions. It is specified for the Lipschitz and degenerate (non-Lipschitz) problem separately.

Once the problem is defined, a numerical scheme for finding an approximation of the solution needs to be developed. We keep sticked to this goal throughout the following two chapters.

Chapter 5

Time discretization

This chapter is based on the article [83] where our main goal is to design a time-discrete numerical scheme for the approximation of an exact solution to the problem (4.5). The Silver-Müller boundary condition (4.2) is coupled with the power law nonlinearity (4.3).

The stabilization of Maxwell's equations with space-time variable coefficients by means of linear or non-linear Silver-Müller boundary condition has been studied in [70]. This is based on some stability estimates that are obtained using the "standard" identity with multiplier and appropriate properties of the feedback.

The decay rates for the energy for the full Maxwell's system have been derived in [30, 31]. The Galerkin approximation of a solution for a linear Silver-Müller BC has been studied in [23].

This chapter splits naturally into a few sections. First, we establish existence and uniqueness of a weak solution in a suitable function space under the minimal regularity assumptions on the boundary Γ and the initial data $\boldsymbol{H}_0$. We design a non-linear time-discrete approximation scheme. Time discretization is performed using the well known Rothe's method, see e.g. [55]. The a priori estimates are helpful in the next section for proving the convergence of our method. The proof of Theorem 5.2 based on Minty-Browder's trick is regarded as the main theoretical result of this chapter. Finally the error estimates for the time discretization are derived in Theorem 5.3. The chapter ends with some numerical experiments confirming the efficiency of the proposed scheme. These results will be presented at the international conference on Mathematical Modeling and Computational Physics 2009 in Dubna.

Taking the degenerate non-Lipschitz power law (4.3) as a boundary condition to the problem (4.5), the variational formulation together with an initial condition reads

$$\begin{aligned} (\partial_t \boldsymbol{H}, \boldsymbol{\varphi}) + (\nabla \times \boldsymbol{H}, \nabla \times \boldsymbol{\varphi}) + \left(|\boldsymbol{H} \times \boldsymbol{\nu}|^{\alpha-1} \boldsymbol{H} \times \boldsymbol{\nu}, \boldsymbol{\varphi} \times \boldsymbol{\nu} \right)_\Gamma &= 0, \\ \boldsymbol{H}(0) &= \boldsymbol{H}_0 \end{aligned} \tag{5.1}$$

for any $\boldsymbol{\varphi} \in \boldsymbol{V}$ and for almost all $t \in (0, T)$.
In this case the space of test functions is denoted by

$$\boldsymbol{V} = \{\boldsymbol{\varphi} \in \mathbf{H}(\mathbf{curl}\,; \Omega);\ \boldsymbol{\varphi} \times \boldsymbol{\nu} \in \mathbf{L}_{1+\alpha}(\Gamma)\},$$

which is a natural choice for our problem. $\boldsymbol{V}$ is a reflexive Banach space endowed with the sum-norm $\|\boldsymbol{\varphi}\|_{\boldsymbol{V}} = \|\boldsymbol{\varphi}\|_{\mathbf{H}(\mathbf{curl}\,;\Omega)} + \|\boldsymbol{\varphi} \times \boldsymbol{\nu}\|_{\mathbf{L}_{1+\alpha}(\Gamma)}$. The dual space to $\boldsymbol{V}$ is denoted by $\boldsymbol{V}^*$.

5.1 Discretization scheme

The time discretization is based on the backward Euler's method as was mentioned. We use an equidistant partitioning with a time step $\tau = \frac{T}{n}$, for any $n \in \mathbb{N}$. Therefore, the time interval $[0, T]$ is divided into n subintervals $[t_{i-1}, t_i]$ with $t_i = i\tau$. For any function z we introduce the following notation

$$z_i = z(t_i), \qquad \delta z_i = \frac{z_i - z_{i-1}}{\tau}.$$

We suggest the non-linear recurrent approximation scheme for $i = 1, \ldots, n$ and $\boldsymbol{\varphi} \in \boldsymbol{V}$

$$\begin{aligned} (\delta \boldsymbol{h}_i, \boldsymbol{\varphi}) + (\nabla \times \boldsymbol{h}_i, \nabla \times \boldsymbol{\varphi}) + \left(|\boldsymbol{h}_i \times \boldsymbol{\nu}|^{\alpha-1} \boldsymbol{h}_i \times \boldsymbol{\nu}, \boldsymbol{\varphi} \times \boldsymbol{\nu} \right)_\Gamma &= 0, \\ \boldsymbol{h}_0 &= \boldsymbol{H}_0. \end{aligned} \tag{5.2}$$

5.1.1 Well–posedness

The existence and uniqueness of a weak solution on each time step is guaranteed by the following lemma.

Lemma 5.1 *Assume $\boldsymbol{H}_0 \in \boldsymbol{V}^*$. Then there exists a uniquely determined $\boldsymbol{h}_i \in \boldsymbol{V}$ solving (5.2) for any $i = 1, \ldots, n$.*

Proof: We apply the theory of monotone operators (see [41, 91]) to show the existence of a weak solution to the boundary value problem (5.2). We consider a non-linear operator $\mathcal{G}(\boldsymbol{h}) : \boldsymbol{V} \to \boldsymbol{V}^*$ defined by

$$(\mathcal{G}(\boldsymbol{h}), \boldsymbol{\varphi}) := \left(\frac{\boldsymbol{h}}{\tau}, \boldsymbol{\varphi}\right) + (\nabla \times \boldsymbol{h}, \nabla \times \boldsymbol{\varphi}) + \left(|\boldsymbol{h} \times \boldsymbol{\nu}|^{\alpha-1} \boldsymbol{h} \times \boldsymbol{\nu}, \boldsymbol{\varphi} \times \boldsymbol{\nu}\right)_\Gamma$$

for any $\boldsymbol{\varphi} \in \boldsymbol{V}$.

Now, we introduce the real-valued function g

$$g(s) = s^{\alpha-1} \qquad \text{for } s > 0. \tag{5.3}$$

Thus, our nonlinearity takes the form $\boldsymbol{G}(\boldsymbol{x}) = g(|\boldsymbol{x}|)\boldsymbol{x}$ for all $\boldsymbol{x} \in \mathbb{R}^3$.

The Gâteaux differential of $\boldsymbol{G}(\boldsymbol{x})$ in the direction $\boldsymbol{h}$ is

$$D\boldsymbol{G}(\boldsymbol{x}, \boldsymbol{h}) = g'(|\boldsymbol{x}|)\frac{\boldsymbol{h} \cdot \boldsymbol{x}}{|\boldsymbol{x}|}\boldsymbol{x} + g(|\boldsymbol{x}|)\boldsymbol{h}.$$

The monotonicity of $\boldsymbol{G}(\boldsymbol{x})$ follows from [91], i.e. for some $\theta \in (0, 1)$ it holds

$$\begin{aligned}
(\boldsymbol{G}(\boldsymbol{x} + \boldsymbol{h}) - \boldsymbol{G}(\boldsymbol{x}), \boldsymbol{h})_\Gamma &= ((D\boldsymbol{G}(\boldsymbol{x} + \theta\boldsymbol{h}), \boldsymbol{h}), \boldsymbol{h})_\Gamma \\
&= g(|\boldsymbol{x} + \theta\boldsymbol{h}|)|\boldsymbol{h}|^2 + g'(|\boldsymbol{x} + \theta\boldsymbol{h}|)\frac{(\boldsymbol{h} \cdot (\boldsymbol{x} + \theta\boldsymbol{h}))^2}{|\boldsymbol{x} + \theta\boldsymbol{h}|} \\
&\geq [g(|\boldsymbol{x} + \theta\boldsymbol{h}|) - |g'(|\boldsymbol{x} + \theta\boldsymbol{h}|)|\, |\boldsymbol{x} + \theta\boldsymbol{h}|]\, |\boldsymbol{h}|^2 \\
&\geq \alpha|\boldsymbol{x} + \theta\boldsymbol{h}|^{\alpha-1}|\boldsymbol{h}|^2 \\
&\geq 0.
\end{aligned} \tag{5.4}$$

Further, we can write

$$(\mathcal{G}(\boldsymbol{h}), \boldsymbol{h}) = \frac{\|\boldsymbol{h}\|^2}{\tau} + \|\nabla \times \boldsymbol{h}\|^2 + \int_\Gamma |\boldsymbol{h} \times \boldsymbol{\nu}|^{1+\alpha}.$$

One can easily see that for $0 < \tau < 1$

$$\frac{(\mathcal{G}(\boldsymbol{h}), \boldsymbol{h})}{\|\boldsymbol{h}\|_{\boldsymbol{V}}} \geq \frac{\|\boldsymbol{h}\|^2_{\mathbf{H}(\mathbf{curl};\Omega)} + \|\boldsymbol{h} \times \boldsymbol{\nu}\|^{1+\alpha}_{\mathbf{L}_{1+\alpha}(\Gamma)}}{\|\boldsymbol{h}\|_{\mathbf{H}(\mathbf{curl};\Omega)} + \|\boldsymbol{h} \times \boldsymbol{\nu}\|_{\mathbf{L}_{1+\alpha}(\Gamma)}} \longrightarrow \infty$$

as $\|\boldsymbol{h}\|_{\boldsymbol{V}} \to \infty$.

The findings above immediately imply that $\mathcal{G}(\boldsymbol{h})$ is monotone, hemi-continuous and $\boldsymbol{V}$-coercive. Thus, according to the theory of monotone operators (cf. Vajnberg [91, Thm. 18.2]) we see that if $\boldsymbol{h}_0 \in \boldsymbol{V}^*$, then for any $i = 1, \ldots, n$ there

exists a weak solution $\boldsymbol{h}_i \in \boldsymbol{V}$. The uniqueness of each weak solution (for any time layer i) follows from

$$(\mathcal{G}(\boldsymbol{u}) - \mathcal{G}(\boldsymbol{v}), \boldsymbol{u} - \boldsymbol{v}) \geq \|\boldsymbol{u} - \boldsymbol{v}\|^2_{\mathbf{H}(\mathbf{curl};\Omega)} .$$

□

5.2 A priori estimates

As a starting point for proving the convergence and estimating the error of the time discrete scheme, a priori estimates are needed to be done. They are derived for $\boldsymbol{h}_i$ for each time step $i = 1, \ldots, n$.

Lemma 5.2 *Assume $\boldsymbol{H}_0 \in \mathbf{L}_2(\Omega)$. Then there exists a positive constant C such that (for any $j = 1, \ldots, n$)*

$$\|\boldsymbol{h}_j\|^2 + \sum_{i=1}^{j} \|\boldsymbol{h}_i - \boldsymbol{h}_{i-1}\|^2 + \sum_{i=1}^{j} \|\nabla \times \boldsymbol{h}_i\|^2 \tau + \sum_{i=1}^{j} \|\boldsymbol{h}_i \times \boldsymbol{\nu}\|^{1+\alpha}_{\mathbf{L}_{1+\alpha}(\Gamma)} \tau \leq C.$$

Proof: Setting $\boldsymbol{\varphi} = \boldsymbol{h}_i$ in (5.2), multiplying by τ and summing up for $i = 1, \ldots, j$ we have

$$\sum_{i=1}^{j} (\delta \boldsymbol{h}_i, \boldsymbol{h}_i) \tau + \sum_{i=1}^{j} \|\nabla \times \boldsymbol{h}_i\|^2 \tau + \sum_{i=1}^{j} \|\boldsymbol{h}_i \times \boldsymbol{\nu}\|^{1+\alpha}_{\mathbf{L}_{1+\alpha}(\Gamma)} \tau = 0.$$

For the first term on the left–hand side we use the Abel summation and we deduce

$$\|\boldsymbol{h}_j\|^2 + \sum_{i=1}^{j} \|\boldsymbol{h}_i - \boldsymbol{h}_{i-1}\|^2 + \sum_{i=1}^{j} \|\nabla \times \boldsymbol{h}_i\|^2 \tau + \sum_{i=1}^{j} \|\boldsymbol{h}_i \times \boldsymbol{\nu}\|^{1+\alpha}_{\mathbf{L}_{1+\alpha}(\Gamma)} \tau \leq C \|\boldsymbol{h}_0\|^2 .$$

□

For next a priori estimates we need the following technical lemma.

Lemma 5.3 *Let $g : \mathbb{R} \to \mathbb{R}$ be a non-negative continuous function such that $G(s) := g(s)s$ is monotonically increasing. Let Φ_G be the primitive function of G. Then for any vectors $\boldsymbol{a}, \boldsymbol{b} \in \mathbb{R}^3$ we have*

$$\Phi_G(|\boldsymbol{b}|) - \Phi_G(|\boldsymbol{a}|) \leq g(|\boldsymbol{b}|)\boldsymbol{b} \cdot (\boldsymbol{b} - \boldsymbol{a}).$$

Proof: From the mean-value theorem and the Cauchy inequality we deduce

$$\begin{aligned}\Phi_G(|\boldsymbol{b}|) - \Phi_G(|\boldsymbol{a}|) &= \int_{|\boldsymbol{a}|}^{|\boldsymbol{b}|} g(s)s \,\mathrm{d}s &&= g(\theta)\theta(|\boldsymbol{b}| - |\boldsymbol{a}|)\\ &\le g(|\boldsymbol{b}|)|\boldsymbol{b}|(|\boldsymbol{b}| - |\boldsymbol{a}|) &&= g(|\boldsymbol{b}|)\left(|\boldsymbol{b}|^2 - |\boldsymbol{b}||\boldsymbol{a}|\right)\\ &\le g(|\boldsymbol{b}|)\boldsymbol{b}\cdot(\boldsymbol{b}-\boldsymbol{a})\end{aligned}$$

for some θ between $|\boldsymbol{a}|$ and $|\boldsymbol{b}|$. □

A slightly higher regularity of the initial data $\boldsymbol{H}_0$ implies better regularity of $\boldsymbol{h}_j$, as the following lemma shows.

Lemma 5.4 *Assume $\boldsymbol{H}_0 \in \boldsymbol{V}$. Then there exists a positive constant C such that (for any $j = 1, \ldots, n$)*

$$\sum_{i=1}^{j} \|\delta \boldsymbol{h}_i\|^2 \tau + \|\nabla \times \boldsymbol{h}_j\|^2 + \sum_{i=1}^{j} \|\nabla \times (\boldsymbol{h}_i - \boldsymbol{h}_{i-1})\|^2 + \|\boldsymbol{h}_j \times \boldsymbol{\nu}\|^{1+\alpha}_{\mathbf{L}_{1+\alpha}(\Gamma)} \le C.$$

Proof: Setting $\boldsymbol{\varphi} = \delta \boldsymbol{h}_i$ in (5.2), multiplying by τ and summing up for $i = 1, \ldots, j$ yields

$$\begin{aligned}&\sum_{i=1}^{j} \|\delta \boldsymbol{h}_i\|^2 \tau + \sum_{i=1}^{j} (\nabla \times \boldsymbol{h}_i, \nabla \times [\boldsymbol{h}_i - \boldsymbol{h}_{i-1}])\\ &+ \sum_{i=1}^{j} \left(|\boldsymbol{h}_i \times \boldsymbol{\nu}|^{\alpha-1} \boldsymbol{h}_i \times \boldsymbol{\nu}, [\boldsymbol{h}_i - \boldsymbol{h}_{i-1}] \times \boldsymbol{\nu}\right)_\Gamma = 0.\end{aligned} \tag{5.5}$$

For the third term we apply Lemma 5.3 and we have

$$\begin{aligned}&\sum_{i=1}^{j} \left(|\boldsymbol{h}_i \times \boldsymbol{\nu}|^{\alpha-1} \boldsymbol{h}_i \times \boldsymbol{\nu}, [\boldsymbol{h}_i - \boldsymbol{h}_{i-1}] \times \boldsymbol{\nu}\right)_\Gamma\\ &\ge \frac{1}{\alpha+1} \sum_{i=1}^{j} \int_\Gamma \left[|\boldsymbol{h}_i \times \boldsymbol{\nu}|^{\alpha+1} - |\boldsymbol{h}_{i-1} \times \boldsymbol{\nu}|^{\alpha+1}\right]\\ &= \frac{1}{\alpha+1} \left(\|\boldsymbol{h}_j \times \boldsymbol{\nu}\|^{1+\alpha}_{\mathbf{L}_{1+\alpha}(\Gamma)} - \|\boldsymbol{h}_0 \times \boldsymbol{\nu}\|^{1+\alpha}_{\mathbf{L}_{1+\alpha}(\Gamma)}\right).\end{aligned}$$

Thus, applying the Abel summation to the second term in (5.5), we obtain

$$\sum_{i=1}^{j} \|\delta \boldsymbol{h}_i\|^2 \tau + \|\nabla \times \boldsymbol{h}_j\|^2 + \sum_{i=1}^{j} \|\nabla \times (\boldsymbol{h}_i - \boldsymbol{h}_{i-1})\|^2 + \|\boldsymbol{h}_j \times \boldsymbol{\nu}\|^{1+\alpha}_{\mathbf{L}_{1+\alpha}(\Gamma)} \le C \|\boldsymbol{h}_0\|_{\boldsymbol{V}}.$$

□

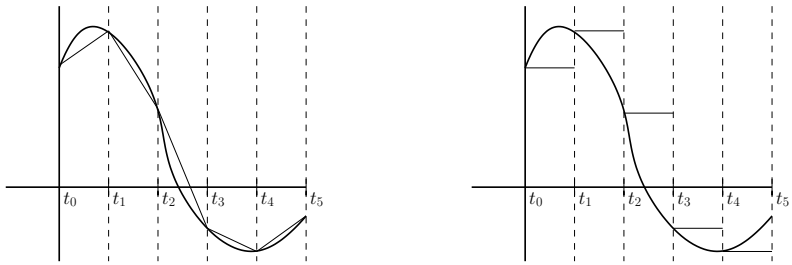

(a) piecewise linear in time function $f_5(t)$

(b) step in time function $\overline{f_5}(t)$

Figure 5.1: Definition of piecewise linear and step in time functions related to a general function $f(t)$ plotted as a curved line

5.3 Convergence

In this section we prove the convergence of our approximate solution to a weak solution of (5.1) in suitable function spaces.

First, we introduce the continuous piecewise linear in time vector field $\boldsymbol{h}_n$ $(i = 1, \ldots, n)$, see Figure 5.1(a), given by

$$\begin{aligned} \boldsymbol{h}_n(0) &= \boldsymbol{H}_0, \\ \boldsymbol{h}_n(t) &= \boldsymbol{h}_{i-1} + (t - t_{i-1})\delta \boldsymbol{h}_i \qquad \text{for } t \in (t_{i-1}, t_i]. \end{aligned}$$

Next, we define the step vector field $\overline{\boldsymbol{h}}_n$, see Figure 5.1(b)

$$\begin{aligned} \overline{\boldsymbol{h}}_n(0) &= \boldsymbol{H}_0, \\ \overline{\boldsymbol{h}}_n(t) &= \boldsymbol{h}_i \qquad \text{for } t \in (t_{i-1}, t_i]. \end{aligned}$$

Using the new notation, we rewrite (5.2) as (for any $\boldsymbol{\varphi} \in \boldsymbol{V}$)

$$(\partial_t \boldsymbol{h}_n, \boldsymbol{\varphi}) + \left(\nabla \times \overline{\boldsymbol{h}}_n, \nabla \times \boldsymbol{\varphi}\right) + \left(\left|\overline{\boldsymbol{h}}_n \times \boldsymbol{\nu}\right|^{\alpha-1} \overline{\boldsymbol{h}}_n \times \boldsymbol{\nu}, \boldsymbol{\varphi} \times \boldsymbol{\nu}\right)_\Gamma = 0. \tag{5.6}$$

Now, we prove that the sequences $\{\boldsymbol{h}_n\}$ and $\{\overline{\boldsymbol{h}}_n\}$ are Cauchy in appropriate function spaces.

Theorem 5.1 *Let $\boldsymbol{H}_0 \in \boldsymbol{V}$. Then there exists a positive C such that*

$$\max_{t\in[0,T]} \|\boldsymbol{h}_n(t) - \boldsymbol{h}_m(t)\|^2 + \int_0^T \left\|\nabla \times [\overline{\boldsymbol{h}}_n - \overline{\boldsymbol{h}}_m]\right\|^2 + \int_0^T \int_\Gamma \left[|\overline{\boldsymbol{h}}_n \times \boldsymbol{\nu}|^{\frac{\alpha+1}{2}} - |\overline{\boldsymbol{h}}_m \times \boldsymbol{\nu}|^{\frac{\alpha+1}{2}}\right]^2 \leq C\left(\frac{1}{n} + \frac{1}{m}\right).$$

Proof: Let n and m be arbitrary natural numbers. We subtract (5.6) for $n = m$ from (5.6). Then we put $\boldsymbol{\varphi} = \overline{\boldsymbol{h}}_n - \overline{\boldsymbol{h}}_m$ and we integrate the equation over $(0, t)$ for any $t \in [0, T]$. We get

$$\begin{aligned} &\int_0^t (\partial_t \boldsymbol{h}_n - \partial_t \boldsymbol{h}_m, \boldsymbol{h}_n - \boldsymbol{h}_m) + \int_0^t \left\|\nabla \times (\overline{\boldsymbol{h}}_n - \overline{\boldsymbol{h}}_m)\right\|^2 \\ &+ \int_0^t \left(|\overline{\boldsymbol{h}}_n \times \boldsymbol{\nu}|^{\alpha-1}\overline{\boldsymbol{h}}_n \times \boldsymbol{\nu} - |\overline{\boldsymbol{h}}_m \times \boldsymbol{\nu}|^{\alpha-1}\overline{\boldsymbol{h}}_m \times \boldsymbol{\nu}, \overline{\boldsymbol{h}}_n \times \boldsymbol{\nu} - \overline{\boldsymbol{h}}_m \times \boldsymbol{\nu}\right)_\Gamma \\ &= \int_0^t \left(\partial_t \boldsymbol{h}_n - \partial_t \boldsymbol{h}_m, \boldsymbol{h}_n - \overline{\boldsymbol{h}}_n + \overline{\boldsymbol{h}}_m - \boldsymbol{h}_m\right). \end{aligned} \tag{5.7}$$

The first term on the left can be written as

$$\int_0^t (\partial_t \boldsymbol{h}_n - \partial_t \boldsymbol{h}_m, \boldsymbol{h}_n - \boldsymbol{h}_m) = \tfrac{1}{2}\|\boldsymbol{h}_n(t) - \boldsymbol{h}_m(t)\|^2.$$

For the second term in (5.7) we use the following algebraic inequality, which can be proved in a standard way and which is valid for any $a, b, y, z \geq 0$

$$4ab\left(y^{\frac{a+b}{2}} - z^{\frac{a+b}{2}}\right)^2 \leq (a+b)^2\left(y^a - z^a\right)\left(y^b - z^b\right). \tag{5.8}$$

From (5.8) and the Cauchy inequality we deduce

$$\begin{aligned} \left(|\boldsymbol{y}|^{\alpha-1}\boldsymbol{y} - |\boldsymbol{z}|^{\alpha-1}\boldsymbol{z}\right)(\boldsymbol{y} - \boldsymbol{z}) &= |\boldsymbol{y}|^{\alpha+1} + |\boldsymbol{z}|^{\alpha+1} - |\boldsymbol{z}|^{\alpha-1}\boldsymbol{z}\boldsymbol{y} - |\boldsymbol{y}|^{\alpha-1}\boldsymbol{z}\boldsymbol{y} \\ &\geq |\boldsymbol{y}|^{\alpha+1} + |\boldsymbol{z}|^{\alpha+1} - |\boldsymbol{z}|^{\alpha}|\boldsymbol{y}| - |\boldsymbol{y}|^{\alpha}|\boldsymbol{z}| \\ &= \left(|\boldsymbol{y}|^{\alpha} - |\boldsymbol{z}|^{\alpha}\right)\left(|\boldsymbol{y}| - |\boldsymbol{z}|\right) \\ &\geq \frac{4\alpha}{(\alpha+1)^2}\left(|\boldsymbol{y}|^{\frac{\alpha+1}{2}} - |\boldsymbol{z}|^{\frac{\alpha+1}{2}}\right)^2. \end{aligned}$$

Therefore, the boundary term in (5.7) can be estimated from below as follows

$$\begin{aligned} &\int_0^t \left(|\overline{\boldsymbol{h}}_n \times \boldsymbol{\nu}|^{\alpha-1}\overline{\boldsymbol{h}}_n \times \boldsymbol{\nu} - |\overline{\boldsymbol{h}}_m \times \boldsymbol{\nu}|^{\alpha-1}\overline{\boldsymbol{h}}_m \times \boldsymbol{\nu}, \overline{\boldsymbol{h}}_n \times \boldsymbol{\nu} - \overline{\boldsymbol{h}}_m \times \boldsymbol{\nu}\right)_\Gamma \\ &\geq \frac{4\alpha}{(\alpha+1)^2}\int_0^t \int_\Gamma \left[|\overline{\boldsymbol{h}}_n \times \boldsymbol{\nu}|^{\frac{\alpha+1}{2}} - |\overline{\boldsymbol{h}}_m \times \boldsymbol{\nu}|^{\frac{\alpha+1}{2}}\right]^2. \end{aligned}$$

The right-hand side in (5.7) can be estimated using the Cauchy inequality. We successively deduce

$$\begin{aligned}
&\int_0^t \left(\partial_t \boldsymbol{h}_n - \partial_t \boldsymbol{h}_m, \boldsymbol{h}_n - \overline{\boldsymbol{h}}_n + \overline{\boldsymbol{h}}_m - \boldsymbol{h}_m\right) \\
&\leq C \int_0^t \left(\|\partial_t \boldsymbol{h}_m\| + \|\partial_t \boldsymbol{h}_n\|\right) \left(\frac{\|\partial_t \boldsymbol{h}_n\|}{n} + \frac{\|\partial_t \boldsymbol{h}_m\|}{m}\right) \\
&\leq C \left(\frac{1}{n} + \frac{1}{m}\right).
\end{aligned}$$

Collecting all estimates we arrive at

$$\begin{aligned}
&\|\boldsymbol{h}_n(t) - \boldsymbol{h}_m(t)\|^2 + \int_0^t \left\|\nabla \times [\overline{\boldsymbol{h}}_n - \overline{\boldsymbol{h}}_m]\right\|^2 \\
&+ \int_0^t \int_\Gamma \left[|\overline{\boldsymbol{h}}_n \times \boldsymbol{\nu}|^{\frac{\alpha+1}{2}} - |\overline{\boldsymbol{h}}_m \times \boldsymbol{\nu}|^{\frac{\alpha+1}{2}}\right]^2 \leq C \left(\frac{1}{n} + \frac{1}{m}\right),
\end{aligned}$$

which is valid for any $t \in [0, T]$. From this we easily derive the desired result.□

Our next step is to show the existence of a weak solution of (5.1). To do this, we use the stability results of the previous lemmas and Theorem 5.1.

Theorem 5.2 (convergence) *Let $\boldsymbol{H}_0 \in \boldsymbol{V}$. Then there exists a $\boldsymbol{H} \in \boldsymbol{V}$ such that*

(i) $\overline{\boldsymbol{h}}_n \to \boldsymbol{H}$ *in* $L_2\left((0,T), \mathbf{H}(\mathbf{curl}\,;\Omega)\right)$

(ii) $\boldsymbol{h}_n \to \boldsymbol{H}$ *in* $L_2\left((0,T), \mathbf{L}_2(\Omega)\right)$

(iii) $\partial_t \boldsymbol{h}_n \rightharpoonup \partial_t \boldsymbol{H}$ *in* $L_2\left((0,T), \mathbf{L}_2(\Omega)\right)$

(iv) $\boldsymbol{\nu} \times |\overline{\boldsymbol{h}}_n \times \boldsymbol{\nu}|^{\alpha-1} \overline{\boldsymbol{h}}_n \times \boldsymbol{\nu} \to \boldsymbol{\nu} \times |\boldsymbol{H} \times \boldsymbol{\nu}|^{\alpha-1} \boldsymbol{H} \times \boldsymbol{\nu}$ *in* $L_{\frac{\alpha+1}{\alpha}}\left((0,T), \mathbf{L}_{\frac{\alpha+1}{\alpha}}(\Gamma)\right)$

(v) $\boldsymbol{H}$ *is the weak solution of (5.1).*

Proof:
(i) and (ii) of Theorem 5.1 claims that $\boldsymbol{h}_n$ is a Cauchy sequence in $L_2\left((0,T), \mathbf{L}_2(\Omega)\right)$. According to Lemma 5.4 we see that

$$\int_0^T \left\|\overline{\boldsymbol{h}}_n - \boldsymbol{h}_n\right\|^2 \leq \frac{C}{n^2} \int_0^T \|\partial_t \boldsymbol{h}_n\|^2 \leq \frac{C}{n^2} \to 0.$$

Thus $\boldsymbol{h}_n$ and $\overline{\boldsymbol{h}}_n$ have the same limit in $L_2\left((0,T),\mathbf{L}_2(\Omega)\right)$. Combined with Theorem 5.1 this implies that $\overline{\boldsymbol{h}}_n$ is a Cauchy sequence in $L_2\left((0,T),\mathbf{H}(\mathbf{curl}\,;\Omega)\right)\subset L_2\left((0,T),\mathbf{L}_2(\Omega)\right)$, from which we easily conclude the proof.

(iii) The assertion follows readily from Lemma 5.4 and

$$(\boldsymbol{h}_n(t),\boldsymbol{\varphi})-(\boldsymbol{H}_0,\boldsymbol{\varphi})=\int_0^t(\partial_t\boldsymbol{h}_n,\boldsymbol{\varphi})$$

passing to the limit for $n\to\infty$.

(iv) Using (i) and the continuous embedding $\gamma:\ \boldsymbol{\varphi}\mapsto\boldsymbol{\varphi}\times\boldsymbol{\nu}$ from $\mathbf{H}(\mathbf{curl}\,;\Omega)$ onto $\mathbf{H}^{-1/2}\left(\mathrm{div},\Gamma\right)$ (cf. Cessenat [19, p.35]) we have

$$\overline{\boldsymbol{h}}_n\times\boldsymbol{\nu}\to\boldsymbol{H}\times\boldsymbol{\nu}\qquad\text{in } L_2\left((0,T),\mathbf{H}^{-1/2}\left(\mathrm{div},\Gamma\right)\right). \tag{5.9}$$

From Lemma 5.4 we see that $\overline{\boldsymbol{h}}_n\times\boldsymbol{\nu}\in L_{\alpha+1}\left((0,T),\mathbf{L}_{\alpha+1}(\Gamma)\right)$, which is a reflexive Banach space. According to (5.9) we deduce that $\overline{\boldsymbol{h}}_n\times\boldsymbol{\nu}\rightharpoonup\boldsymbol{H}\times\boldsymbol{\nu}$ in $L_{\alpha+1}\left((0,T),\mathbf{L}_{\alpha+1}(\Gamma)\right)$. In particular, the trace of $\boldsymbol{H}(t)$ belongs to $\mathbf{L}_{\alpha+1}(\Gamma)$ a.e. in $(0,T)$, so $\boldsymbol{H}(t)$ belongs to $\boldsymbol{V}$ a.e. in $(0,T)$.

Now, we are going to use the Minty-Browder trick (cf. [36]), which exploits the monotone structure of a non-linear operator. Due to the monotonicity (see Lemma 5.1) we can write

$$\int_0^T\left(|\overline{\boldsymbol{h}}_n\times\boldsymbol{\nu}|^{\alpha-1}\overline{\boldsymbol{h}}_n\times\boldsymbol{\nu}-|\boldsymbol{u}\times\boldsymbol{\nu}|^{\alpha-1}\boldsymbol{u}\times\boldsymbol{\nu},\overline{\boldsymbol{h}}_n\times\boldsymbol{\nu}-\boldsymbol{u}\times\boldsymbol{\nu}\right)_\Gamma\geq 0, \tag{5.10}$$

which is valid for any vector field $\boldsymbol{u}$ with $\boldsymbol{u}\times\boldsymbol{\nu}\in L_{\alpha+1}\left((0,T),\mathbf{L}_{\alpha+1}(\Gamma)\right)$.

Now, we let $n\to\infty$ in (5.10). We have

$$\begin{aligned}&\int_0^T\left(|\boldsymbol{u}\times\boldsymbol{\nu}|^{\alpha-1}\boldsymbol{u}\times\boldsymbol{\nu},\overline{\boldsymbol{h}}_n\times\boldsymbol{\nu}-\boldsymbol{u}\times\boldsymbol{\nu}\right)_\Gamma\\ \to&\int_0^T\left(|\boldsymbol{u}\times\boldsymbol{\nu}|^{\alpha-1}\boldsymbol{u}\times\boldsymbol{\nu},\boldsymbol{H}\times\boldsymbol{\nu}-\boldsymbol{u}\times\boldsymbol{\nu}\right)_\Gamma.\end{aligned}$$

From Lemma 5.4 we see that $\boldsymbol{\nu}\times|\overline{\boldsymbol{h}}_n\times\boldsymbol{\nu}|^{\alpha-1}\overline{\boldsymbol{h}}_n\times\boldsymbol{\nu}\in L_{\frac{\alpha+1}{\alpha}}\left((0,T),\mathbf{L}_{\frac{\alpha+1}{\alpha}}(\Gamma)\right)$, which is a reflexive Banach space. Therefore, $\boldsymbol{\nu}\times|\overline{\boldsymbol{h}}_n\times\boldsymbol{\nu}|^{\alpha-1}\overline{\boldsymbol{h}}_n\times\boldsymbol{\nu}\rightharpoonup\boldsymbol{\nu}\times\boldsymbol{z}\times\boldsymbol{\nu}$ in $L_{\frac{\alpha+1}{\alpha}}\left((0,T),\mathbf{L}_{\frac{\alpha+1}{\alpha}}(\Gamma)\right)$. Thus

$$\int_0^T\left(|\overline{\boldsymbol{h}}_n\times\boldsymbol{\nu}|^{\alpha-1}\overline{\boldsymbol{h}}_n\times\boldsymbol{\nu},\boldsymbol{u}\times\boldsymbol{\nu}\right)_\Gamma\to\int_0^T\left(\boldsymbol{z}\times\boldsymbol{\nu},\boldsymbol{u}\times\boldsymbol{\nu}\right)_\Gamma.$$

Further, we obtain

$$\begin{aligned}
\lim_{n\to\infty}\int_0^T\int_\Gamma |\overline{\boldsymbol{h}}_n\times\boldsymbol{\nu}|^{\alpha+1} &= \lim_{n\to\infty}\int_0^T \left(|\overline{\boldsymbol{h}}_n\times\boldsymbol{\nu}|^{\alpha-1}\overline{\boldsymbol{h}}_n\times\boldsymbol{\nu},\overline{\boldsymbol{h}}_n\times\boldsymbol{\nu}\right)_\Gamma \\
&= \lim_{n\to\infty}\int_0^T -\left(\partial_t\boldsymbol{h}_n,\overline{\boldsymbol{h}}_n\right)-\left(\nabla\times\overline{\boldsymbol{h}}_n,\nabla\times\overline{\boldsymbol{h}}_n\right) \\
&= \int_0^T -\left(\partial_t\boldsymbol{H},\boldsymbol{H}\right)-\left(\nabla\times\boldsymbol{H},\nabla\times\boldsymbol{H}\right) \\
&= \lim_{n\to\infty}\int_0^T -\left(\partial_t\boldsymbol{h}_n,\boldsymbol{H}\right)-\left(\nabla\times\overline{\boldsymbol{h}}_n,\nabla\times\boldsymbol{H}\right) \\
&= \lim_{n\to\infty}\int_0^T \left(|\overline{\boldsymbol{h}}_n\times\boldsymbol{\nu}|^{\alpha-1}\overline{\boldsymbol{h}}_n\times\boldsymbol{\nu},\boldsymbol{H}\times\boldsymbol{\nu}\right)_\Gamma \\
&= \int_0^T \left(\boldsymbol{z}\times\boldsymbol{\nu},\boldsymbol{H}\times\boldsymbol{\nu}\right)_\Gamma .
\end{aligned} \tag{5.11}$$

Therefore, passing to the limit for $n\to\infty$ in (5.10) we obtain

$$\int_0^T \left(\boldsymbol{z}\times\boldsymbol{\nu}-|\boldsymbol{u}\times\boldsymbol{\nu}|^{\alpha-1}\boldsymbol{u}\times\boldsymbol{\nu},\boldsymbol{H}\times\boldsymbol{\nu}-\boldsymbol{u}\times\boldsymbol{\nu}\right)_\Gamma \geq 0.$$

Now, we set $\boldsymbol{u}=\boldsymbol{H}+\varepsilon\boldsymbol{w}$ for any $\boldsymbol{w}$ with $\boldsymbol{w}\times\boldsymbol{\nu}\in L_{\alpha+1}\left((0,T),\mathbf{L}_{\alpha+1}(\Gamma)\right)$ and any $\varepsilon>0$. We get

$$\int_0^T \left(\boldsymbol{z}\times\boldsymbol{\nu}-|\left(\boldsymbol{H}+\varepsilon\boldsymbol{w}\right)\times\boldsymbol{\nu}|^{\alpha-1}\left(\boldsymbol{H}+\varepsilon\boldsymbol{w}\right)\times\boldsymbol{\nu},\boldsymbol{w}\times\boldsymbol{\nu}\right)_\Gamma \leq 0.$$

Passing $\varepsilon\to 0$ we can write

$$\int_0^T \left(\boldsymbol{\nu}\times\boldsymbol{z}\times\boldsymbol{\nu}-\boldsymbol{\nu}\times|\boldsymbol{H}\times\boldsymbol{\nu}|^{\alpha-1}\boldsymbol{H}\times\boldsymbol{\nu},\boldsymbol{w}\right)_\Gamma \leq 0.$$

Now, replacing $\boldsymbol{w}$ by $-\boldsymbol{w}$, we deduce that also the reverse inequality holds and therefore

$$\int_0^T \left(\boldsymbol{\nu}\times\boldsymbol{z}\times\boldsymbol{\nu}-\boldsymbol{\nu}\times|\boldsymbol{H}\times\boldsymbol{\nu}|^{\alpha-1}\boldsymbol{H}\times\boldsymbol{\nu},\boldsymbol{w}\right)_\Gamma = 0,$$

which yields the desired result

$$\boldsymbol{\nu}\times\boldsymbol{z}\times\boldsymbol{\nu}=\boldsymbol{\nu}\times|\boldsymbol{H}\times\boldsymbol{\nu}|^{\alpha-1}\boldsymbol{H}\times\boldsymbol{\nu}$$

in the dual space of admissible test fields.

Hence, the relation (5.11) implies

$$\lim_{n\to\infty}\int_0^T\int_\Gamma |\overline{\boldsymbol{h}}_n\times\boldsymbol{\nu}|^{\alpha+1}=\int_0^T\int_\Gamma |\boldsymbol{H}\times\boldsymbol{\nu}|^{\alpha+1}.$$

This, together with the fact that

$$\boldsymbol{\nu}\times|\overline{\boldsymbol{h}}_n\times\boldsymbol{\nu}|^{\alpha-1}\overline{\boldsymbol{h}}_n\times\boldsymbol{\nu}\rightharpoonup\boldsymbol{\nu}\times\boldsymbol{z}\times\boldsymbol{\nu}=\boldsymbol{\nu}\times|\boldsymbol{H}\times\boldsymbol{\nu}|^{\alpha-1}\boldsymbol{H}\times\boldsymbol{\nu}$$

in $L_{\frac{\alpha+1}{\alpha}}\Big((0,T),\mathbf{L}_{\frac{\alpha+1}{\alpha}}(\Gamma)\Big)$ implies the strong convergence in this space.

(v) We start from (5.6). Integrating this identity over $(0,t)$ for any $t\in(0,T)$ yields

$$\int_0^t(\partial_t\boldsymbol{h}_n,\boldsymbol{\varphi})+\int_0^t\big(\nabla\times\overline{\boldsymbol{h}}_n,\nabla\times\boldsymbol{\varphi}\big)+\int_0^t\Big(\big|\overline{\boldsymbol{h}}_n\times\boldsymbol{\nu}\big|^{\alpha-1}\overline{\boldsymbol{h}}_n\times\boldsymbol{\nu},\boldsymbol{\varphi}\times\boldsymbol{\nu}\Big)_\Gamma=0.$$

We pass to the limit for $n\to\infty$. For the first term we use (iii), for the second term (i) and finally for the third term we apply (iv). We arrive at

$$\int_0^t(\partial_t\boldsymbol{H},\boldsymbol{\varphi})+\int_0^t(\nabla\times\boldsymbol{H},\nabla\times\boldsymbol{\varphi})+\int_0^t\Big(|\boldsymbol{H}\times\boldsymbol{\nu}|^{\alpha-1}\boldsymbol{H}\times\boldsymbol{\nu},\boldsymbol{\varphi}\times\boldsymbol{\nu}\Big)_\Gamma=0.$$

Finally, differentiating the resulting identity with respect to the time variable t, concludes the proof. □

5.4 Error estimates

Let us note that Theorem 5.1 immediately implies the error estimates for the time discretization method.

Theorem 5.3 (error estimates) *Let $\boldsymbol{H}_0\in\boldsymbol{V}$. Then there exists a positive constant C such that*

$$\max_{t\in[0,T]}\|\boldsymbol{h}_n(t)-\boldsymbol{H}(t)\|^2+\int_0^T\big\|\nabla\times[\overline{\boldsymbol{h}}_n-\boldsymbol{H}]\big\|^2$$
$$+\int_0^T\int_\Gamma\Big[|\overline{\boldsymbol{h}}_n\times\boldsymbol{\nu}|^{\frac{\alpha+1}{2}}-|\boldsymbol{H}\times\boldsymbol{\nu}|^{\frac{\alpha+1}{2}}\Big]^2\le C\tau.$$

Proof: The proof follows exactly the same line as in Theorem 5.1, therefore we omit it. Formally it can be obtained from Theorem 5.1 by letting $m\to\infty$. □

5.5 Numerical experiments

The efficiency of the backward Euler method (5.2) is demonstrated on several numerical examples. To find the exact solution that solve original problem (5.1) is not completely trivial. Therefore we choose exact solution and accordingly we adapt the right-hand side and the boundary condition of the original problem. The problem becomes more complicated, but on the other hand we are able to evaluate the exact error of the method.

The test problem reads as follows:

$$\begin{aligned} \partial_t \boldsymbol{H} + \nabla \times \nabla \times \boldsymbol{H} &= \boldsymbol{F} && \text{in } \Omega\,, \\ \boldsymbol{\nu} \times \nabla \times \boldsymbol{H} &= \boldsymbol{\nu} \times (|\boldsymbol{H} \times \boldsymbol{\nu}|^{\alpha-1} \boldsymbol{H} \times \boldsymbol{\nu}) + \boldsymbol{J} && \text{on } \Gamma. \end{aligned} \tag{5.12}$$

Applying the backward Euler method yields

$$\begin{aligned} \frac{1}{\tau}\left(\boldsymbol{H}_i, \boldsymbol{\varphi}\right) + \left(\nabla \times \boldsymbol{H}_i, \nabla \times \boldsymbol{\varphi}\right) + \left(|\boldsymbol{H}_i \times \boldsymbol{\nu}|^{\alpha-1} \boldsymbol{H}_i \times \boldsymbol{\nu}, \boldsymbol{\varphi} \times \boldsymbol{\nu}\right)_\Gamma + \left(\boldsymbol{J}, \boldsymbol{\varphi}\right)_\Gamma \\ = \left(\boldsymbol{F}, \boldsymbol{\varphi}\right) + \frac{1}{\tau}\left(\boldsymbol{H}_{i-1}, \boldsymbol{\varphi}\right). \end{aligned}$$

Even though the problem is discretized in time, it still retains its nonlinear character. Therefore we apply the Newton method, see Appendix, as a standard tool for solving nonlinear PDEs.

First, an auxiliary functional $F(\boldsymbol{v})$ for $\boldsymbol{v} \in \boldsymbol{V}$ with its Fréchet derivative has to be defined. We can write

$$\begin{aligned} (F(\boldsymbol{v}), \boldsymbol{\varphi}) &= \frac{1}{\tau}\left(\boldsymbol{v}, \boldsymbol{\varphi}\right) + \left(\nabla \times \boldsymbol{v}, \nabla \times \boldsymbol{\varphi}\right) + \left(|\boldsymbol{v} \times \boldsymbol{\nu}|^{\alpha-1} \boldsymbol{v} \times \boldsymbol{\nu}, \boldsymbol{\varphi} \times \boldsymbol{\nu}\right)_\Gamma \\ &\quad + \left(\boldsymbol{J}, \boldsymbol{\varphi}\right)_\Gamma - \left(\boldsymbol{F}, \boldsymbol{\varphi}\right) - \frac{1}{\tau}\left(\boldsymbol{H}_{i-1}, \boldsymbol{\varphi}\right), \\ (DF(\boldsymbol{v})\boldsymbol{\varphi}_i, \boldsymbol{\varphi}_j) &= \frac{1}{\tau}(\boldsymbol{\varphi}_i, \boldsymbol{\varphi}_j) + (\nabla \times \boldsymbol{\varphi}_i, \nabla \times \boldsymbol{\varphi}_j) \\ &\quad + |\boldsymbol{v} \times \boldsymbol{\nu}|^{\alpha-1} \left[\frac{(\alpha-1) < \boldsymbol{v} \times \boldsymbol{\nu}, \boldsymbol{\varphi}_i \times \boldsymbol{\nu} >< \boldsymbol{v} \times \boldsymbol{\nu}, \boldsymbol{\varphi}_j \times \boldsymbol{\nu} >}{|\boldsymbol{v} \times \boldsymbol{\nu}|^2}\right]_\Gamma \\ &\quad + |\boldsymbol{v} \times \boldsymbol{\nu}|^{\alpha-1} \left[< \boldsymbol{\varphi}_i \times \boldsymbol{\nu}, \boldsymbol{\varphi}_j \times \boldsymbol{\nu} >\right]_\Gamma, \end{aligned}$$

where $\boldsymbol{\varphi}_i, \boldsymbol{\varphi}_j \in \boldsymbol{V}$.

On each time level Newton's method solves:

$$F(\boldsymbol{H}_i) = 0\,.$$

Starting with an initial guess $\boldsymbol{H}_0 = \boldsymbol{0}$ one computes

$$DF(\boldsymbol{H}_{i_m})\boldsymbol{d}_m = F(\boldsymbol{H}_{i_m}) \qquad \text{for } m > 0$$

and sets

$$\boldsymbol{H}_{i_{m+1}} = \boldsymbol{H}_{i_m} - \boldsymbol{d}_m$$

until $\|\boldsymbol{d}_m\| < 1.0 \cdot 10^{-6}$.

The parameter of nonlinearity α is chosen following the theory, i.e. $\alpha \in (0, 1]$. The closer to zero this parameter is, the more nonlinear the nature of the problem is and hence more difficult to solve. For $\alpha = 1$ the problem acquires linear character and our scheme is "flawless".[1]

The efficiency of the combination of Newton's and backward Euler's method is studied on the basis of the absolute error from Theorem 5.3:

$$\begin{aligned} \max_{t\in[0,T]} \|\boldsymbol{h}_n(t) - \boldsymbol{H}(t)\|^2 + \int_0^T \left\|\nabla \times [\overline{\boldsymbol{h}}_n - \boldsymbol{H}]\right\|^2 \\ + \int_0^T \int_\Gamma \left[|\overline{\boldsymbol{h}}_n \times \boldsymbol{\nu}|^{\frac{\alpha+1}{2}} - |\boldsymbol{H} \times \boldsymbol{\nu}|^{\frac{\alpha+1}{2}}\right]^2 . \end{aligned} \tag{5.13}$$

5.5.1 Exact solution linear in space and quadratic in time

First, we consider the problem (5.12), where the vector fields $\boldsymbol{F}$ and $\boldsymbol{J}$ are given in such a way that the exact solution $\boldsymbol{H}(\boldsymbol{x}, t)$ fulfills

$$\mathbf{H}(\boldsymbol{x}, t) = \begin{pmatrix} 5x_2 - 8x_1 + t^2 \\ 8x_0 - 10x_2 + 2t^2 + 1 \\ 10x_1 - 5x_0 + 3t^2 \end{pmatrix}. \tag{5.14}$$

Theorem 5.3 states the linear dependency of the absolute error of the numerical scheme on the choice of discretization parameter τ. In our experiments two parameters of nonlinearity, namely $\alpha = 0.1$ and $\alpha = 0.7$, were chosen. The accuracy of the numerical scheme was tested for six different lengths of the time step τ. As one can see in Figure 5.2, the absolute error decreases linearly with the decreasing value of the parameter τ.

We have also studied the sensibility of our problem to the size of the mesh. As Tables 5.1 and 5.2 show, the accuracy of the calculated solutions does not depend on the mesh refinement. This is due to the fact that the exact solution to our test problem is linear in space and as such exactly fits by Whitney's elements even on a coarse grid. As a consequence the absolute error is not decreasing; on the contrary, a slight increase is observed because of accumulation of calculation

[1] The computational error between our approximation and the exact solution gains values in $*.10^{-31}$. Such a number is considered a machine zero.

error. In the case of big nonlinearity, $\alpha = 0.1$, the length of the time step $\tau = 0.1$ is not adequate to the choice of the discretization parameter h. In other words, the combination of a too big time step with a too fine mesh causes divergence of the numerical scheme.

The influence of different values of $\alpha \in \{0.03, 0.1, 0.2, \ldots, 0.9, 1\}$ is plotted in Figure 5.3. Parameter α approaching zero renders the problem more nonlinear and the absolute error bigger.

We can conclude that the performed experiments converge in line with our expectations.

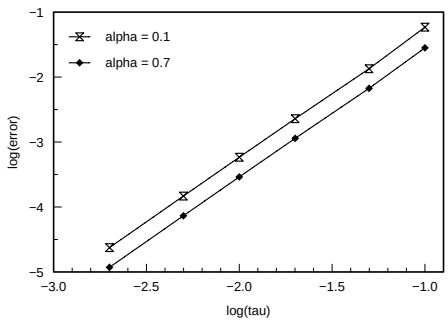

Figure 5.2: The linear dependence of the absolute error (5.13) of the numerical scheme (5.2) on the choice of the time step τ and the nonlinearity parameter α. The smaller τ, the more accurate the approximation is. Smaller α yields bigger absolute error. Exact solution (5.14) and mesh of 604 DOFs are considered.

τ	0.1	0.05	0.02	0.01	0.005	0.002
1 ref.	2.734e-02	6.519e-03	1.106e-03	2.820e-04	7.12e-05	1.15e-05
2 ref.	2.818e-02	6.708e-03	1.139e-03	2.903e-04	7.33e-05	1.18e-05
3 ref.	2.866e-02	6.827e-03	1.159e-03	2.954e-04	7.46e-05	1.20e-05
4 ref.	2.908e-02	6.925e-03	1.176e-03	2.997e-04	7.57e-05	1.22e-05

Table 5.1: The dependence of the absolute error (5.13) of the numerical scheme (5.2) on the choice of the time step τ and refinement of the mesh. The error decreases with the decreasing time step. The refinement of the mesh has no effect on the accuracy. Exact solution (5.14) and parameter of nonlinearity $\alpha = 0.7$ are considered.

τ	0.1	0.05	0.02	0.01	0.005	0.002
1 ref.	5.690e-02	1.312e-02	2.233e-03	5.697e-04	1.43e-04	2.31e-05
2 ref.	5.861e-02	1.343e-02	2.287e-03	5.835e-04	1.47e-04	2.37e-05
3 ref.	DIV	1.369e-02	2.327e-03	5.939e-04	1.49e-04	2.41e-05
4 ref.	DIV	1.389e-02	2.364e-03	6.033e-04	1.52e-04	2.45e-05

Table 5.2: The dependence of the absolute error (5.13) of the numerical scheme (5.2) on the choice of the time step τ and refinement of the mesh. The error decreases with decreasing time step. The refinement of the mesh has no effect on accuracy. For some inconvenient combination of discretization parameters the method diverges. Exact solution (5.14) and parameter of nonlinearity $\alpha = 0.1$ are considered.

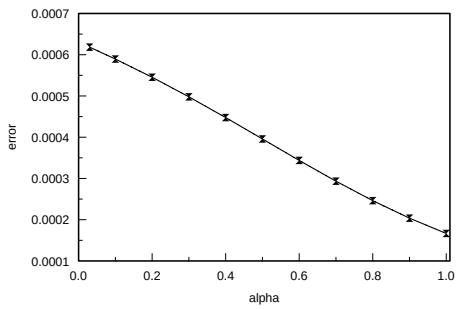

Figure 5.3: The absolute error (5.13) of the approximation scheme (5.2) increases with α approaching zero. The exact solution (5.14), the time step $\tau = 0.01$ and the mesh of 604 DOFs are considered.

5.5.2 Exact solution nonlinear in space

Now, we consider the problem (5.12), where the vector fields $\boldsymbol{F}$ and $\boldsymbol{J}$ are given in such a way that the exact solution $\boldsymbol{H}(\boldsymbol{x}, t)$ fulfills

$$\mathbf{H}(\boldsymbol{x}, t) = \begin{pmatrix} 5\sin(x_2) - 8\sin(x_1) + t^4 \\ 8\sin(x_0) - 10\sin(x_2) + 2t^4 + 1 \\ 10\sin(x_1) - 5\sin(x_0) + 3t^4 + 2 \end{pmatrix}. \tag{5.15}$$

The convergence of the method with diminishing τ agrees with our theoretical results. The accuracy of the numerical scheme is tested for six different lengths of the time step τ. As one can see in Table 5.3, the absolute error decreases with decreasing values of parameter τ.

Here, the impact of the mesh refinement on the accuracy of the numerical scheme is obvious as well, because the periodic solution (5.15) cannot be fitted with Whitney's elements precisely. The efficiency of the method is studied for the mesh refined 1,2,3,4 and 5 times. The finer the mesh we work on, the more precise the approximation we get.

With diminishing τ and with the mesh fine enough we are able to improve the absolute error of our approximation from 0.725 to 0.002. The only problem is that the computations on the mesh with 238688 DOFs (five times refined basic mesh) are very time demanding, see Table 5.4.

τ	0.1	0.05	0.02	0.01	0.005	0.002
1 ref.	7.251e-01	5.633e-01	5.721e-01	5.832e-01	5.890e-01	5.926e-01
2 ref.	3.424e-01	1.696e-01	1.476e-01	1.454e-01	1.461e-01	1.469e-01
3 ref.	2.488e-01	7.206e-02	4.260e-02	3.794e-02	3.690e-02	3.673e-02
4 ref.	2.257e-01	4.769e-02	1.631e-02	1.101e-02	9.645e-03	9.284e-03
5 ref.	2.199e-01	4.159e-02	9.709e-03	3.977e-03	2.622e-03	2.388e-03

Table 5.3: The dependence of the absolute error (5.13) of the numerical scheme (5.2) on the choice of the time step τ and refinement of the mesh. Exact solution (5.15) and parameter of nonlinearity $\alpha = 0.7$ are considered.

τ	0.1	0.05	0.02	0.01	0.005	0.002
1 ref.	00:00:23	00:00:35	00:01:24	00:04:22	00:06:25	00:10:09
2 ref.	00:01:26	00:02:18	00:05:31	00:10:43	00:20:31	00:46:22
3 ref.	00:05:54	00:09:21	00:23:00	00:45:21	01:25:57	03:22:24
4 ref.	00:27:51	00:45:20	01:40:58	03:14:54	06:30:47	14:26:45
5 ref.	03:03:56	04:24:50	08:37:33	18:09:40	39:46:55	70:00:19

Table 5.4: Computational time of the simulations from Table 5.3 (hh:mm:ss).

5.6 Conclusions

We have studied the initial boundary value problem (5.1) describing the evolution of electromagnetic fields in a bounded domain, in case of a non–perfect contact of two different materials is considered on the boundary. The nonlinear time–discrete approximation scheme (5.2) based on the backward Euler method has been proposed. Convergence of the approximate solution towards the exact one has been proved and the results have also been confirmed by numerical experiments.

For solving the nonlinear steady–state PDE the Newton method was used. In numerical analysis, it is the best known method for finding the roots of a real-valued function. The advantage of the Newton method is, that if the iteration process begins sufficiently close to the desired root, the convergence is remarkably quick. Unfortunately, when iteration begins far from the solution, the method can easily lead to incorrect results. The meaning of "sufficiently close" and "remarkably quick" depends on the problem. Thus, good implementation of the method together with "well-behaved" problem overcome possible convergence failures. Furthermore, depending on the complexity of the problem, an appropriate ratio between the discretization parameters has to be chosen, otherwise the method can diverge, as we could see on an example with too fine mesh and too big time step (Table 5.2). Additionally, by setting up all parameters adequately we can avoid an excessive consumption of computational time, Table 5.4.

In [80] the authors consider a similar degenerate problem where the nonlinearity is not assumed on the boundary but inside the domain. Such a problem setting describes the processes of magnetization of type-II superconductors. The rate of the convergence numerically obtained by Slodička and Buša in [80] is slower than ours. This conclusion is not surprising, as the nonlinearity in the whole domain may cause more inaccuracy than the nonlinearity acting only on the boundary.

The numerical experiments were presented on some academic examples. Without loss of generality, we formulated the problems as simply as possible with the electromagnetic parameters σ and μ equal to 1. These examples serve as a good starting point, but it would of course be interesting to test the derived scheme on problems with real data and monitor the convergence rate in this case.

Chapter 6

Full discretization

By applying discretization in time to the time–dependent nonlinear problem (4.6), this changes into the recurrent steady–state scheme of the form

$$\begin{aligned} (\delta \boldsymbol{h}_i, \boldsymbol{\varphi}) + (\nabla \times \boldsymbol{h}_i, \nabla \times \boldsymbol{\varphi}) + (\boldsymbol{G}(\boldsymbol{h}_i \times \boldsymbol{\nu}), \boldsymbol{\varphi} \times \boldsymbol{\nu})_\Gamma &= 0, \\ \boldsymbol{h}_0 &= \boldsymbol{H}_0 \end{aligned} \tag{6.1}$$

for any $\boldsymbol{\varphi} \in \boldsymbol{V}$.

The problem is that the scheme (6.1) is still nonlinear. Thus, we first linearize the scheme. Afterwards, discretization in space is performed.

The main goal of this chapter is to use the results from the previous chapter to design a linear time- and space-discrete numerical method for the approximation of the exact solution to the nonlinear boundary value problem (4.6).

From now on the constitutive law (4.4) is considered, so we refer to this case as to the non-degenerate Lipschitz continuous case.

The chapter is organized as follows. First, we discuss the additional properties of the nonlinear vector function $\boldsymbol{G}$ in case it is Lipschitz continuous. Thanks to the new character of the nonlinearity, the error estimates of the time-discretized scheme can be improved in comparison with the results for the non-Lipschitz case derived in Chapter 5. As a next step we linearize our problem using the well-known fixed-point principle. Finally, discretization in space is performed. Here, Whitney's edge elements are employed. The fully-discretized linear scheme is proposed in Section 6.3. We derive error estimates depending on the choice of the discretization parameters, on basis of which the convergence is shown. The numerical experiments confirming the efficiency of the developed scheme can be found in the last section.

The results of this chapter were presented at the international conference ICNAAM 2008 and are summarized in the proceedings of this conference [97]. The whole article [98] was submitted to the Journal of Mathematical Analysis and Applications.

6.1 Time discretization

The backward Euler method is a standard tool for discretization in time, see Section 5.1. The suggested non-linear recurrent approximation scheme (6.1) is valid for $i = 1, \dots, n$ and $\boldsymbol{\varphi} \in \boldsymbol{V}$.

We consider the following space of test functions

$$\boldsymbol{V} = \{\boldsymbol{\varphi} \in \mathbf{H}(\mathbf{curl}\,;\Omega);\ \boldsymbol{\varphi} \times \boldsymbol{\nu} \in \mathbf{L}_2\,(\Gamma)\}$$

throughout this chapter. The space $\boldsymbol{V}$ is a reflexive Banach space endowed with the sum-norm $\|\boldsymbol{\varphi}\|_{\boldsymbol{V}} = \|\boldsymbol{\varphi}\|_{\mathbf{H}(\mathbf{curl}\,;\Omega)} + \|\boldsymbol{\varphi} \times \boldsymbol{\nu}\|_{\mathbf{L}_2(\Gamma)}$.

In the previous chapter we have proved the well–posedness of the problem for the general case, namely we considered a non-Lipschitz continuous nonlinear vector function $\boldsymbol{G}$ defined by (4.3). Note, that the proof of the existence and uniqueness of $\boldsymbol{h}_i$ for each time step $i = 1, \dots n$ (Lemma 5.1) is also valid for a less general case, thus, it can be omitted.

As in Chapter 5, we define the nonlinearity $\boldsymbol{G}(\boldsymbol{x}) = g(|\boldsymbol{x}|)\boldsymbol{x}$ where the auxiliary function g is given by

$$g(s) = \begin{cases} a^{\alpha-1} & 0 \le s < a, \\ s^{\alpha-1} & a \le s \le b, \\ b^{\alpha-1} & b < s \end{cases}$$

for some fixed positive constants $0 < a < b$.

As our problem is now Lipschitz continuous, the error estimates can be improved. To obtain new results we use the following properties of the nonlinear vector field $\boldsymbol{G}$:

Lemma 6.1 *For all $\boldsymbol{s}, \boldsymbol{t} \in \mathbb{R}^3$ there holds*

$$(\boldsymbol{G}(\boldsymbol{s} \times \boldsymbol{\nu}) - \boldsymbol{G}(\boldsymbol{t} \times \boldsymbol{\nu}), (\boldsymbol{s} - \boldsymbol{t}) \times \boldsymbol{\nu}) \ge \alpha b^{\alpha-1} |(\boldsymbol{s} - \boldsymbol{t}) \times \boldsymbol{\nu}|^2$$

and

$$|\boldsymbol{G}(\boldsymbol{s} \times \boldsymbol{\nu}) - \boldsymbol{G}(\boldsymbol{t} \times \boldsymbol{\nu})| \le a^{\alpha-1} |(\boldsymbol{s} - \boldsymbol{t}) \times \boldsymbol{\nu}| \qquad \textit{(Lipschitz continuity)}.$$

Proof: The lemma is easy to prove by writing out the Gâteaux differential of $\boldsymbol{G}(\boldsymbol{x})$ in the direction $\boldsymbol{h}$:

$$D\boldsymbol{G}(\boldsymbol{x},\boldsymbol{h}) = \begin{cases} a^{\alpha-1}\boldsymbol{h} & 0 \le |\boldsymbol{x}| < a, \\ (\alpha-1)|\boldsymbol{x}|^{\alpha-3}(\boldsymbol{x}\cdot\boldsymbol{h})\boldsymbol{x} + |\boldsymbol{x}|^{\alpha-1}\boldsymbol{h} & a \le |\boldsymbol{x}| \le b, \\ b^{\alpha-1}\boldsymbol{h} & b < |\boldsymbol{x}|. \end{cases}$$

Consequently,

$$(D\boldsymbol{G}(\boldsymbol{x},\boldsymbol{h}),\boldsymbol{h}) \ge \begin{cases} a^{\alpha-1}|\boldsymbol{h}|^2 & 0 \le |\boldsymbol{x}| < a, \\ \alpha|\boldsymbol{x}|^{\alpha-1}|\boldsymbol{h}|^2 & a \le |\boldsymbol{x}| \le b, \\ b^{\alpha-1}|\boldsymbol{h}|^2 & b < |\boldsymbol{x}|. \end{cases}$$

Thus, we obtain

$$(\boldsymbol{G}(\boldsymbol{x}+\boldsymbol{h}) - \boldsymbol{G}(\boldsymbol{x}),\boldsymbol{h}) = (D\boldsymbol{G}(\boldsymbol{x}+\theta\boldsymbol{h},\boldsymbol{h}),\boldsymbol{h}) \ge C|\boldsymbol{h}|^2 \quad \text{for } \theta \in (0,1)$$

with constant $C = \alpha b^{\alpha-1}$, where $\alpha \in (0,1]$.
The Lipschitz continuity follows from the fact that

$$|[g(|x|)x]'| \le a^{\alpha-1} \quad \text{for } \forall x \in \mathbb{R},\ \alpha \in (0,1]\,.$$

□

6.1.1 A priori estimates

Next, we derive suitable a priori estimates for $\boldsymbol{h}_i$ on each time level $i = 1,\dots,n$. We start with the following compatibility condition needed for Lemma 6.2.

$$(\partial_t\boldsymbol{H}(0),\boldsymbol{\varphi}) + (\nabla\times\boldsymbol{H}(0),\nabla\times\boldsymbol{\varphi}) + (\boldsymbol{G}(\boldsymbol{H}(0)\times\boldsymbol{\nu}),\boldsymbol{\varphi}\times\boldsymbol{\nu})_\Gamma = 0 \tag{6.2}$$

for any $\boldsymbol{\varphi} \in \boldsymbol{V}$. This condition expresses compatibility between the boundary data and the initial condition where $\boldsymbol{H}_0 \in \boldsymbol{V}$ and says that the variational equation (4.6) is satisfied at the time $t = 0$. Next, we define

$$\delta\boldsymbol{h}_0 := \partial_t\boldsymbol{H}_0 := -\nabla\times\nabla\times\boldsymbol{H}_0\,.$$

As far as the compatibility is defined, the following stability result can be obtained.

Lemma 6.2 *Let the vector field $\boldsymbol{G}$ satisfy Lemma 6.1. Moreover assume $\boldsymbol{H}_0 \in \boldsymbol{V}$ satisfies (6.2). Then there exists a positive constant C such that*

$$\|\delta \boldsymbol{h}_j\|^2 + \sum_{i=1}^{j} \|\delta \boldsymbol{h}_i - \delta \boldsymbol{h}_{i-1}\|^2 + \sum_{i=1}^{j} \tau \|\nabla \times \delta \boldsymbol{h}_i\|^2 + \sum_{i=1}^{j} \tau \|\delta \boldsymbol{h}_i \times \boldsymbol{\nu}\|_\Gamma^2 \leq C$$

holds for any $j = 1, \ldots, n$.

Proof: We subtract (6.1) for $i = i - 1$ from (6.1), then we set $\boldsymbol{\varphi} = \delta \boldsymbol{h}_i$ and finally sum up the result for $i = 1, \ldots, j$. This yields

$$\begin{aligned} &\sum_{i=1}^{j} (\delta \boldsymbol{h}_i - \delta \boldsymbol{h}_{i-1}, \delta \boldsymbol{h}_i) + \sum_{i=1}^{j} (\nabla \times (\boldsymbol{h}_i - \boldsymbol{h}_{i-1}), \nabla \times \delta \boldsymbol{h}_i) \\ &\quad + \sum_{i=1}^{j} (\boldsymbol{G}(\boldsymbol{h}_i \times \boldsymbol{\nu}) - \boldsymbol{G}(\boldsymbol{h}_{i-1} \times \boldsymbol{\nu}), \delta \boldsymbol{h}_i \times \boldsymbol{\nu})_\Gamma = 0 . \end{aligned}$$

For $i = 0$ we use the compatibility condition. Further we employ the properties of $\boldsymbol{G}$ (Lemma 6.1) together with Abel's summation applied to the first term to get the desired result. □

6.1.2 Error estimate

First, we introduce the continuous piecewise linear in time vector field $\boldsymbol{h}_n$ given by

$$\begin{aligned} \boldsymbol{h}_n(0) &= \boldsymbol{H}_0, \\ \boldsymbol{h}_n(t) &= \boldsymbol{h}_{i-1} + (t - t_{i-1}) \delta \boldsymbol{h}_i \qquad \text{for } t \in (t_{i-1}, t_i] \end{aligned}$$

and define the step in time vector field $\overline{\boldsymbol{h}}_n$

$$\begin{aligned} \overline{\boldsymbol{h}}_n(0) &= \boldsymbol{H}_0, \\ \overline{\boldsymbol{h}}_n(t) &= \boldsymbol{h}_i \qquad \text{for } t \in (t_{i-1}, t_i] . \end{aligned}$$

Using the new notation we rewrite (6.1) as (for any $\boldsymbol{\varphi} \in \boldsymbol{V}$)

$$(\partial_t \boldsymbol{h}_n, \boldsymbol{\varphi}) + \big(\nabla \times \overline{\boldsymbol{h}}_n, \nabla \times \boldsymbol{\varphi}\big) + \big(\boldsymbol{G}(\overline{\boldsymbol{h}}_n \times \boldsymbol{\nu}), \boldsymbol{\varphi} \times \boldsymbol{\nu}\big)_\Gamma = 0 . \tag{6.3}$$

Now, we are in a position to derive that, if the vector field $\boldsymbol{G}$ satisfies Lemma 6.1, then the error of the approximation scheme (6.1) is quadratically dependent on the choice of discretization parameter τ.

Theorem 6.1 *Let the assumptions of Lemma 6.2 be fulfilled. Then there exists a positive constant C such that*

$$\max_{t\in[0,T]} \|\boldsymbol{h}_n(t) - \boldsymbol{H}(t)\|^2 + \int_0^T \left\|\nabla \times (\overline{\boldsymbol{h}}_n - \boldsymbol{H})\right\|^2 + \int_0^T \left\|(\overline{\boldsymbol{h}}_n - \boldsymbol{H}) \times \boldsymbol{\nu}\right\|_\Gamma^2 \le C\tau^2.$$

Proof: Subtracting (4.6) from (6.3) and sequentially setting $\boldsymbol{\varphi} = \boldsymbol{h}_n - \boldsymbol{H}$ one gets

$$\begin{aligned}(\partial_t(\boldsymbol{h}_n - \boldsymbol{H}), \boldsymbol{h}_n - \boldsymbol{H}) + \big(\nabla \times (\overline{\boldsymbol{h}}_n - \boldsymbol{H}), \nabla \times (\boldsymbol{h}_n - \boldsymbol{H})\big)\\ + \big(\boldsymbol{G}(\overline{\boldsymbol{h}}_n \times \boldsymbol{\nu}) - \boldsymbol{G}(\boldsymbol{H} \times \boldsymbol{\nu}), (\boldsymbol{h}_n - \boldsymbol{H}) \times \boldsymbol{\nu}\big)_\Gamma = 0\,.\end{aligned}$$

After integration in time we arrive at

$$\begin{aligned}\frac{1}{2}\|\boldsymbol{h}_n(t) - \boldsymbol{H}(t)\|^2 + \int_0^t \left\|\nabla \times (\overline{\boldsymbol{h}}_n - \boldsymbol{H})\right\|^2\\ + \int_0^t \big(\boldsymbol{G}(\overline{\boldsymbol{h}}_n \times \boldsymbol{\nu}) - \boldsymbol{G}(\boldsymbol{H} \times \boldsymbol{\nu}), (\overline{\boldsymbol{h}}_n - \boldsymbol{H}) \times \boldsymbol{\nu}\big)_\Gamma\\ = \int_0^t \big(\nabla \times (\overline{\boldsymbol{h}}_n - \boldsymbol{H}), \nabla \times (\overline{\boldsymbol{h}}_n - \boldsymbol{h}_n)\big)\\ + \int_0^t \big(\boldsymbol{G}(\overline{\boldsymbol{h}}_n \times \boldsymbol{\nu}) - \boldsymbol{G}(\boldsymbol{H} \times \boldsymbol{\nu}), (\overline{\boldsymbol{h}}_n - \boldsymbol{h}_n) \times \boldsymbol{\nu}\big)_\Gamma\,.\end{aligned}$$

Applying Lemma 6.1 and Young's inequality to the right–hand side one obtains

$$\begin{aligned}\frac{1}{2}\|\boldsymbol{h}_n(t) - \boldsymbol{H}(t)\|^2 + \int_0^t \left\|\nabla \times (\overline{\boldsymbol{h}}_n - \boldsymbol{H})\right\|^2 + \alpha b^{\alpha-1}\int_0^t \left\|(\overline{\boldsymbol{h}}_n - \boldsymbol{H}) \times \boldsymbol{\nu}\right\|_\Gamma^2\\ \le \varepsilon \int_0^t \left\|\nabla \times (\overline{\boldsymbol{h}}_n - \boldsymbol{H})\right\|^2 + C_\varepsilon \int_0^t \left\|\nabla \times (\overline{\boldsymbol{h}}_n - \boldsymbol{h}_n)\right\|^2\\ +\varepsilon \int_0^t \left\|\boldsymbol{G}(\overline{\boldsymbol{h}}_n \times \boldsymbol{\nu}) - \boldsymbol{G}(\boldsymbol{H} \times \boldsymbol{\nu})\right\|_\Gamma^2 + C_\varepsilon \int_0^t \left\|(\overline{\boldsymbol{h}}_n - \boldsymbol{h}_n) \times \boldsymbol{\nu}\right\|_\Gamma^2\,.\end{aligned}$$

Using Lemma 6.2 and invoking the Lipschitz continuity of $\boldsymbol{G}$ we obtain

$$\begin{aligned}\frac{1}{2}\|\boldsymbol{h}_n(t) - \boldsymbol{H}(t)\|^2 + (1-\varepsilon)\int_0^t \left\|\nabla \times (\overline{\boldsymbol{h}}_n - \boldsymbol{H})\right\|^2\\ +(\alpha b^{\alpha-1} - a^{2(\alpha-1)}\varepsilon)\int_0^t \left\|(\overline{\boldsymbol{h}}_n - \boldsymbol{H}) \times \boldsymbol{\nu}\right\|_\Gamma^2 \le C_\varepsilon \tau^2\,.\end{aligned}$$

The last inequality is valid for any $t > 0$. Therefore

$$\begin{aligned}\frac{1}{2}\max_{t\in[0,T]}\|\boldsymbol{h}_n(t) - \boldsymbol{H}(t)\|^2 + (1-\varepsilon)\int_0^t \left\|\nabla \times (\overline{\boldsymbol{h}}_n - \boldsymbol{H})\right\|^2\\ +(\alpha b^{\alpha-1} - a^{2(\alpha-1)}\varepsilon)\int_0^t \left\|(\overline{\boldsymbol{h}}_n - \boldsymbol{H}) \times \boldsymbol{\nu}\right\|_\Gamma^2 \le C_\varepsilon \tau^2\,.\end{aligned}$$

Choosing an appropriate ε we conclude the proof. $\square$

6.2 Space discretization

Whitney finite elements is our tool for discretization in space. Because they satisfy the continuity conditions between two elements, they are convenient for approximating the fields $\boldsymbol{E}$ and $\boldsymbol{B}$. The existence and uniqueness of the approximation is based on the Lax-Milgram lemma. The dependence of the approximation error on the choice of an approximation space results from Céa's lemma. Both statements can be found in the Appendix, Thm. 10.5 and Thm. 10.6.

6.2.1 Finite elements

The finite element method originates from the need for solving complex elasticity and structural analysis problems in civil and aeronautical engineering. Its development can be traced back to the work by Alexander Hrennikoff (1941) and Richard Courant (1942). Their different approaches share one essential characteristic: discretization of a continuous domain into a set of discrete subdomains, usually called elements. In the seventies, the French mathematician Ciarlet [21] introduced finite elements as a triple consisting of

i) a *geometric domain* T. In general we make a decomposition of the computational domain Ω into sub-domains T (triangles, rectangles), i.e. we can write $\Omega = \bigcup_{i=1}^{n} T_i$.

ii) a finite-dimensional *vector space of functions* on a single element T that are convenient to implement, e.g. polynomials P_T.

iii) a set of *degrees of freedom* Σ_T. If this set of linear functionals on P_T is chosen in such a way, that the value given for each degree of freedom uniquely determines a function in P_T, then the finite element is said to be unisolvent.

The last what is needed to be defined is operator $r(f) \in P_T$ interpolating sufficiently smooth function f defined on T to the finite dimensional space. An interpolation operator satisfies $\sigma(r(f) - f) = 0$ for all $\sigma \in \Sigma_T$.

More details on finite elements in general and their applications in electromagnetism can be found in [65].

6.2.2 Edge Whitney's elements

For our purposes we use Whitney's finite elements as introduced by Whitney [96] in 1957. Different types of Whitney's elements are known, e.g. nodal, edge, facial, ... The most suitable for the approximation of the magnetic intensity field $\boldsymbol{H}$ are Whitney's edge elements. Indeed, this particular approximating element is continuous in the tangential part when moving through neighboring elements, which coincides with the continuity property of the field $\boldsymbol{H}$. In the literature, this property is known as $\mathbf{H}(\mathbf{curl}\,;\Omega)$-conformity and a proof can be found in [42] or [65].

To characterize edge Whitney's elements precisely, the definition of the triple (T, P_T, Σ_T) from the previous section has to be given.

We assume our computational domain to be polyhedral and divided into tetrahedra. Thereby we get the tetrahedral mesh $\mathcal{M}$ with a tetrahedron as a basic element T. The set of all tetrahedra is denoted by $\mathcal{T}$. Each element consists of 4 vertices, 6 edges and 4 faces. Speaking of a *conforming* mesh, the tetrahedra can intersect either along a common face, an edge, in the node or they do not intersect at all. The mesh $\mathcal{M}$ is said to be *regular* if there exist constants $C, h > 0$ such that

$$h_T/\rho_T \leq C \quad \forall T \in \mathcal{T}. \tag{6.4}$$

Here, h_T is the diameter of the smallest sphere containing $\overline{T}$, ρ_T is the diameter of the largest sphere contained in $\overline{T}$ and

$$h = \max_{T \in \mathcal{T}} \{h_T\}.$$

From now on we use for the mesh the symbol $\mathcal{M}_h$ to emphasize the connection with the specific discretization parameter h. Our aim is to show that the finer the mesh we construct ($h \to 0$), the more exact the approximation is.

The space of functions P_T is generated by polynomials of degree one. We define it as follows

$$P_T := \{\mathbf{p}(\mathbf{x}) = \mathbf{a} \times \mathbf{x} + \mathbf{c} \,|\, \mathbf{a}, \mathbf{c} \in \mathbb{R}^3, \mathbf{x} \in T\}. \tag{6.5}$$

Let e_i, $i = 1, \ldots, 6$ be the edges of the tetrahedron T and let $\mathbf{u}$ be a function belonging to $\boldsymbol{W}^{1,s}(T)$ for some $s > 2$. Then the set of degrees of freedom reads

$$\Sigma_T := \{M_{e_i}, i = 1, \ldots, 6\}, \tag{6.6}$$

where

$$M_{e_i}(\mathbf{u}) := \int_{e_i} \mathbf{u} \cdot \boldsymbol{\tau}_{e_i} \, \mathrm{d}s. \tag{6.7}$$

The vector $\boldsymbol{\tau}_{e_i}$ represents the unit directional vector of the edge e_i.

To finish the definition of edge elements, the *basis functions* have to be specified. Let $e = \{0, 1\}$ be one edge of the tetrahedron $T = \{0, 1, 2, 3\}$. Then the basis function $\mathbf{w}_e$ associated with the edge e is defined by the relation

$$\mathbf{w}_e = w_0 \nabla w_1 - w_1 \nabla w_0. \tag{6.8}$$

By w_i we denote the linear function taking value 1 in the vertex i and value 0 in all other vertices of the tetrahedron, i.e. $w_i(j) = \delta_{i,j}$[1] for $i, j = 0, \ldots, 3$ and $w_i + w_j = 1$ on the edge $\{i, j\}$. The vector ∇w_i denotes the gradient of the function w_i.

We proceed with the computation of the circulation of $\mathbf{w}_e$ along the edge e. We work with one single tetrahedron $T = \{0, 1, 2, 3\}$. Let A be the orthogonal projection of the vertex 0 to the plane given by the vertices 1,2,3. Furthermore, h_0 denotes the height of the tetrahedron in the vertex 0 and $\boldsymbol{h}_0 = \overrightarrow{A0}$. As $w_0 = 0$ in the plane $1, 2, 3$, its gradient ∇w_0, is perpendicular to this plane. The whole situation is depicted in Figure 6.1(a).

To evaluate $M_e(\mathbf{w}_e)$ we can write

$$\begin{aligned} M_e(\mathbf{w}_e) &= \int_e \mathbf{w}_e \cdot \boldsymbol{\tau}_e \, \mathrm{d}s = \int_e w_0 \nabla w_1 \cdot \boldsymbol{\tau}_e \, \mathrm{d}s - \int_e w_1 \nabla w_0 \cdot \boldsymbol{\tau}_e \, \mathrm{d}s \\ &= \nabla w_1 \cdot \boldsymbol{\tau}_e \int_e w_0 \, \mathrm{d}s - \nabla w_0 \cdot \boldsymbol{\tau}_e \int_e w_1 \, \mathrm{d}s. \end{aligned}$$

The scalar product satisfies $\nabla w_0 \cdot \boldsymbol{\tau}_e = |\nabla w_0||\boldsymbol{\tau}_e| \cos\alpha$, where α is the angle between the vectors ∇w_0 and $\boldsymbol{\tau}_e$, see Figure 6.1(b). Because of the identity $|e| \cos\alpha = -h_0$, with $|e|$ denoting the length of the edge e, one obtains

$$\nabla w_0 \cdot \boldsymbol{\tau}_e = |\nabla w_0||\boldsymbol{\tau}_e| \cos\alpha = -h_0 |\nabla w_0||e|^{-1} = -|e|^{-1},$$

where the last equality follows from the mean value theorem

$$(\nabla w_0, \boldsymbol{h}_0) = w_0(0) - w_0(A) = 1.$$

Analogously, $\nabla w_1 \cdot \boldsymbol{\tau}_e = |e|^{-1}$. Finally, the circulation of $\mathbf{w}_e$ along the edge e equals

$$M_e(\mathbf{w}_e) = |e|^{-1} \int_e w_0 + w_1 \mathrm{d}s = 1.$$

[1] In literature the symbol $\delta_{i,j}$ denotes the Kronecker's δ–function.

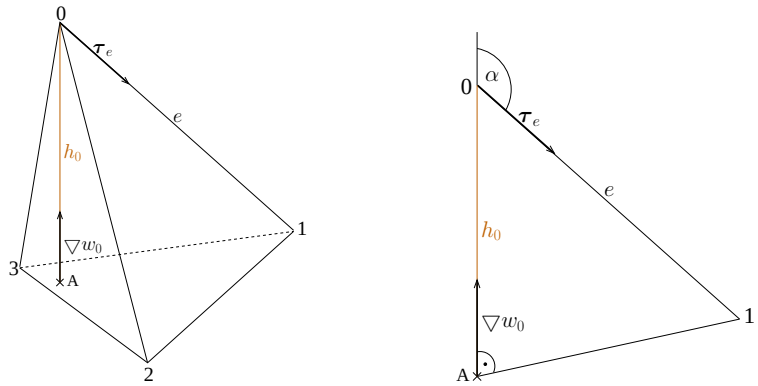

(a) Geometry of tetrahedron.

(b) Computation of the scalar product.

Figure 6.1: Whitney's edge elements

One can verify that the latter relation equals zero along the other edges of the tetrahedron. Thus, we conclude $M_{e_i}(\mathbf{w}_{e_j}) = \delta_{i,j}$ for $i, j = 1, \ldots, 6$.

For detailed proofs and an overview of all kinds of Whitney's elements we refer to [24, Chapter 3] and [53, Chapter 4].

6.2.3 Approximation properties

In this section we give some approximation properties of Whitney's edge elements. These are helpful for obtaining error estimates later on.
In the following lemmas we suppose that the mesh $\mathcal{M}_h$ is regular and the interpolation operator r_h is defined by

$$M_{e_i}(\boldsymbol{u} - r_h(\boldsymbol{u})) = 0 \qquad \forall i = 1, \ldots, 6. \tag{6.9}$$

Lemma 6.3 *Let $\mathcal{M}_h$ be a regular mesh on Ω. If $\boldsymbol{u} \in \boldsymbol{H}^s(\Omega)$ and $\nabla \times \boldsymbol{u} \in \boldsymbol{H}^s(\Omega)$ for some $\frac{1}{2} + \delta < s \leq 1$ with $\delta > 0$, then*

$$\|\boldsymbol{u} - r_h\boldsymbol{u}\|_{\mathbf{L}^2(\Omega)} + \|\nabla \times (\boldsymbol{u} - r_h\boldsymbol{u})\|_{\mathbf{L}^2(\Omega)} \leq Ch^s \left(\|\boldsymbol{u}\|_{\boldsymbol{H}^s(\Omega)} + \|\nabla \times \boldsymbol{u}\|_{\boldsymbol{H}^s(\Omega)} \right).$$

Lemma 6.4 *Suppose $\boldsymbol{u} \in \boldsymbol{H}^s(\Omega)$ and $\nabla \times \boldsymbol{u} \in \boldsymbol{H}^s(\Omega)$ for some $\frac{1}{2} < s \leq 1$. Then*

$$\|\boldsymbol{\nu} \times (\boldsymbol{u} - r_h\boldsymbol{u}) \times \boldsymbol{\nu}\|_{\mathbf{L}^2_t(\Gamma)} \leq Ch^{s-1/2} \left(\|\boldsymbol{u}\|_{\boldsymbol{H}^s(\Omega)} + \|\nabla \times \boldsymbol{u}\|_{\boldsymbol{H}^s(\Omega)} \right).$$

The space $\mathbf{L}^2_t(\Gamma)$ is defined as follows:

$$\mathbf{L}^2_t(\Gamma) = \{\boldsymbol{u} \in (\mathbf{L}_2(\Gamma))^3 \mid \boldsymbol{\nu} \cdot \boldsymbol{u} = 0 \text{ on } \Gamma\}.$$

6.3 Fully discretized linear scheme

Finally we suggest a linear numerical scheme discretized in time and space for finding an approximation of the solution to the problem (4.6). First we put $\boldsymbol{u}_0^h = r_h \boldsymbol{H}_0$. Then for each $i > 0$ and $k > 0$ $\boldsymbol{u}_{i,k}^h \in \boldsymbol{V}^h$ is the solution of the boundary value problem

$$\begin{aligned}&(\boldsymbol{u}_{i,k}^h, \boldsymbol{\varphi}^h) + \tau(\nabla \times \boldsymbol{u}_{i,k}^h, \nabla \times \boldsymbol{\varphi}^h) + \tau L(\boldsymbol{u}_{i,k}^h \times \boldsymbol{\nu}, \boldsymbol{\varphi}^h \times \boldsymbol{\nu})_\Gamma \\ &= (\boldsymbol{u}_{i-1}^h, \boldsymbol{\varphi}^h) + \tau L(\boldsymbol{u}_{i,k-1}^h \times \boldsymbol{\nu}, \boldsymbol{\varphi}^h \times \boldsymbol{\nu})_\Gamma - \tau(\boldsymbol{G}(\boldsymbol{u}_{i,k-1}^h \times \boldsymbol{\nu}), \boldsymbol{\varphi}^h \times \boldsymbol{\nu})_\Gamma\end{aligned} \tag{6.10}$$

valid for all $\boldsymbol{\varphi}^h \in \boldsymbol{V}^h$. We define the stopping criterion for some $\eta \geq 1$:

$$\begin{aligned}&\text{If } \left\|\boldsymbol{u}_{i,k_i}^h - \boldsymbol{u}_{i,k_i-1}^h\right\| \leq \tau^\eta \text{ and } \left\|(\boldsymbol{u}_{i,k_i}^h - \boldsymbol{u}_{i,k_i-1}^h) \times \boldsymbol{\nu}\right\|_\Gamma \leq \tau^\eta \\ &\qquad \Longrightarrow \text{ STOP and } \boldsymbol{u}_i^h := \boldsymbol{u}_{i,k_i}^h\,.\end{aligned} \tag{6.11}$$

The exact value of τ^η will be discussed later.
The described algorithm is depicted in Figure 6.2. The parameter h denotes the mesh refinement, i the time layer and k_i the number of iterations in one time step (which can differ from one time step to the other). The vector field $\boldsymbol{G}$ follows definition (4.4). The linearization coefficient $L > 0$ is chosen such that quick convergence of the proposed iteration scheme is assured. We can derive, similarly as in [54, Remark 1], the optimal value for this parameter. We come back to this question later (see Remark 6.1). The existence and uniqueness of a weak solution is guaranteed by the Lax-Milgram lemma.

Further we need to define a real function $b(s) := g(s) - L$ and an auxiliary operator

$$\boldsymbol{B}(\boldsymbol{s} \times \boldsymbol{\nu}) = \boldsymbol{G}(\boldsymbol{s} \times \boldsymbol{\nu}) - L\boldsymbol{s} \times \boldsymbol{\nu}. \tag{6.12}$$

Now we need to check if the introduced stopping criterion (6.11) is appropriate. In other words, we need to prove the convergence of the sequences $\{\boldsymbol{u}_{i,k}^h\}$, $\{\boldsymbol{u}_{i,k}^h \times \boldsymbol{\nu}\}$ for $k \to \infty$. The following property of the auxiliary vector field $\boldsymbol{B}$ is used in the proof:

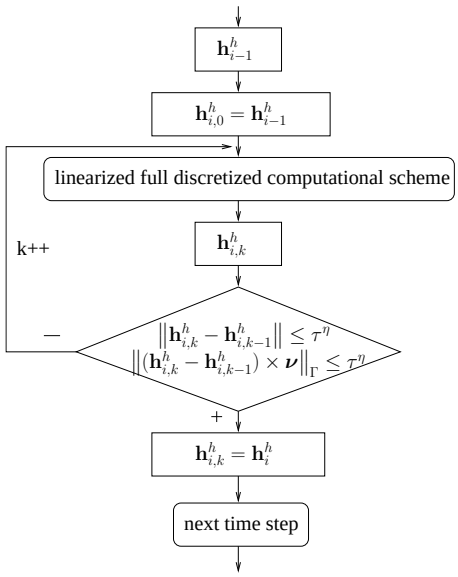

Figure 6.2: Flowchart of the proposed fully discretized scheme

Lemma 6.5 *For all* $\boldsymbol{s}, \boldsymbol{t} \in \mathbb{R}^3$ *the following inequality holds*

$$|\boldsymbol{B}(\boldsymbol{s} \times \boldsymbol{\nu}) - \boldsymbol{B}(\boldsymbol{t} \times \boldsymbol{\nu})|_\Gamma \leq M|(\boldsymbol{s} - \boldsymbol{t}) \times \boldsymbol{\nu}|_\Gamma \,,$$

where $M(L) > 0$ *equals*

$$M = M(L) = \max\{|a^{\alpha-1} - L|, |\alpha b^{\alpha-1} - L|\} \qquad \textit{for } \alpha \in (0, 1] \,.$$

Proof: We follow the idea of the proof of [54, Lemma 1].
The mean value theorem is used in the form

$$|b(s)s - b(q)q| \leq \max_{\theta \geq 0}\{[b(\theta)\theta]'\}|s - q| \qquad \text{for } \forall s, q \geq 0.$$

Using the definition of real functions g and b, we obtain the first derivative of the scalar function $b(\theta)\theta$:

$$[b(\theta)\theta]' = \begin{cases} a^{\alpha-1} - L & 0 < \theta < a, \\ \alpha\theta^{\alpha-1} - L & a < \theta < b, \\ b^{\alpha-1} - L & b < \theta. \end{cases} \tag{6.13}$$

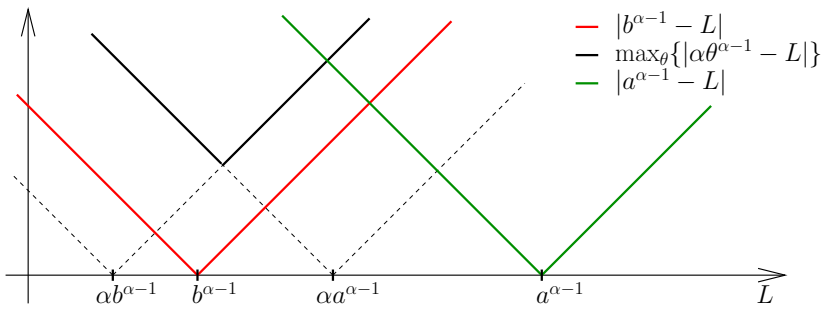

Figure 6.3: Evaluation of the value of M in Lemma 6.5.

Now, our task is to find the $\sup\{[b(\theta)\theta]'\}$ for all $\theta \geq 0$. It is easy to see that it is one of these three functions, specifically

$$\sup_{\theta\geq 0}\{|[b(\theta)\theta]'|\} = \max\{|a^{\alpha-1} - L|, \max_{a<\theta<b}\{|\alpha\theta^{\alpha-1} - L|\}, |b^{\alpha-1} - L|\}.$$

A sketch of these functions can be found in Figure 6.3. After introducing the new notation $M(L) = \max_{\theta\geq 0}\{|[b(\theta)\theta]'|\}$, we conclude that

$$M = M(L) = \max\{|a^{\alpha-1} - L|, |\alpha b^{\alpha-1} - L|\} \text{ for } \alpha \in (0, 1].$$

Thus, for all non-negative real numbers s, q it holds

$$|b(s)s - b(q)q| \leq M|s - q|. \tag{6.14}$$

The fact that

$$|b(s)| \leq \max\{|a^{\alpha-1} - L|, |b^{\alpha-1} - L|\} \leq M \tag{6.15}$$

can easily be verified as well for all $s > 0$.
We continue with the algebraic identity valid for all vectors $\boldsymbol{s}, \boldsymbol{t} \in \mathbb{R}^3$

$$\begin{aligned} |\boldsymbol{B}(\boldsymbol{s}) - \boldsymbol{B}(\boldsymbol{t})|^2 &= |b(|\boldsymbol{s}|)\boldsymbol{s} - b(|\boldsymbol{t}|)\boldsymbol{t}|^2 \\ &= [b(|\boldsymbol{s}|)|\boldsymbol{s}| - b(|\boldsymbol{t}|)|\boldsymbol{t}|]^2 + 2b(|\boldsymbol{s}|)b(|\boldsymbol{t}|)[|\boldsymbol{s}||\boldsymbol{t}| - (\boldsymbol{s}, \boldsymbol{t})]. \end{aligned} \tag{6.16}$$

Using the Cauchy inequality

$$|\boldsymbol{s}||\boldsymbol{t}| - (\boldsymbol{s}, \boldsymbol{t}) \geq 0$$

together with (6.14) and (6.15) we obtain from (6.16)

$$|\boldsymbol{B}(\boldsymbol{s}) - \boldsymbol{B}(\boldsymbol{t})|^2 \leq M^2||\boldsymbol{s}| - |\boldsymbol{t}||^2 + 2M^2[|\boldsymbol{s}||\boldsymbol{t}| - (\boldsymbol{s}, \boldsymbol{t})] = M^2|\boldsymbol{s} - \boldsymbol{t}|^2,$$

which completes the proof. □

6.3.1 Convergence to the auxiliary problem

We show that (6.10) converges for $k \to \infty$ to the following auxiliary problem: Find $\boldsymbol{v}_i^h \in \boldsymbol{V}^h, \boldsymbol{v}_0 = \boldsymbol{u}_0 = r_h \boldsymbol{H}_0$ such that

$$(\boldsymbol{v}_i^h, \boldsymbol{\varphi}^h) + \tau(\nabla \times \boldsymbol{v}_i^h, \nabla \times \boldsymbol{\varphi}^h) + \tau(G(\boldsymbol{v}_i^h \times \boldsymbol{\nu}), \boldsymbol{\varphi}^h \times \boldsymbol{\nu})_\Gamma = (\boldsymbol{u}_{i-1}^h, \boldsymbol{\varphi}^h) \quad (6.17)$$

holds for any $\boldsymbol{\varphi}^h \in \boldsymbol{V}^h$. The existence of a unique solution $\boldsymbol{v}_i$ can be proved using the previously mentioned theory of monotone operators (see [91]). Therefore the proof is omitted.

Theorem 6.2 *Suppose Lemma 6.5 is satisfied. If $\boldsymbol{u}_{i,k}^h$ and $\boldsymbol{v}_i^h$ are the solutions to the boundary value problem (6.10) and the auxiliary problem (6.17), then*

$$\begin{aligned}
\left\|\boldsymbol{u}_{i,k}^h - \boldsymbol{v}_i^h\right\| &\leq \sqrt{\tau L}\left(\frac{M}{L}\right)^k \left\|(\boldsymbol{v}_i^h - \boldsymbol{u}_{i,0}^h) \times \boldsymbol{\nu}\right\|_\Gamma , \\
\left\|\nabla \times (\boldsymbol{u}_{i,k}^h - \boldsymbol{v}_i^h)\right\| &\leq \sqrt{L}\left(\frac{M}{L}\right)^k \left\|(\boldsymbol{v}_i^h - \boldsymbol{u}_{i,0}^h) \times \boldsymbol{\nu}\right\|_\Gamma , \\
\left\|(\boldsymbol{u}_{i,k}^h - \boldsymbol{v}_i^h) \times \boldsymbol{\nu}\right\|_\Gamma &\leq \left(\frac{M}{L}\right)^k \left\|(\boldsymbol{v}_i^h - \boldsymbol{u}_{i,0}^h) \times \boldsymbol{\nu}\right\|_\Gamma
\end{aligned}$$

holds for any $k > 0$, $i > 0$, $h > 0$ and $\tau < 1$.

Proof: Rewriting equation (6.17) yields

$$\begin{aligned}
&(\boldsymbol{v}_i^h, \boldsymbol{\varphi}^h) + \tau(\nabla \times \boldsymbol{v}_i^h, \nabla \times \boldsymbol{\varphi}^h) + \tau L(\boldsymbol{v}_i^h \times \boldsymbol{\nu}, \boldsymbol{\varphi}^h \times \boldsymbol{\nu})_\Gamma \\
&= (\boldsymbol{u}_{i-1}^h, \boldsymbol{\varphi}^h) + \tau L(\boldsymbol{v}_i^h \times \boldsymbol{\nu}, \boldsymbol{\varphi}^h \times \boldsymbol{\nu})_\Gamma - \tau(G(\boldsymbol{v}_i^h \times \boldsymbol{\nu}), \boldsymbol{\varphi}^h \times \boldsymbol{\nu})_\Gamma .
\end{aligned} \quad (6.18)$$

Subtracting (6.18) from (6.10) and recalling (6.12) we obtain

$$\begin{aligned}
(\boldsymbol{u}_{i,k}^h - \boldsymbol{v}_i^h, \boldsymbol{\varphi}^h) + \tau\left(\nabla \times (\boldsymbol{u}_{i,k}^h - \boldsymbol{v}_i^h), \nabla \times \boldsymbol{\varphi}^h\right) + \tau L\left((\boldsymbol{u}_{i,k}^h - \boldsymbol{v}_i^h) \times \boldsymbol{\nu}, \boldsymbol{\varphi}^h \times \boldsymbol{\nu}\right)_\Gamma \\
= \tau\left(\boldsymbol{B}(\boldsymbol{v}_i^h \times \boldsymbol{\nu}) - \boldsymbol{B}(\boldsymbol{u}_{i,k-1}^h \times \boldsymbol{\nu}), \boldsymbol{\varphi}^h \times \boldsymbol{\nu}\right)_\Gamma .
\end{aligned}$$

Next, we set $\boldsymbol{\varphi}^h = \boldsymbol{u}^h_{i,k} - \boldsymbol{v}^h_i$:

$$\begin{aligned}\left\|\boldsymbol{u}^h_{i,k} - \boldsymbol{v}^h_i\right\|^2 + \tau\left\|\nabla\times(\boldsymbol{u}^h_{i,k} - \boldsymbol{v}^h_i)\right\|^2 + \tau L\left\|(\boldsymbol{u}^h_{i,k} - \boldsymbol{v}^h_i)\times\boldsymbol{\nu}\right\|^2_\Gamma \\ = \tau\left(\boldsymbol{B}(\boldsymbol{v}^h_i\times\boldsymbol{\nu}) - \boldsymbol{B}(\boldsymbol{u}^h_{i,k-1}\times\boldsymbol{\nu}), (\boldsymbol{u}^h_{i,k} - \boldsymbol{v}^h_i)\times\boldsymbol{\nu}\right)_\Gamma .\end{aligned}$$

Using Cauchy's inequality and the boundedness of the auxiliary operator $\boldsymbol{B}$, proved in Lemma 6.5, one gets

$$\begin{aligned}\left\|\boldsymbol{u}^h_{i,k} - \boldsymbol{v}^h_i\right\|^2 &+ \tau\left\|\nabla\times(\boldsymbol{u}^h_{i,k} - \boldsymbol{v}^h_i)\right\|^2 + \tau L\left\|(\boldsymbol{u}^h_{i,k} - \boldsymbol{v}^h_i)\times\boldsymbol{\nu}\right\|^2_\Gamma \\ &\le \tau\left\|\boldsymbol{B}(\boldsymbol{v}^h_i\times\boldsymbol{\nu}) - \boldsymbol{B}(\boldsymbol{u}^h_{i,k-1}\times\boldsymbol{\nu})\right\|_\Gamma\cdot\left\|(\boldsymbol{u}^h_{i,k} - \boldsymbol{v}^h_i)\times\boldsymbol{\nu}\right\|_\Gamma \\ &\le \tau M\left\|(\boldsymbol{v}^h_i - \boldsymbol{u}^h_{i,k-1})\times\boldsymbol{\nu}\right\|_\Gamma\cdot\left\|(\boldsymbol{u}^h_{i,k} - \boldsymbol{v}^h_i)\times\boldsymbol{\nu}\right\|_\Gamma .\end{aligned}$$

Starting from the last inequality we can estimate the boundary term as follows

$$\begin{aligned}\tau L\left\|(\boldsymbol{u}^h_{i,k} - \boldsymbol{v}^h_i)\times\boldsymbol{\nu}\right\|^2_\Gamma &\le \tau M\left\|(\boldsymbol{v}^h_i - \boldsymbol{u}^h_{i,k-1})\times\boldsymbol{\nu}\right\|_\Gamma\cdot\left\|(\boldsymbol{u}^h_{i,k} - \boldsymbol{v}^h_i)\times\boldsymbol{\nu}\right\|_\Gamma \\ \Longrightarrow \left\|(\boldsymbol{u}^h_{i,k} - \boldsymbol{v}^h_i)\times\boldsymbol{\nu}\right\|_\Gamma &\le \frac{M}{L}\left\|(\boldsymbol{v}^h_i - \boldsymbol{u}^h_{i,k-1})\times\boldsymbol{\nu}\right\|_\Gamma \\ \Longrightarrow \left\|(\boldsymbol{u}^h_{i,k} - \boldsymbol{v}^h_i)\times\boldsymbol{\nu}\right\|_\Gamma &\le \left(\frac{M}{L}\right)^k\left\|(\boldsymbol{v}^h_i - \boldsymbol{u}^h_{i,0})\times\boldsymbol{\nu}\right\|_\Gamma .\end{aligned}$$

Using this result, the "curl" term estimation is processed

$$\left\|\nabla\times(\boldsymbol{u}^h_{i,k} - \boldsymbol{v}^h_i)\right\|^2 \le L\left(\frac{M}{L}\right)^{2k}\left\|(\boldsymbol{v}^h_i - \boldsymbol{u}^h_{i,0})\times\boldsymbol{\nu}\right\|^2_\Gamma .$$

Analogously we get the last missing estimate.

Because of Lemma 6.6, which proves the existence of a parameter $L > 0$ such that $M(L) < L$, we conclude that $\{\boldsymbol{u}^h_{i,k}\}$ and $\{\boldsymbol{u}^h_{i,k}\times\boldsymbol{\nu}\}$ are convergent sequences for $k\to\infty$. □

Lemma 6.6 *There exists $L > 0$ such that $M(L) < L$.*

Proof: If $L \ge (a^{\alpha-1} + \alpha b^{\alpha-1})/2$ then $M = L - \alpha b^{\alpha-1}$ for $\alpha\in(0,1]$ and the statement of the lemma is fulfilled directly. □

Remark 6.1 (Optimal value of the parameter L)
To get a satisfying convergence the ratio $M(L)/L$ has to be minimized. Let us consider the derivative of the mentioned function. For $\alpha\in(0,1]$ we consider two cases:

i) *If* $L > (a^{\alpha-1} + \alpha b^{\alpha-1})/2$ *then* $M(L) = L - \alpha b^{\alpha-1}$. *The derivative is then given by*

$$\partial_L \left(\frac{M(L)}{L} \right) = \frac{\alpha b^{\alpha-1}}{L^2} > 0 \,.$$

The minimal value is obtained for $L = (a^{\alpha-1} + \alpha b^{\alpha-1})/2$.

ii) *If* $0 < L < (a^{\alpha-1} + \alpha b^{\alpha-1})/2$ *then* $M(L) = a^{\alpha-1} - L$. *For the derivative we obtain*

$$\partial_L \left(\frac{M(L)}{L} \right) = \frac{-a^{\alpha-1}}{L^2} < 0 \,.$$

Then the function is decreasing and the minimum is obtained for $L = (a^{\alpha-1} + \alpha b^{\alpha-1})/2$ *as well.*

From these two cases we conclude that $L = (a^{\alpha-1} + \alpha b^{\alpha-1})/2$ *is the optimal value of the parameter* L.

6.3.2 A priori estimates

For the final result the following a priori estimate is essential.

Theorem 6.3 *Let the operators* $\boldsymbol{G}$ *and* $\boldsymbol{B}$ *satisfy Lemma 6.1 and Lemma 6.5. Then there exists a constant* $C > 0$ *such that*

$$\left\|\delta \boldsymbol{u}_j^h\right\|^2 + \sum_{i=1}^{j} \left\|\delta \boldsymbol{u}_i^h - \delta \boldsymbol{u}_{i-1}^h\right\|^2 + \sum_{i=1}^{j} \tau \left\|\nabla \times \delta \boldsymbol{u}_i^h\right\|^2 + \sum_{i=1}^{j} \tau \left\|\delta \boldsymbol{u}_i^h \times \boldsymbol{\nu}\right\|_\Gamma^2 \leq C \,.$$

Proof: We start from the discrete linearized system

$$\begin{aligned} (\delta \boldsymbol{u}_{i,k}^h, \boldsymbol{\varphi}^h) + (\nabla \times \boldsymbol{u}_{i,k}^h, \nabla \times \boldsymbol{\varphi}^h) + (\boldsymbol{G}(\boldsymbol{u}_{i,k}^h \times \boldsymbol{\nu}), \boldsymbol{\varphi}^h \times \boldsymbol{\nu})_\Gamma \\ = (\boldsymbol{B}(\boldsymbol{u}_{i,k}^h \times \boldsymbol{\nu}) - \boldsymbol{B}(\boldsymbol{u}_{i,k-1}^h \times \boldsymbol{\nu}), \boldsymbol{\varphi}^h \times \boldsymbol{\nu})_\Gamma \,. \end{aligned} \tag{6.19}$$

Now we perform the following operations. First we set $k = k_i$, then we subtract (6.19) for $i = i - 1$ from (6.19). Next we set $\boldsymbol{\varphi}^h = \delta \boldsymbol{u}_i^h$ and after summation for

$i = 1, \ldots, j$ we get

$$\begin{aligned}
&\sum_{i=1}^{j}(\delta \boldsymbol{u}_i^h - \delta \boldsymbol{u}_{i-1}^h, \delta \boldsymbol{u}_i^h) + \sum_{i=1}^{j}(\nabla \times (\boldsymbol{u}_i^h - \boldsymbol{u}_{i-1}^h), \nabla \times \delta \boldsymbol{u}_i^h) \\
&\qquad + \sum_{i=1}^{j}(\boldsymbol{G}(\boldsymbol{u}_i^h \times \boldsymbol{\nu}) - \boldsymbol{G}(\boldsymbol{u}_{i-1}^h \times \boldsymbol{\nu}), \delta \boldsymbol{u}_i^h \times \boldsymbol{\nu})_\Gamma \\
&\qquad = \sum_{i=1}^{j}(\boldsymbol{B}(\boldsymbol{u}_{i,k_i}^h \times \boldsymbol{\nu}) - \boldsymbol{B}(\boldsymbol{u}_{i,k_i-1}^h \times \boldsymbol{\nu}), \delta \boldsymbol{u}_i^h \times \boldsymbol{\nu})_\Gamma \\
&\quad - \sum_{i=1}^{j}(\boldsymbol{B}(\boldsymbol{u}_{i-1,k_{i-1}}^h \times \boldsymbol{\nu}) - \boldsymbol{B}(\boldsymbol{u}_{i-1,k_{i-1}-1}^h \times \boldsymbol{\nu}), \delta \boldsymbol{u}_i^h \times \boldsymbol{\nu})_\Gamma \,.
\end{aligned}$$

The left–hand side is estimated by applying Abel's summation and the property of the nonlinear operator $\boldsymbol{G}$. The Cauchy-Schwartz inequality, the boundedness of the auxiliary operator $\boldsymbol{B}$ and the stopping criterion (6.11) are used for the estimation of the right–hand side. This yields

$$\begin{aligned}
&\frac{1}{2}\left\|\delta \boldsymbol{u}_j^h\right\|^2 + \frac{1}{2}\sum_{i=1}^{j}\left\|\delta \boldsymbol{u}_i^h - \delta \boldsymbol{u}_{i-1}^h\right\|^2 + \sum_{i=1}^{j}\tau\left\|\nabla \times \delta \boldsymbol{u}_i^h\right\|^2 \\
&+\alpha b^{\alpha-1}\sum_{i=1}^{j}\tau\left\|\delta \boldsymbol{u}_i^h \times \boldsymbol{\nu}\right\|_\Gamma^2 \le \frac{1}{2}\left\|\delta \boldsymbol{u}_0^h\right\|^2 + 2\sum_{i=1}^{j} M\tau^\eta\left\|\delta \boldsymbol{u}_i^h \times \boldsymbol{\nu}\right\|_\Gamma \,.
\end{aligned}$$

Further by Young's inequality one obtains

$$\begin{aligned}
\frac{1}{2}\left\|\delta \boldsymbol{u}_j^h\right\|^2 + &\quad \frac{1}{2}\sum_{i=1}^{j}\left\|\delta \boldsymbol{u}_i^h - \delta \boldsymbol{u}_{i-1}^h\right\|^2 + \sum_{i=1}^{j}\tau\left\|\nabla \times \delta \boldsymbol{u}_i^h\right\|^2 \\
+ &\quad (\alpha b^{\alpha-1} - \varepsilon)\sum_{i=1}^{j}\tau\left\|\delta \boldsymbol{u}_i^h \times \boldsymbol{\nu}\right\|_\Gamma^2 \\
\le &\quad \frac{1}{2}\left\|\delta \boldsymbol{u}_0^h\right\|^2 + C_\varepsilon\sum_{i=1}^{j} M^2\tau^{2\eta-1} \\
\le &\quad C_\varepsilon(1 + \tau^{2\eta-2}) \\
\le &\quad C \,.
\end{aligned}$$

Choosing some small fixed $\varepsilon > 0$ concludes the rest of the proof. □

6.3.3 Convergence to fully discretized linear problem

First we define the continuous piecewise linear in time vector field $\boldsymbol{u}_n^h$ given by

$$\begin{aligned} \boldsymbol{u}_0^h &= r_h \boldsymbol{H}_0, \\ \boldsymbol{u}_n^h(t) &= \boldsymbol{u}_{i-1}^h + (t - t_{i-1})\delta \boldsymbol{u}_i^h \qquad \text{for } t \in (t_{i-1}, t_i] \end{aligned}$$

and the step in time vector field $\overline{\boldsymbol{u}}_n^h$

$$\begin{aligned} \overline{\boldsymbol{u}}_0^h &= r_h \boldsymbol{H}_0, \\ \overline{\boldsymbol{u}}_n^h(t) &= \boldsymbol{u}_i^h \qquad \text{for } t \in (t_{i-1}, t_i]. \end{aligned}$$

The next theorem provides the estimate of the error between the weak solution to variational problem (4.6) and the step vector field $\overline{\boldsymbol{u}}_n^h$–solution to the approximation scheme (6.10).

Theorem 6.4 *Let the operator $\boldsymbol{G}$ be Lipschitz continuous. Suppose $\boldsymbol{H} \in \boldsymbol{H}^1(\Omega)$ and $\nabla \times \boldsymbol{H} \in \boldsymbol{H}^1(\Omega)$. Then the following estimate holds (for $h, \tau < 1$ and $\eta \geq 1$)*

$$\max_{t \in [0,T]} \left\| \boldsymbol{H}(t) - \overline{\boldsymbol{u}}_n^h(t) \right\|^2 \leq C(\tau^2 + h)\,.$$

Proof: We subtract the discrete linearized system (6.19) from the approximation scheme (6.1) for $\boldsymbol{\varphi} = \boldsymbol{\varphi}^h$ and set $k = k_i$. We assume the test function $\boldsymbol{\varphi}^h = r_h \boldsymbol{h}_i - \boldsymbol{u}_i^h$. Next we multiply the obtained equation by τ and sum it up for $i = 1, \ldots, j$.

$$\begin{aligned} &\sum_{i=1}^{j} \tau \left(\delta(\boldsymbol{h}_i - \boldsymbol{u}_i^h), \boldsymbol{h}_i - \boldsymbol{u}_i^h \right) + \sum_{i=1}^{j} \tau \left(\nabla \times (\boldsymbol{h}_i - \boldsymbol{u}_i^h), \nabla \times (\boldsymbol{h}_i - \boldsymbol{u}_i^h) \right) \\ &\qquad + \sum_{i=1}^{j} \tau \left(\boldsymbol{G}(\boldsymbol{h}_i \times \boldsymbol{\nu}) - \boldsymbol{G}(\boldsymbol{u}_i^h \times \boldsymbol{\nu}), (\boldsymbol{h}_i - \boldsymbol{u}_i^h) \times \boldsymbol{\nu} \right)_\Gamma \\ &= \sum_{i=1}^{j} \tau \left(\delta(\boldsymbol{h}_i - \boldsymbol{u}_i^h), \boldsymbol{h}_i - r_h \boldsymbol{h}_i \right) + \sum_{i=1}^{j} \tau \left(\nabla \times (\boldsymbol{h}_i - \boldsymbol{u}_i^h), \nabla \times (\boldsymbol{h}_i - r_h \boldsymbol{h}_i) \right) \\ &\qquad + \sum_{i=1}^{j} \tau \left(\boldsymbol{G}(\boldsymbol{h}_i \times \boldsymbol{\nu}) - \boldsymbol{G}(\boldsymbol{u}_i^h \times \boldsymbol{\nu}), (\boldsymbol{h}_i - r_h \boldsymbol{h}_i) \times \boldsymbol{\nu} \right)_\Gamma \\ &\quad + \sum_{i=1}^{j} \tau \left(\boldsymbol{B}(\boldsymbol{u}_{i,k_i-1}^h \times \boldsymbol{\nu}) - \boldsymbol{B}(\boldsymbol{u}_{i,k_i}^h \times \boldsymbol{\nu}), (r_h \boldsymbol{h}_i - \boldsymbol{h}_i + \boldsymbol{h}_i - \boldsymbol{u}_i^h) \times \boldsymbol{\nu} \right)_\Gamma . \end{aligned}$$

Using the Abel summation on the first term on the left–hand side and embracing the first property of the operator $\boldsymbol{G}$ (Lemma 6.1), Cauchy-Schwartz's inequality,

Hölder's inequality and Young's inequality with some small fixed $\varepsilon > 0$, one obtains

$$
\begin{aligned}
&\frac{1}{2}\left\|\boldsymbol{h}_j - \boldsymbol{u}_j^h\right\|^2 + \frac{1}{2}\sum_{i=1}^{j}\left((\boldsymbol{h}_i - \boldsymbol{u}_i^h) - (\boldsymbol{h}_{i-1} - \boldsymbol{u}_{i-1}^h)\right)^2 \\
&+\sum_{i=1}^{j}\tau\left\|\nabla\times(\boldsymbol{h}_i - \boldsymbol{u}_i^h)\right\|^2 + \alpha b^{\alpha-1}\sum_{i=1}^{j}\tau\left\|(\boldsymbol{h}_i - \boldsymbol{u}_i^h)\times\boldsymbol{\nu}\right\|_\Gamma^2 \\
&\leq \frac{1}{2}\left\|\boldsymbol{H}_0 - \boldsymbol{u}_0^h\right\|^2 + \sqrt{\sum_{i=1}^{j}\tau\left\|\delta(\boldsymbol{h}_i - \boldsymbol{u}_i^h)\right\|^2}\sqrt{\sum_{i=1}^{j}\tau\left\|\boldsymbol{h}_i - r_h\boldsymbol{h}_i\right\|^2} \\
&+\varepsilon\sum_{i=1}^{j}\tau\left\|\nabla\times(\boldsymbol{h}_i - \boldsymbol{u}_i^h)\right\|^2 + C_\varepsilon\sum_{i=1}^{j}\tau\left\|\nabla\times(\boldsymbol{h}_i - r_h\boldsymbol{h}_i)\right\|^2 \\
&+\varepsilon\sum_{i=1}^{j}\tau\left\|\boldsymbol{G}(\boldsymbol{h}_i\times\boldsymbol{\nu}) - \boldsymbol{G}(\boldsymbol{u}_i^h\times\boldsymbol{\nu})\right\|_\Gamma^2 \\
&+C_\varepsilon\sum_{i=1}^{j}\tau\left\|(\boldsymbol{h}_i - r_h\boldsymbol{h}_i)\times\boldsymbol{\nu}\right\|_\Gamma^2 + C_\varepsilon\sum_{i=1}^{j}\tau\left\|\boldsymbol{B}(\boldsymbol{u}_{i,k_i-1}^h\times\boldsymbol{\nu}) - \boldsymbol{B}(\boldsymbol{u}_{i,k_i}^h\times\boldsymbol{\nu})\right\|_\Gamma^2 \\
&+\varepsilon\left(\sum_{i=1}^{j}\tau\left\|(r_h\boldsymbol{h}_i - \boldsymbol{h}_i)\times\boldsymbol{\nu}\right\|_\Gamma^2 + \sum_{i=1}^{j}\tau\left\|(\boldsymbol{h}_i - \boldsymbol{u}_i^h)\times\boldsymbol{\nu}\right\|_\Gamma^2\right).
\end{aligned}
$$

Using the results from Lemma 6.2 and Theorem 6.3, the boundedness of the operator $\boldsymbol{B}$ (Lemma 6.5) followed by stopping criterion (6.11) and finally the Lipschitz continuity of $\boldsymbol{G}$, we successively deduce that

$$
\begin{aligned}
&\frac{1}{2}\left\|\boldsymbol{h}_j - \boldsymbol{u}_j^h\right\|^2 + (1-\varepsilon)\sum_{i=1}^{j}\tau\left\|\nabla\times(\boldsymbol{h}_i - \boldsymbol{u}_i^h)\right\|^2 \\
&+(\alpha b^{\alpha-1} - \varepsilon a^{2(\alpha-1)} - \varepsilon)\sum_{i=1}^{j}\tau\left\|(\boldsymbol{h}_i - \boldsymbol{u}_i^h)\times\boldsymbol{\nu}\right\|_\Gamma^2 \\
&\leq \frac{1}{2}\left\|\boldsymbol{H}_0 - \boldsymbol{u}_0^h\right\|^2 + C\sqrt{\sum_{i=1}^{j}\tau\left\|\boldsymbol{h}_i - r_h\boldsymbol{h}_i\right\|^2} \\
&+C_\varepsilon\left(\sum_{i=1}^{j}\tau\left\|\nabla\times(\boldsymbol{h}_i - r_h\boldsymbol{h}_i)\right\|^2 + \sum_{i=1}^{j}\tau\left\|(\boldsymbol{h}_i - r_h\boldsymbol{h}_i)\times\boldsymbol{\nu}\right\|_\Gamma^2 + \tau^{2\eta}\right).
\end{aligned}
$$

Rewriting this in the notation of the piecewise continuous and piecewise constant

functions and recalling that $\overline{\boldsymbol{u}}_0^h = r_h \boldsymbol{H}_0$ we have

$$\begin{aligned}
&\frac{1}{2}\left\|\overline{\boldsymbol{h}}_n(t) - \overline{\boldsymbol{u}}_n^h(t)\right\|^2 + (1-\varepsilon)\int_0^t \left\|\nabla \times (\overline{\boldsymbol{h}}_n - \overline{\boldsymbol{u}}_n^h)\right\|^2 \\
&\quad +(\alpha b^{\alpha-1} - \varepsilon a^{2(\alpha-1)} - \varepsilon)\int_0^t \left\|(\overline{\boldsymbol{h}}_n - \overline{\boldsymbol{u}}_n^h)\times \boldsymbol{\nu}\right\|_\Gamma^2 \\
&\quad \le \frac{1}{2}\left\|\boldsymbol{H}_0 - r_h \boldsymbol{H}_0\right\|^2 + C\sqrt{\int_0^t \left\|\overline{\boldsymbol{h}}_n - r_h\overline{\boldsymbol{h}}_n\right\|^2} \\
&+C_\varepsilon\left(\int_0^t \left\|\nabla\times(\overline{\boldsymbol{h}}_n - r_h\overline{\boldsymbol{h}}_n)\right\|^2 + \int_0^t \left\|(\overline{\boldsymbol{h}}_n - r_h\overline{\boldsymbol{h}}_n)\times\boldsymbol{\nu}\right\|_\Gamma^2 + \tau^{2\eta}\right).
\end{aligned}$$

Using the continuity of the interpolant r_h we arrive at

$$\begin{aligned}
\left\|\overline{\boldsymbol{h}}_n(t) - \overline{\boldsymbol{u}}_n^h(t)\right\|^2 &\le \left\|\boldsymbol{H}_0 - r_h\boldsymbol{H}_0\right\|^2 + C\sqrt{\int_0^t \left\|\boldsymbol{H} - r_h\boldsymbol{H}\right\|^2} \\
&+C_\varepsilon\left(\int_0^t \left\|\nabla\times(\boldsymbol{H} - r_h\boldsymbol{H})\right\|^2 + \int_0^t \left\|(\boldsymbol{H} - r_h\boldsymbol{H})\times\boldsymbol{\nu}\right\|_\Gamma^2 + \tau^{2\eta}\right).
\end{aligned}$$

To assure the convergence of the method, the three differences $\|\boldsymbol{H} - r_h\boldsymbol{H}\|$, $\|\nabla\times(\boldsymbol{H} - r_h\boldsymbol{H})\|$ and $\|(\boldsymbol{H} - r_h\boldsymbol{H})\times\boldsymbol{\nu}\|_\Gamma$ have to be estimated with respect to the $\mathbf{L}_2$ norm. At this point we use the statements from Lemma 6.3 and Lemma 6.4, where the approximation properties of Whitney's elements are summarized. These estimates depend on the regularity of the solution $\boldsymbol{H}$. To estimate the boundary term we bring into account the following equality:

$$\|(\boldsymbol{H} - r_h\boldsymbol{H})\times\boldsymbol{\nu}\|_\Gamma = \|\boldsymbol{\nu}\times(\boldsymbol{H} - r_h\boldsymbol{H})\times\boldsymbol{\nu}\|_\Gamma .$$

The triangle inequality

$$\left\|\boldsymbol{H}(t) - \overline{\boldsymbol{u}}_n^h(t)\right\|^2 \le \frac{1}{2}\left\|\boldsymbol{H}(t) - \boldsymbol{h}_n(t)\right\|^2 + \frac{1}{2}\left\|\boldsymbol{h}_n(t) - \overline{\boldsymbol{h}}_n(t)\right\|^2 + \frac{1}{2}\left\|\overline{\boldsymbol{h}}_n(t) - \overline{\boldsymbol{u}}_n^h(t)\right\|^2$$

together with Theorem 6.1 concludes the proof. □

It can be shown that the error estimate between the weak solution to the variational problem (4.6) and the piecewise linear vector field $\boldsymbol{u}_n^h$ has the same dependence on the discretization parameters.

Theorem 6.5 *Let the operator $\boldsymbol{G}$ be Lipschitz continuous. If $\boldsymbol{H} \in \boldsymbol{H}^1(\Omega)$ and $\nabla\times\boldsymbol{H} \in \boldsymbol{H}^1(\Omega)$, then for $h, \tau < 1$ and $\eta \ge 1$ one has*

$$\max_{t\in[0,T]} \left\|\boldsymbol{H}(t) - \boldsymbol{u}_n^h(t)\right\|^2 \le C(\tau^2 + h).$$

Proof: The proof follows from the triangle inequality and the previous theorem:

$$\begin{aligned}\left\|\boldsymbol{H}(t)-\boldsymbol{u}_n^h(t)\right\|^2 &\leq \frac{1}{2}\left\|\boldsymbol{H}(t)-\overline{\boldsymbol{u}}_n^h(t)\right\|^2+\frac{1}{2}\left\|\overline{\boldsymbol{u}}_n^h(t)-\boldsymbol{u}_n^h(t)\right\|^2\\ &\leq C(\tau^2+h).\end{aligned}$$

□

6.4 Numerical experiments

In this section we present some numerical examples to confirm the effectivity of the linearized scheme (6.10), (6.11). The dependence of the relative error

$$\max_{t\in[0,T]}\frac{\left\|\boldsymbol{H}(t)-\overline{\boldsymbol{u}}_n^h(t)\right\|}{\|\boldsymbol{H}(t)\|} \tag{6.20}$$

on each parameter of the method, i.e. α,η,τ and h, is studied separately. The choice of the parameter $\alpha\in(0,1]$ coincides with the theory. The linearization parameter L is chosen to be optimal in the sense of Remark 6.1.

Let the computational domain Ω occupied by the ferromagnetic material be a unit cube in $\mathbb{R}^3$. On the boundary Γ we consider a Neumann boundary condition. As the exact solution is known, we can calculate the error of the method accurately. Consequently, the problem becomes more complex, namely: Find $\boldsymbol{H}\in\boldsymbol{V}$ such that

$$\begin{aligned}\boldsymbol{H}+\nabla\times\nabla\times\boldsymbol{H} &= \boldsymbol{F} && \text{in } \Omega,\\ \boldsymbol{\nu}\times\nabla\times\boldsymbol{H} &= \boldsymbol{\nu}\times\boldsymbol{G}(\boldsymbol{H}\times\boldsymbol{\nu})+\boldsymbol{J} && \text{on } \Gamma_{Neu},\\ \boldsymbol{H}_0 &= \boldsymbol{0} && \text{in } \Omega.\end{aligned} \tag{6.21}$$

The numerical scheme (6.10) is slightly changed to

$$\begin{aligned}&\frac{1}{\tau}(\boldsymbol{u}_{i,k}^h,\boldsymbol{\varphi}^h)+(\nabla\times\boldsymbol{u}_{i,k}^h,\nabla\times\boldsymbol{\varphi}^h)+L(\boldsymbol{u}_{i,k}^h\times\boldsymbol{\nu},\boldsymbol{\varphi}^h\times\boldsymbol{\nu})_\Gamma\\ &\qquad=(\boldsymbol{F},\boldsymbol{\varphi}^h)-(\boldsymbol{J},\boldsymbol{\varphi}^h)_\Gamma+\frac{1}{\tau}(\boldsymbol{u}_{i-1}^h,\boldsymbol{\varphi}^h)\\ &+L(\boldsymbol{u}_{i,k-1}^h\times\boldsymbol{\nu},\boldsymbol{\varphi}^h\times\boldsymbol{\nu})_\Gamma-\Big(\boldsymbol{G}(\boldsymbol{u}_{i,k-1}^h\times\boldsymbol{\nu}),\boldsymbol{\varphi}^h\times\boldsymbol{\nu}\Big)_\Gamma,\end{aligned} \tag{6.22}$$

and is combined with the stopping criterion (6.11).
The nonlinear vector field $\boldsymbol{G}$ is defined as follows

$$\boldsymbol{G}(\boldsymbol{H}\times\boldsymbol{\nu})=\begin{cases}0.01^{\alpha-1}\boldsymbol{H}\times\boldsymbol{\nu} & 0\leq|\boldsymbol{H}\times\boldsymbol{\nu}|<0.01,\\ |\boldsymbol{H}\times\boldsymbol{\nu}|^{\alpha-1}\boldsymbol{H}\times\boldsymbol{\nu} & 0.01\leq|\boldsymbol{H}\times\boldsymbol{\nu}|\leq 100,\\ 100^{\alpha-1}\boldsymbol{H}\times\boldsymbol{\nu} & 100<|\boldsymbol{H}\times\boldsymbol{\nu}|.\end{cases} \tag{6.23}$$

We solve the system (6.21),(6.23) for three different types of exact solutions:

▷ exact solution linear in space and time

$$\boldsymbol{H}_1(\boldsymbol{x},t) = \begin{pmatrix} 5x_2 - 8x_1 + t \\ 8x_0 - 10x_2 + t \\ 10x_1 - 5x_0 + t \end{pmatrix}; \tag{6.24}$$

▷ exact solution linear in space and nonlinear in time

$$\boldsymbol{H}_2(\boldsymbol{x},t) = \begin{pmatrix} (5x_2 - 8x_1)(\sin(2\pi t) + 2) \\ (8x_0 - 10x_2)(\sin(2\pi t) + 2) \\ (10x_1 - 5x_0)(\sin(2\pi t) + 2) \end{pmatrix}; \tag{6.25}$$

▷ exact solution nonlinear in space and linear in time

$$\boldsymbol{H}_3(\boldsymbol{x},t) = \begin{pmatrix} 5\sin(x_2) - 8\sin(x_1) + t \\ 8\sin(x_0) - 10\sin(x_2) + t \\ 10\sin(x_1) - 5\sin(x_0) + t \end{pmatrix}. \tag{6.26}$$

The data functions $\boldsymbol{F}$ and $\boldsymbol{J}$ acting in (6.21) depend on the choice of the exact solution.

6.4.1 Dependence of the relative error on the parameters of the method

The impact of the parameter η on the relative error is tested on the problem with linear exact solution (6.24) and is given in Figure 6.4. We observe that the value of $\eta = 3$ gives satisfactory results and therefore this value of parameter is used for the rest of the experiments. Note that based on the theory the choice of $\eta = 1$ should be enough. By choice of $\eta = 3$ we want to make sure that the iteration error can be neglected.

Next, we investigate the dependence on the parameter of nonlinearity α. If $\alpha = 1$, the problem (6.21), (6.23) acquires linear character and the computational scheme (6.22), (6.11) is quick and precise. If α tends to zero, the nature of the problem becomes more nonlinear with impact on increase of the relative error. The evolution of the error in time is plotted in Figures 6.5 and 6.6.

The dependence of the error on the length of the time step τ is studied on the problems with exact solutions (6.24) and (6.25), see Figures 6.7 and 6.8. The problem with linear exact solution (6.24) yields better results than the theory

predicts; the dependence of the error on τ can be approximately fitted by the function $f(\tau) = \tau^{2.9}$. Possibly, this result is influenced by the choice of the exact solution and is not valid in general. If the problem with sinusoidal exact solution (6.25) is considered the dependence of the error on the length of the time step is linear, which is in line with the derived theoretical results.

Finally we study the sensibility of our problem to the size of the mesh which we use for computations. As Table 6.2 shows, the accuracy of the approximation does not depend on the size of the mesh if the exact solution (6.24) is considered. The reason is that the linear solution (6.24) can be fitted by Whitney's elements exactly, thus the "coarse mesh" is suitable enough to reach satisfying accuracy of our model. In this case, the best approach is to use the basic mesh consisting of 6 elements. Otherwise, by refining, calculation errors accumulate. The impact of the mesh refinement on the relative error is well visible in Figure 6.9. In order to see this dependence, the problem with the sinusoidal in space exact solution (6.26) is taken. Here, the exact solution cannot be interpolated by Whitney's elements precisely. This discretization (interpolation) error is reported in Table 6.1. The discretization error is the minimal attainable error. By refining the mesh we are able to obtain a better approximation of the exact solution, but still we have to set up all parameters adequately in order to avoid an excessive consumption of computational time.[2]

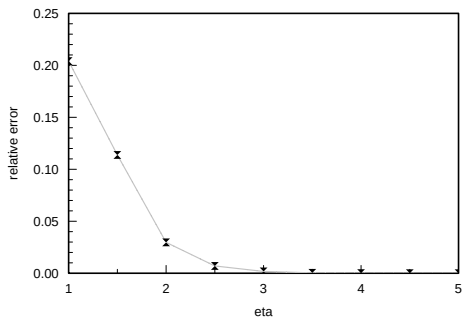

Figure 6.4: The dependence of the relative error (6.20) of the numerical scheme (6.22), (6.11) on the parameter η. Linear in time exact solution (6.24) is considered. The parameters $\alpha = 0.2$, $\tau = 0.05, h = \sqrt{3}$ and $L = 19.9$ are fixed. The relative error can be decreased by choosing $\eta \geq 3$.

[2]If we refine the basic mesh 4 times, we compute on 24 576 elements what requires much patience if solving more complicated problems.

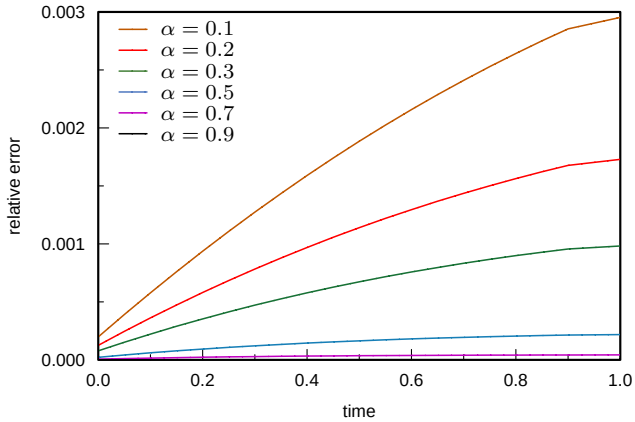

Figure 6.5: The dependence of the relative error (6.20) of the numerical scheme (6.22), (6.11) in time on different choice of nonlinearity parameter α. The smaller α is chosen, the more nonlinear the problem and the less precise the approximation of the exact solution. Linear in time exact solution (6.24), $\tau = 0.05, h = \sqrt{3}$ and $\eta = 3$ are considered.

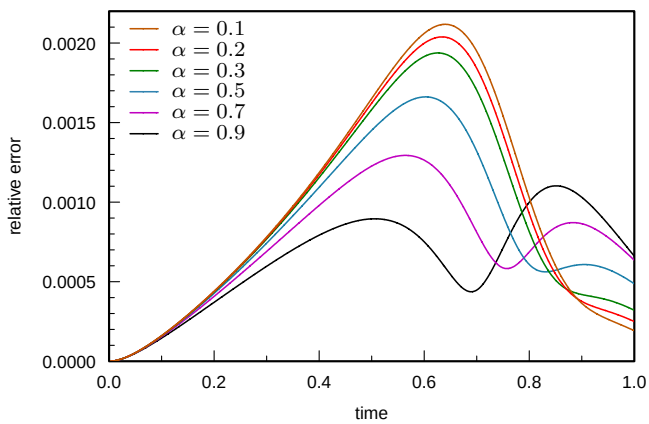

Figure 6.6: The dependence of the relative error (6.20) of the numerical scheme (6.22), (6.11) in time on the parameter of nonlinearity α. Sinusoidal in time exact solution (6.25) is considered. A smaller time step is needed, in comparison with the problem with linear exact solution (Figure 6.5), to obtain satisfactory accuracy. The parameters $\tau = 0.001, h = \sqrt{3}$ and $\eta = 3$ are considered.

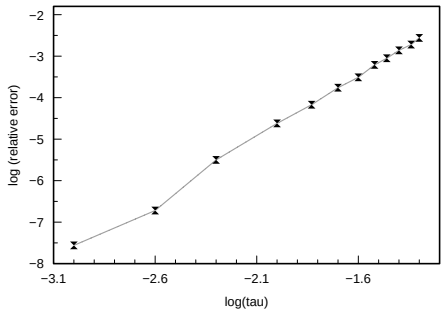

Figure 6.7: The dependence of the relative error (6.20) of the numerical scheme (6.22), (6.11) on the length of the time step τ. Linear in time exact solution (6.24) is considered. The fixed parameters $\alpha = 0.2, h = \sqrt{3}, \eta = 3$ and $L = 19.9$ are used. The rate of convergence is approximately 2.9, which is much better result than our estimate from Theorem 6.5.

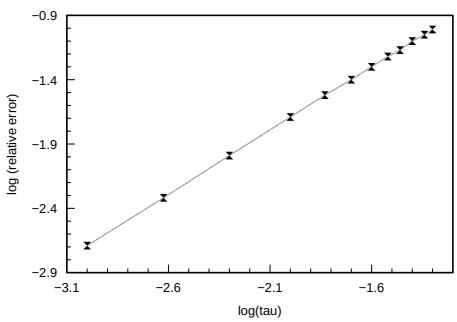

Figure 6.8: The dependence of the relative error (6.20) of the numerical scheme (6.22), (6.11) on the length of the time step τ. Sinusoidal in time exact solution (6.25) is considered. The fixed parameters $\alpha = 0.2, h = \sqrt{3}, \eta = 3$ and $L = 19.9$ are used. The rate of convergence is 0.99, which coincides with our estimate from Theorem 6.5.

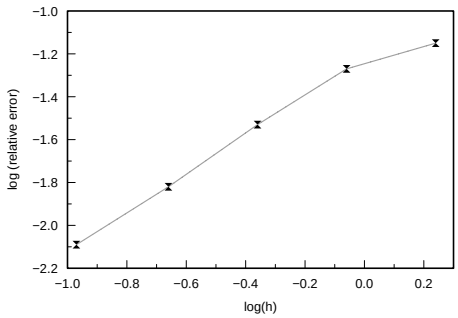

Figure 6.9: The dependence of the relative error (6.20) of the numerical scheme (6.22), (6.11) on the choice of the discretization parameter h. The exact solution (6.26) with sinusoidal behavior in the space variable is considered. The parameters $\alpha = 0.2, \tau = 0.05, \eta = 3$ and $L = 19.9$ are fixed. The rate of convergence is 0.9, which is better result than our estimate from Theorem 6.5.

n° ref.	h	discret. error	relative error	comput. time
0	$\sqrt{3}$	0.072319	0.071533	00:00:02
1	$\sqrt{3}/2$	0.053718	0.053352	00:00:14
2	$\sqrt{3}/4$	0.029336	0.029259	00:01:42
3	$\sqrt{3}/8$	0.014982	0.014973	00:13:08
4	$\sqrt{3}/16$	0.007530	0.008050	02:00:25

Table 6.1: Summarized results from Figure 6.9. The dependence of the relative error tracks the values of the discretization error $\|\boldsymbol{H}_0 - r_h \boldsymbol{H}_0\|$.

6.4.2 Convergence of the approximation in one time layer

In the previous subsection the development of the relative error in time was shown, depending on all the method parameters. Here, we investigate the convergence of our approximation within one particular time layer. As one can see in Figure 6.2, it is an iterative process which stops when the difference between two consecutive iterations in the domain as well as on the boundary is smaller than some fixed value τ^η.

n° ref.	h	relative error	comput. time
0	$\sqrt{3}$	0.001729	00:00:02
1	$\sqrt{3}/2$	0.001401	00:00:15
2	$\sqrt{3}/4$	0.002083	00:01:50
3	$\sqrt{3}/8$	0.002808	00:13:02
4	$\sqrt{3}/16$	0.003336	02:01:01

Table 6.2: The dependence of the relative error (6.20) of the numerical scheme (6.22), (6.11) on the mesh refinement. Linear in time exact solution (6.24) is considered. The parameters $\tau = 0.05, \alpha = 0.2, \eta = 3$ and $L = 19.9$ are fixed. With more refinements the relative error increases slightly because of accumulation of calculation errors.

We consider fixed parameters h, τ and η. For each parameter of nonlinearity α, an optimal value of L is chosen in line with Remark 6.1.

If the parameter α approaches zero, more iterations are required to obtain the same accuracy. This phenomenon is visible both when the linear exact solution (6.24) or the periodical one (6.26) is considered, see Tables 6.3 and 6.4, respectively. Such a behavior was expected, because with smaller α the nature of the problem becomes more nonlinear and consequently more complex.

In the previous subsection we discussed that the sinusoidal exact solution (6.26) can be fitted by Whitney's elements only with precision reported as discretization error. The magnitude of the discretization error for the basic mesh and mesh $1, 2, 3$ and 4 times refined can be found in Table 6.1. Thus, if the mesh consists of 3072 elements (3 refinements of the basic mesh), the exact solution (6.26) is fitted by Whitney's edge elements with an error of about 1.5%. The discretization error is the minimal error which can be reached. If the relative error reaches this "limit" value, no more iterations are needed, see Figure 6.10. The convergence of the method is fast, its slope depends on parameter α.

			relative error	
α	L	n° iter.	first iter.	last iter.
0.1	31.55	40	0.014701	0.000858
0.2	19.91	29	0.014483	0.000507
0.3	12.56	21	0.014355	0.000295
0.5	5.025	11	0.014244	0.000109
0.7	2.078	6	0.014206	0.000043
0.9	1.076	4	0.014190	0.000003

Table 6.3: The evolution of the relative error (6.20) of the approximation scheme (6.22), (6.11) in one time layer. The problem with linear exact solution (6.24) is considered. The parameters $\tau = 0.05, \eta = 3$ and an optimal L are fixed. The mesh consists of 48 elements (1 refinement).

Remark 6.2 (The situation on the boundary)
The convergence of our approximation on the boundary within one particular time layer is studied using the relative error

$$\max_{t\in[0,T]} \frac{\left\|\boldsymbol{H}(t) - \overline{\boldsymbol{u}}_n^h(t)\right\|_\Gamma}{\left\|\boldsymbol{H}(t)\right\|_\Gamma}. \tag{6.27}$$

Again, if the parameter α approaches zero, more iterations are required in order to obtain the same accuracy, see Table 6.5.

If the mesh consists of 3072 elements (3 refinements of the basic mesh), the exact solution (6.26) is fit on the boundary by Whitney's edge elements with an error of about 0.9%. The discretization error is the minimal error which can be reached. If the relative error reaches this "limit" value, no more iterations are needed, see Figure 6.11.

			relative error	
α	L	n° iter.	first iter.	last iter.
0.1	31.55	47	0.022021	0.015079
0.2	19.91	36	0.021783	0.014975
0.3	12.56	27	0.021642	0.014919
0.5	5.03	14	0.021521	0.014865
0.7	2.08	7	0.021471	0.014831
0.9	1.08	4	0.021441	0.014809

Table 6.4: The evolution of the relative error (6.20) of the approximation scheme (6.22), (6.11) in one time layer. Problem with sinusoidal exact solution (6.26) is considered. The parameters $\tau = 0.05, \eta = 3$ and an optimal L are fixed. The mesh consists of 3072 elements (3 refinements).

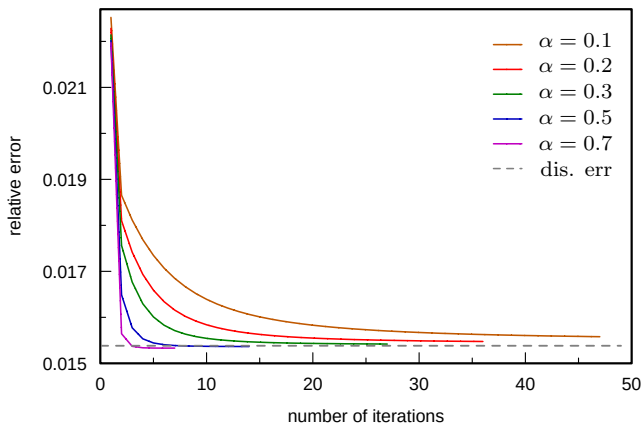

Figure 6.10: The relative error (6.20) of the approximation scheme (6.22), (6.11) depending on the number of iterations. The nonlinearity is given by (6.23) and sinusoidal in space exact solution (6.26) is considered. The mesh consists of 3072 elements. The exact solution can be fitted by Whitney's elements with a discretization error of 1.5%. Hence, it is the smallest error which can be reached.

			relative error on Γ	
α	L	n° iter.	first iter.	last iter.
0.1	31.55	47	0.016554	0.010162
0.2	19.91	36	0.015999	0.009795
0.3	12.56	27	0.015643	0.009610
0.5	5.03	14	0.015330	0.009473
0.7	2.08	7	0.015213	0.009408
0.9	1.08	4	0.015159	0.009371

Table 6.5: The evolution of the relative error (6.27) of the approximation scheme (6.22), (6.11) in one time layer on the boundary of the domain. Problem (6.26) with sinusoidal exact solution is considered. The parameters $\tau = 0.05, \eta = 3$ and an optimal L are fixed. The mesh consists of 3072 elements (3 refinements).

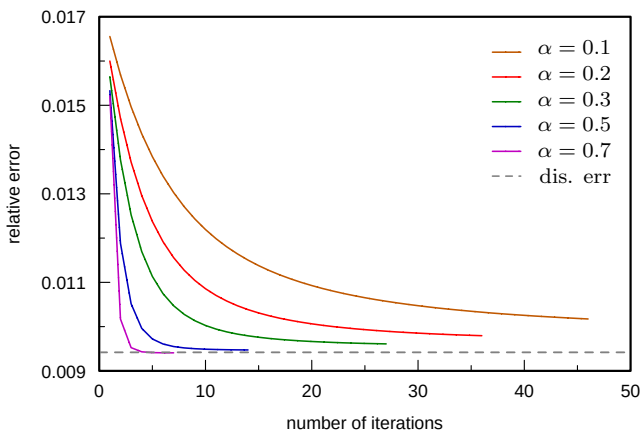

Figure 6.11: The same situation as in Figure 6.10, but the norm is calculated only on the boundary. The exact solution can be fitted on the boundary by Whitney's elements with a discretization error of 0.9%. Hence, it is the smallest error which can be reached.

6.5 Conclusions

In this chapter we have proved theoretically and also numerically the convergence of the proposed scheme (6.10), (6.11) to the boundary value problem (4.6) with constitutive law (4.4). This nonlinear scheme describes the evolution of electromagnetic fields in a bounded domain, when a non–perfect contact between two different materials is considered on the boundary.

Thanks to the new character of the nonlinear vector function $\boldsymbol{G}$ (by using a cut-off for large and small values of magnetic field, see (4.4)), the error estimate for the time discretization was improved in comparison with Chapter 5.

The convergence of the approximation scheme with respect to the length of the time step τ coincides with the theory. The convergence with respect to the size of the mesh h is even faster than the derived estimates predict. However, the numerical experiments can be influenced by the choice of the exact solution.

The linearization scheme is based on the fixed-point principle. One could have expected the method to be slow, see [53], where the author needs several hundred internal iterations to reach the stopping criterion. Nevertheless, based on our numerical results we regard the method as fast, robust and stable. The main reason is that the nonlinearity in the whole domain, as was investigated by Janíková in [53], causes more difficulties and decelerates the method more than the nonlinearity acting only on the boundary.

Figures 6.10 and 6.11 illustrate that the internal iterations have the same character. The relative error decreases rapidly at the beginning and stays relatively constant after a while. The reason is that the relative error is obtained as a sum of the linearization and the space discretization error. In the beginning the linearization error is dominant but with increasing number of iterations it becomes subjacent to the discretization one. Thus, we can conclude that the finer the mesh, the smaller the relative error. However, the mesh diameter has to be chosen reasonably to avoid an excessive increase of computational time and memory consumption.

Part II

Direct problems in high-frequency electromagnetism

Chapter 7

Problem formulation

The high-frequency domain includes the study of electromagnetic waves and propagation of energy through matter. Because a high–frequency domain is difficult to define, we assume a domain of electromagnetic fields in which the displacement currents cannot be neglected.

If the computing domain Ω coincides with the complement of a bounded domain Ω_{int}, $\Omega = \mathbb{R}^3 - \Omega_{int}$, we speak of an exterior boundary value problem. Numerical methods for the solution of exterior problems have received special attention in the past. Since the pioneering work of Engquist and Majda [35] in 1977, the method of Artificial Boundary Condition (ABC) has been widely used for wave problems. On top of standard boundary conditions imposed on the domain boundary, an additional condition at infinity must be added. This condition represents an ABC used for truncation of an unbounded propagation domain to a bounded one suitable for computations. An ABC is then given as a relation linking the traces of the wave on the fictitious boundary and approximately models the propagation of the wave through the surface, from the computational domain to its exterior. Moreover, it is a guaranty of unique and well-posed solution to the differential problem.

There are many important areas of applications where artificial boundaries are used. We can also find them in the literature under the name *dynamic* or *evolution*, because they describe the processes outside the computational domain which change dynamically and develop in the time. Typical examples are found in local weather prediction, see [32, 72], geophysical calculations involving acoustic and elastic waves, see [14, 56]. The dynamic BCs are very natural in

many mathematical models as heat transfer in a solid in contact with moving fluid, thermoelasticity and diffusion phenomena, see [73]. They also appear in study of the Stefan problem when the boundary material has a large thermal conductivity and sufficiently small thickness. Hence, the boundary material is regarded as the boundary of the domain. A degenerate elliptic–parabolic problem with nonlinear dynamic BCs and with applications in the Stefan problem is considered, for instance, in [4].

In [26] the stability of parabolic problems with special type of nonlinear dynamic BC, namely Wentzell BC, is studied. Such a boundary value problem can model a diffusion process, for example, the heat equation with a heat source on the boundary. Specially in [26] the authors discussed the situation when the heat source on the boundary depends nonlinearly on the heat flow across and the temperature on the boundary and the heat can transfer along the boundary. For more information about the parabolic problems with dynamic Wentzell BCs, see [25, 39, 94].

The monograph [90] is devoted to the heat equation in the perforated domain. There the authors deal with the case in which the perforations are periodically distributed and their size is uniform. The dynamic BC is considered on the surface of the holes.

Heat equation supplied with dynamic BCs of reactive type is studied in [92].

Arrieta, Quittner and Bernal also treat parabolic problems with nonlinear dynamic BCs. In [6] they are interested in the largest possible growth of the nonlinear terms in appropriate spaces.

The wave equation with second order nonstandard dynamic BCs is discussed, for instance, in [93]. A one dimensional model describes transversal small oscillations of an elastic rod with a tip mass on one endpoint, while the other one is pinched (see [27, 46]). A two dimensional model introduced in [43] deals with a vibrating membrane. A three dimensional model elaborated in [10] describes small irrotational perturbation from the rest state of a gas contained in a locally reacting chamber.

In this and the following chapter, an ABC with linear character is assumed. Unlike in the low-frequency part, see Chapters 5 and 6, the difficulties with the nonlinearity fall out. The complexity of the exterior boundary problem originates in its mathematical description by the full system of Maxwell's equations whereas at high frequencies, the electric and magnetic fields are interdependent.

Let Ω be a bounded domain of $\mathbb{R}^3$ whose boundary $\partial\Omega$ consists of two disconnected parts Σ and Γ that are both regular enough to define a normal vector $\boldsymbol{\nu}$ outwardly directed to $\partial\Omega$. The geometry of the computational domain is depicted in Figure 7.1(b). The boundary Γ corresponds to the surface limiting a regular body, namely the scatterer, which is perfectly conducting. The boundary Σ is also regular, satisfies $\Gamma \cap \Sigma = \emptyset$ and it is the exterior boundary of Ω.

The way we deal with the ABC is motivated by the work of H. Barucq [7], where the theory of propagating electromagnetic waves in an unbounded domain is elaborated in two dimensions. She studied a TE-polarized electromagnetic field $(\boldsymbol{E}, H)$ described by the Maxwell equations

$$\begin{array}{ll} \varepsilon\partial_t \boldsymbol{E} - \mathbf{Curl}\, H = \mathbf{0}, \quad \mu\partial_t H + \mathrm{curl}\boldsymbol{E} = 0 & \text{in } O \times (0,\infty), \\ \mathrm{div}\, \boldsymbol{E} = 0 & \text{in } O \times (0,\infty), \\ \boldsymbol{E}(\boldsymbol{x},0) = \boldsymbol{E}_0(\boldsymbol{x}), \quad H(\boldsymbol{x},0) = H_0(\boldsymbol{x}) & \text{in } O, \\ \boldsymbol{E} \times \boldsymbol{\nu} = J & \text{on } \Gamma \times (0,\infty). \end{array} \tag{7.1}$$

The parameters ε and μ are the dielectric constants, O is an unbounded domain of $\mathbb{R}^2$. The boundary of O is denoted by Γ and is regular enough to define a normal vector $\boldsymbol{\nu}$ outwardly directed to O. If ∂_1 and ∂_2 denote the spatial derivatives, the operators $\mathbf{Curl}$ and curl are respectively defined by

$$\mathbf{Curl}\, \varphi = (\partial_2\varphi, -\partial_1\varphi)^t, \qquad \mathrm{curl}\boldsymbol{v} = \partial_1 v_2 - \partial_2 v_1$$

and they coincide with the usual definition of the curl operator $\mathbf{curl} = \nabla\times$ as follows. Consider the vector $\boldsymbol{\varphi} = (0,0,\varphi)^t$ where φ only depends on x_1 and x_2. Then, $\mathbf{curl}\, \boldsymbol{\varphi} = \mathbf{Curl}\, \varphi$. In the same way, if $\boldsymbol{v} = (v_1, v_2, 0)^t$ with v_1 and v_2 only depending on x_1 and x_2, then $\mathbf{curl}\, \boldsymbol{v} = (0, 0, \mathrm{curl}\ \boldsymbol{v})^t$. The source J is assumed to be compactly time-supported in $[0, T]$.

Barucq showed that the unbounded domain O can be truncated by an auxiliary surface Σ in O. She also characterized the propagation of $(\boldsymbol{E}, H)$ from the interior of Σ to its exterior by a first order condition

$$\partial_t(\boldsymbol{E} \times \boldsymbol{\nu} + H) = \alpha(\boldsymbol{x})\boldsymbol{E} \times \boldsymbol{\nu} + \beta(\boldsymbol{x})H \qquad \text{on } \Sigma \times (0,\infty). \tag{7.2}$$

Here the functions α and β are regular functions defined on Σ, given by

$$\alpha(\boldsymbol{x}) = \frac{\kappa(\boldsymbol{x})}{4} - \gamma(\boldsymbol{x}) \qquad \text{and} \qquad \beta(\boldsymbol{x}) = -\frac{\kappa(\boldsymbol{x})}{4} - \gamma(\boldsymbol{x}), \tag{7.3}$$

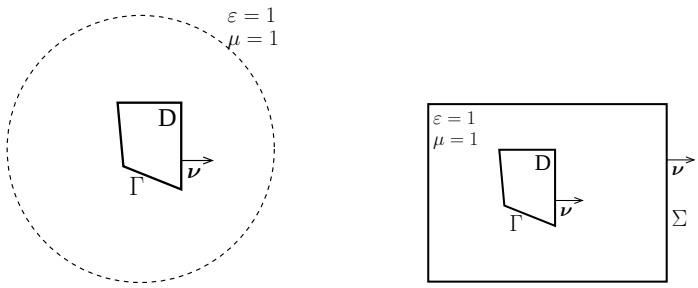

(a) Unbounded domain. Background of scatterer surrounded by air or vacuum.

(b) Bounded domain suitable for computations. An absorbing boundary condition prescribed on the auxiliary boundary Σ.

Figure 7.1: Geometry of the scatterer and the boundaries. The boundary Γ of the scatterer is perfectly conducting. An unbounded domain of propagation of electromagnetic waves is truncated by introducing an artificial boundary Σ limiting the computational domain. A suitable boundary condition is assumed on this artificial boundary.

where γ is an arbitrary regular function defined on Σ and κ is the curvature of Σ. From the convexity of the area one can conclude that κ is non-negative. The condition (7.2) has been derived using pseudodifferential calculus, see [86]. Barucq analyzed the Maxwell system along with (7.2) and showed the well-posedness and long time behavior of the solution. Her work stimulated us to extend the mentioned problem to three dimensions.

Thus, the 3D case of (7.1) is studied. We consider the mixed problem[1]: Find $\{\boldsymbol{E}, \boldsymbol{H}\}$ solution to

$$\begin{aligned}
&\partial_t \boldsymbol{E} - \nabla \times \boldsymbol{H} = \boldsymbol{0}, \quad \partial_t \boldsymbol{H} + \nabla \times \boldsymbol{E} = \boldsymbol{0} && \text{in } \Omega \times (0, \infty), \\
&\boldsymbol{E}(\boldsymbol{x}, 0) = \boldsymbol{E}_0(\boldsymbol{x}), \quad \boldsymbol{H}(\boldsymbol{x}, 0) = \boldsymbol{H}_0(\boldsymbol{x}) && \text{in } \Omega, \\
&\boldsymbol{E} \times \boldsymbol{\nu} = \boldsymbol{0} && \text{on } \Gamma \times (0, \infty), \\
&\partial_t \left(\boldsymbol{E} \times \boldsymbol{\nu} - \boldsymbol{H} \times \boldsymbol{\nu} \times \boldsymbol{\nu} \right) = \alpha \boldsymbol{E} \times \boldsymbol{\nu} - \beta \boldsymbol{H} \times \boldsymbol{\nu} \times \boldsymbol{\nu} && \text{on } \Sigma \times (0, \infty).
\end{aligned} \tag{7.4}$$

Note that the last equation in (7.4) represents a 3D analogue of (7.2) – see also [37, p. 354].

[1]For simplicity, we put $\varepsilon = \mu = 1$, $\boldsymbol{J} = \boldsymbol{0}$.

Throughout the following chapter we assume that

$$\exists K < 0 : \; 0 > \alpha(\boldsymbol{x}) > K \;\text{ and }\; 0 > \alpha(\boldsymbol{x}) \geq \beta(\boldsymbol{x}) \quad \forall \boldsymbol{x} = (x_1, x_2, x_3)^t \in \Sigma, \tag{7.5}$$

which means that the boundary Σ has a positive curvature.

Further, in Chapter 8, we formulate the variational formulation to the boundary value problem (7.4) and specify the appropriate function spaces of test functions. The goal of the next chapter is to design a numerical scheme for solving the mentioned variational problem.

Let us note that our analysis is also valid in 2D.

Chapter 8

Time discretization

The aim of this chapter is to propose an efficient numerical approximation of the solution to the scattering problem arising from the propagation of electromagnetic fields through an unbounded domain, see Figure 7.1(a). We study a system of time-dependent Maxwell's equations (7.4) with a first order boundary condition on an artificial part of the boundary.

One of the simplest ABCs is the Silver-Müller condition with dissipative character (cf. [22, 40]). The combination of the second order Maxwell system with the first order BC has been studied in [8], where the asymptotic analysis has been worked out. Model of absorbing boundary was suggested by Bérenger [12, 13] in 1994. The revolutionary method of *Perfectly Match Layer (PML)* yields no reflection at any wave number and any angle of incidence of the scattered wave at the "sponge" layer interface.

This chapter, based on the article [84], is organized as follows. After the rigorous definition of the problem we propose the time-discretization scheme using the backward Euler method, as we have done in previous chapters. Consequently the well-posedness of the problem in 3D is proved in Lemma 8.1. In Section 8.2 the long-time stability results for the time discrete approximate solution are derived. The main results are formulated in Theorems 8.1 and 8.2. Here, the linear dependence of the error of proposed time-discrete scheme on the choice of the time step τ is shown.

Most of the theoretical results of this chapter were presented at the international conference NumAn 2008 and are summarized in the paper [82], published in the proceedings of the conference.

Considering the problem setting (7.4) introduced in Chapter 7, the related variational formulation reads

$$\begin{aligned}
&(\partial_t \boldsymbol{E}, \boldsymbol{\varphi}) - (\nabla \times \boldsymbol{H}, \boldsymbol{\varphi}) &&= 0,\\
&(\partial_t \boldsymbol{H}, \boldsymbol{\psi}) + (\boldsymbol{E}, \nabla \times \boldsymbol{\psi}) &&= (\boldsymbol{E} \times \boldsymbol{\nu}, \boldsymbol{\psi})_\Sigma\,,\\
&(\partial_t\,(\boldsymbol{E} \times \boldsymbol{\nu} - \boldsymbol{H} \times \boldsymbol{\nu} \times \boldsymbol{\nu})\,, \boldsymbol{\xi})_\Sigma &&= (\alpha \boldsymbol{E} \times \boldsymbol{\nu} - \beta \boldsymbol{H} \times \boldsymbol{\nu} \times \boldsymbol{\nu}, \boldsymbol{\xi})_\Sigma
\end{aligned} \tag{8.1}$$

for any $\boldsymbol{\varphi} \in \boldsymbol{V}, \boldsymbol{\psi} \in \boldsymbol{W}, \boldsymbol{\xi} \in \mathbf{L}_2\,(\Sigma)$ and for a.e. $t \in [0, \infty)$. The spaces of test functions are defined as follows

$$\begin{aligned}
\boldsymbol{V} &= \{\boldsymbol{\varphi} \in \mathbf{H}(\mathbf{curl}\,;\Omega);\ \boldsymbol{\varphi} \times \boldsymbol{\nu} = \mathbf{0} \ \text{ on } \Gamma,\ \boldsymbol{\varphi} \times \boldsymbol{\nu} \in \mathbf{L}_2\,(\Sigma)\},\\
\boldsymbol{W} &= \{\boldsymbol{\varphi} \in \mathbf{H}(\mathbf{curl}\,;\Omega);\ \boldsymbol{\varphi} \times \boldsymbol{\nu} \in \mathbf{L}_2\,(\Sigma)\}.
\end{aligned}$$

Both spaces are endowed with the same graph norm

$$\|\boldsymbol{\varphi}\|^2_{\boldsymbol{V}} = \|\boldsymbol{\varphi}\|^2_{\boldsymbol{W}} = \|\boldsymbol{\varphi}\|^2_{\mathbf{H}(\mathbf{curl}\,;\Omega)} + \|\boldsymbol{\varphi} \times \boldsymbol{\nu}\|^2_{\mathbf{L}_2(\Sigma)}\,.$$

8.1 Discretization scheme

Using the standard backward Euler method for time discretization, we suggest the following linear recurrent approximation scheme for $i \in \mathbb{N}$:

(1) start from $\boldsymbol{e}_{i-1}, \boldsymbol{h}_{i-1}$, taking into account $\boldsymbol{e}_0 = \boldsymbol{E}_0\,, \boldsymbol{h}_0 = \boldsymbol{H}_0\,.$

(2) solve the system of PDEs with unknowns $\boldsymbol{e}_i, \boldsymbol{h}_i$

$$\begin{aligned}
&(\delta \boldsymbol{e}_i, \boldsymbol{\varphi}) - (\nabla \times \boldsymbol{h}_i, \boldsymbol{\varphi}) &&= 0,\\
&(\delta \boldsymbol{h}_i, \boldsymbol{\psi}) + (\boldsymbol{e}_i, \nabla \times \boldsymbol{\psi}) &&= (\boldsymbol{e}_i \times \boldsymbol{\nu}, \boldsymbol{\psi})_\Sigma\,,\\
&(\delta \boldsymbol{e}_i \times \boldsymbol{\nu} - \delta \boldsymbol{h}_i \times \boldsymbol{\nu} \times \boldsymbol{\nu}, \boldsymbol{\xi})_\Sigma &&= (\alpha \boldsymbol{e}_i \times \boldsymbol{\nu} - \beta \boldsymbol{h}_i \times \boldsymbol{\nu} \times \boldsymbol{\nu}, \boldsymbol{\xi})_\Sigma
\end{aligned} \tag{8.2}$$

for any $\boldsymbol{\varphi} \in \boldsymbol{V}, \boldsymbol{\psi} \in \boldsymbol{W}, \boldsymbol{\xi} \in \mathbf{L}_2\,(\Sigma)\,.$

First we analyze the BC on Σ :

$$\begin{aligned}
\delta\,(\boldsymbol{e}_i \times \boldsymbol{\nu} - \boldsymbol{h}_i \times \boldsymbol{\nu} \times \boldsymbol{\nu}) &= \alpha \boldsymbol{e}_i \times \boldsymbol{\nu} - \beta \boldsymbol{h}_i \times \boldsymbol{\nu} \times \boldsymbol{\nu}\\
&= \alpha\,(\boldsymbol{e}_i \times \boldsymbol{\nu} - \boldsymbol{h}_i \times \boldsymbol{\nu} \times \boldsymbol{\nu}) + (\alpha - \beta) \boldsymbol{h}_i \times \boldsymbol{\nu} \times \boldsymbol{\nu}.
\end{aligned}$$

Applying the backward Euler method to the discretization in time one obtains the following solution

$$\begin{aligned}
&\boldsymbol{e}_i \times \boldsymbol{\nu} - \boldsymbol{h}_i \times \boldsymbol{\nu} \times \boldsymbol{\nu} =\\
&(1 - \tau\alpha)^{-i}[\boldsymbol{e}_0 \times \boldsymbol{\nu} - \boldsymbol{h}_0 \times \boldsymbol{\nu} \times \boldsymbol{\nu}] + \tau(\alpha - \beta) \sum_{j=1}^{i} (1 - \tau\alpha)^{j-i-1} \boldsymbol{h}_j \times \boldsymbol{\nu} \times \boldsymbol{\nu}\,.
\end{aligned} \tag{8.3}$$

This can be recast as

$$\boldsymbol{e}_i \times \boldsymbol{\nu} - \boldsymbol{h}_i \times \boldsymbol{\nu} \times \boldsymbol{\nu} \quad = \boldsymbol{B}_{i-1} + \tau(\alpha - \beta)(1 - \tau\alpha)^{-1} \boldsymbol{h}_i \times \boldsymbol{\nu} \times \boldsymbol{\nu}, \tag{8.4}$$

where

$$\boldsymbol{B}_{i-1} = (1 - \tau\alpha)^{-i}[\boldsymbol{e}_0 \times \boldsymbol{\nu} - \boldsymbol{h}_0 \times \boldsymbol{\nu} \times \boldsymbol{\nu}] + \tau(\alpha - \beta) \sum_{j=1}^{i-1} (1 - \tau\alpha)^{j-i-1} \boldsymbol{h}_j \times \boldsymbol{\nu} \times \boldsymbol{\nu}\,.$$

Hence, we find

$$\boldsymbol{e}_i \times \boldsymbol{\nu} = \boldsymbol{B}_{i-1} + \left[1 + \tau(\alpha - \beta)(1 - \tau\alpha)^{-1}\right] \boldsymbol{h}_i \times \boldsymbol{\nu} \times \boldsymbol{\nu}.$$

The next lemma shows the existence of $\boldsymbol{e}_i, \boldsymbol{h}_i$ on each time step.

8.1.1 Well–posedness

Lemma 8.1 *Let $\boldsymbol{E}_0, \boldsymbol{H}_0 \in \mathbf{L}_2(\Omega)$ and $\boldsymbol{E}_0 \times \boldsymbol{\nu}, \boldsymbol{H}_0 \times \boldsymbol{\nu} \in \mathbf{L}_2(\Sigma)$. Assume (7.5). Then for any $i \in \mathbb{N}$ and any fixed sufficiently small τ, there exist uniquely determined $\boldsymbol{e}_i \in \boldsymbol{V}, \boldsymbol{h}_i \in \boldsymbol{W}$ satisfying (8.2).*

Proof: Suppose that we want to prove the existence and uniqueness of the solution for the following system

$$\begin{aligned} &(\boldsymbol{e}, \boldsymbol{\varphi}) - \tau\,(\nabla \times \boldsymbol{h}, \boldsymbol{\varphi}) && = (\boldsymbol{a}, \boldsymbol{\varphi})\,, \\ &(\boldsymbol{h}, \boldsymbol{\psi}) + \tau\,(\boldsymbol{e}, \nabla \times \boldsymbol{\psi}) + \tau\,(K\boldsymbol{h} \times \boldsymbol{\nu}, \boldsymbol{\psi} \times \boldsymbol{\nu})_\Sigma && = (\boldsymbol{b}, \boldsymbol{\psi}) + \tau\,(\boldsymbol{B}, \boldsymbol{\psi})_\Sigma\,, \end{aligned} \tag{8.5}$$

where

$$\begin{aligned} &K = [1 + \tau(\alpha - \beta)(1 - \tau\alpha)^{-1}] \geq 1\,, && (\boldsymbol{a}, \boldsymbol{\varphi}) = (\boldsymbol{e}_{i-1}, \boldsymbol{\varphi})\,, \\ &(\boldsymbol{B}, \boldsymbol{\psi})_\Sigma = (\boldsymbol{B}_{i-1}, \boldsymbol{\psi})_\Sigma\,, && (\boldsymbol{b}, \boldsymbol{\psi}) = (\boldsymbol{h}_{i-1}, \boldsymbol{\psi}) \end{aligned} \tag{8.6}$$

for any $\boldsymbol{\varphi} \in \boldsymbol{V}, \boldsymbol{\psi} \in \boldsymbol{W}$ and some $\boldsymbol{a}, \boldsymbol{b} \in \mathbf{L}_2(\Omega)\,, \boldsymbol{B} \in \mathbf{L}_2(\Sigma)$.

We approximate the spaces $\boldsymbol{V}, \boldsymbol{W}$ by their finite dimensional subspaces $\boldsymbol{V}_k = [\boldsymbol{\varphi}_1, \ldots, \boldsymbol{\varphi}_k]$ and $\boldsymbol{W}_l = [\boldsymbol{\psi}_1, \ldots, \boldsymbol{\psi}_l]$, respectively. Assume the following approximation property

$$\lim_{k \to \infty} \|\boldsymbol{\varphi} - P_k \boldsymbol{\varphi}\|_{\boldsymbol{V}} = \lim_{l \to \infty} \|\boldsymbol{\psi} - P_l \boldsymbol{\psi}\|_{\boldsymbol{W}} = 0 \tag{8.7}$$

for any $\boldsymbol{\varphi} \in \boldsymbol{V}, \boldsymbol{\psi} \in \boldsymbol{W}$. Here $P_k\,, P_l$ denote the projectors on $\boldsymbol{V}_k, \boldsymbol{W}_l$, respectively. The approximation of (8.5) reads

$$\begin{aligned} &(\boldsymbol{e}_k, \boldsymbol{\varphi}) - \tau\,(\nabla \times \boldsymbol{h}_l, \boldsymbol{\varphi}) && = (\boldsymbol{a}, \boldsymbol{\varphi})\,, \\ &(\boldsymbol{h}_l, \boldsymbol{\psi}) + \tau\,(\boldsymbol{e}_k, \nabla \times \boldsymbol{\psi}) + \tau\,(K\boldsymbol{h}_l \times \boldsymbol{\nu}, \boldsymbol{\psi} \times \boldsymbol{\nu})_\Sigma && = (\boldsymbol{b}, \boldsymbol{\psi}) + \tau\,(\boldsymbol{B}, \boldsymbol{\psi})_\Sigma \end{aligned} \tag{8.8}$$

for any $\boldsymbol{\varphi} \in \boldsymbol{V}_k,\ \boldsymbol{\psi} \in \boldsymbol{W}_l$.

We are looking for $\boldsymbol{e}_k, \boldsymbol{h}_l$ of the form $\boldsymbol{e}_k = \sum_{i=1}^{k} e_i \boldsymbol{\varphi}_i$ and $\boldsymbol{h}_l = \sum_{i=1}^{l} h_i \boldsymbol{\psi}_i$. Substituting this into (8.8), we obtain the following linear algebraic system (where the superscript T denotes the transpose)

$$\begin{aligned} \mathbb{A}\boldsymbol{e}_k - \mathbb{C}\boldsymbol{h}_l &= \boldsymbol{f}, \\ \mathbb{C}^T\boldsymbol{e}_k + \mathbb{B}\boldsymbol{h}_l &= \boldsymbol{g} + \boldsymbol{h} \end{aligned} \tag{8.9}$$

with

$$\begin{aligned} \mathbb{A} &= ((\boldsymbol{\varphi}_i, \boldsymbol{\varphi}_j)_\Omega)_{i,j=1,\dots,k} \\ \mathbb{B} &= ((\boldsymbol{\psi}_i, \boldsymbol{\psi}_j)_\Omega + \tau(K\boldsymbol{\psi}_i \times \boldsymbol{\nu}, \boldsymbol{\psi}_j \times \boldsymbol{\nu})_\Sigma)_{i,j=1,\dots,l} \\ \mathbb{C} &= \tau((\nabla \times \boldsymbol{\psi}_i, \boldsymbol{\varphi}_j)_\Omega)_{i=1,\dots l\,;j=1\dots k} \\ \boldsymbol{f} &= ((\boldsymbol{a}, \boldsymbol{\varphi}_j)_\Omega)^T_{j=1,\dots,k} \\ \boldsymbol{g} &= ((\boldsymbol{b}, \boldsymbol{\psi}_j)_\Omega)^T_{j=1,\dots,l} \\ \boldsymbol{h} &= \tau((\boldsymbol{B}, \boldsymbol{\psi}_j)_\Sigma)^T_{j=1,\dots,l}. \end{aligned} \tag{8.10}$$

The matrices $\mathbb{A}$ and $\mathbb{B}$ are symmetric and positive definite. Eliminating $\boldsymbol{e}_k$ from (8.9a) and setting the result into (8.9b) yields

$$\begin{aligned} &\boldsymbol{e}_k = \mathbb{A}^{-1}\boldsymbol{f} + \mathbb{A}^{-1}\mathbb{C}\boldsymbol{h}_l\,, \\ &\left[\mathbb{B} + \mathbb{C}^T\mathbb{A}^{-1}\mathbb{C}\right]\boldsymbol{h}_l = \boldsymbol{g} + \boldsymbol{h} - \mathbb{C}^T\mathbb{A}^{-1}\boldsymbol{f}. \end{aligned} \tag{8.11}$$

Due to the fact that the matrix $\mathbb{B} + \mathbb{C}^T\mathbb{A}^{-1}\mathbb{C}$ is regular, we have proved the existence of a unique solution $\boldsymbol{e}_k \in \boldsymbol{V}_k$ and $\boldsymbol{h}_l \in \boldsymbol{W}_l$ of (8.8).

As a next step we need uniform a priori estimates for $\boldsymbol{e}_k$ and $\boldsymbol{h}_l$ with respect to k and l. Therefore we set $\boldsymbol{\varphi} = \boldsymbol{e}_k\,, \boldsymbol{\psi} = \boldsymbol{h}_l$ in (8.8) and sum both equations. We get

$$\|\boldsymbol{e}_k\|^2 + \|\boldsymbol{h}_l\|^2 + \tau\,(K\boldsymbol{h}_l \times \boldsymbol{\nu}, \boldsymbol{h}_l \times \boldsymbol{\nu})_\Sigma = (\boldsymbol{a}, \boldsymbol{e}_k) + (\boldsymbol{b}, \boldsymbol{h}_l) + \tau(\boldsymbol{B}, \boldsymbol{h}_l)_\Sigma.$$

After applying Young's inequalities to the scalar product on the right-hand side, we obtain

$$\|\boldsymbol{e}_k\|^2 + \|\boldsymbol{h}_l\|^2 + \|\boldsymbol{h}_l \times \boldsymbol{\nu}\|^2_\Sigma \le C(\tau)\left(\|\boldsymbol{a}\|^2 + \|\boldsymbol{b}\|^2 + \|\boldsymbol{B}\|^2_\Sigma\right),$$

which is valid for any $k, l \in \mathbb{N}$.
Further we deduce

$$\begin{aligned} |(\nabla \times \boldsymbol{h}_l, \boldsymbol{\varphi})| &= |(\nabla \times \boldsymbol{h}_l, \boldsymbol{\varphi} - P_k\boldsymbol{\varphi}) + (\nabla \times \boldsymbol{h}_l, P_k\boldsymbol{\varphi})| \\ &= \left|(\boldsymbol{h}_l, \nabla \times (\boldsymbol{\varphi} - P_k\boldsymbol{\varphi})) - (\boldsymbol{h}_l \times \boldsymbol{\nu}, \boldsymbol{\varphi} - P_k\boldsymbol{\varphi})_\Sigma + \frac{1}{\tau}\,(\boldsymbol{e}_k - \boldsymbol{a}, P_k\boldsymbol{\varphi})\right| \\ &\le \|\boldsymbol{h}_l\|\,\|\nabla \times (\boldsymbol{\varphi} - P_k\boldsymbol{\varphi})\| + \|\boldsymbol{h}_l \times \boldsymbol{\nu}\|_\Sigma\,\|\boldsymbol{\varphi} - P_k\boldsymbol{\varphi}\|_\Sigma + \frac{1}{\tau}\,\|\boldsymbol{e}_k - \boldsymbol{a}\|\,\|P_k\boldsymbol{\varphi}\| \\ &\le C(\tau)\,\|\boldsymbol{\varphi}\|_{\boldsymbol{V}}\,, \end{aligned}$$

which yields that

$$\|\nabla \times \boldsymbol{h}_l\|_{\boldsymbol{V}^*} = \sup_{\|\boldsymbol{\varphi}\|_{\boldsymbol{V}} \leq 1} (\nabla \times \boldsymbol{h}_l, \boldsymbol{\varphi}) \leq C(\tau).$$

Due to the reflexivity of $\mathbf{L}_2(\Omega), \mathbf{L}_2(\Sigma)$ and $\boldsymbol{V}^*$ we can choose subsequences from $\boldsymbol{e}_k$ and $\boldsymbol{h}_l$ (denoted by the same symbol again) such that

$$\begin{array}{lll} \boldsymbol{e}_k & \rightharpoonup \boldsymbol{e} & \text{in } \mathbf{L}_2(\Omega), \\ \boldsymbol{h}_l & \rightharpoonup \boldsymbol{h} & \text{in } \mathbf{L}_2(\Omega), \\ \boldsymbol{h}_l \times \boldsymbol{\nu} & \rightharpoonup \boldsymbol{u} \times \boldsymbol{\nu} & \text{in } \mathbf{L}_2(\Sigma), \\ \nabla \times \boldsymbol{h}_l & \rightharpoonup \boldsymbol{w} & \text{in } \boldsymbol{V}^*. \end{array} \tag{8.12}$$

Now, for any $\boldsymbol{\varphi} \in \mathbf{H}_0(\mathbf{curl}\,;\Omega) \subset \boldsymbol{V}$ it holds

$$\begin{array}{ccc} (\nabla \times \boldsymbol{h}_l, \boldsymbol{\varphi}) & = & (\boldsymbol{h}_l, \nabla \times \boldsymbol{\varphi}) \\ \downarrow & & \downarrow \\ (\boldsymbol{w}, \boldsymbol{\varphi}) & = & (\boldsymbol{h}, \nabla \times \boldsymbol{\varphi}), \end{array}$$

which implies that $\boldsymbol{w} = \nabla \times \boldsymbol{h}$.

Further, for any $\boldsymbol{\varphi} \in \boldsymbol{V}$ we have

$$\begin{array}{ccccc} (\nabla \times \boldsymbol{h}_l, \boldsymbol{\varphi}) & = & (\boldsymbol{h}_l, \nabla \times \boldsymbol{\varphi}) & - & (\boldsymbol{h}_l \times \boldsymbol{\nu}, \boldsymbol{\varphi})_\Sigma \\ \downarrow & & \downarrow & & \downarrow \\ (\nabla \times \boldsymbol{h}, \boldsymbol{\varphi}) & = & (\boldsymbol{h}, \nabla \times \boldsymbol{\varphi}) & - & (\boldsymbol{u} \times \boldsymbol{\nu}, \boldsymbol{\varphi})_\Sigma, \end{array}$$

which implies that $\boldsymbol{u} \times \boldsymbol{\nu} = \boldsymbol{h} \times \boldsymbol{\nu}$.

In view of the approximation property (8.7), we deduce for any $\boldsymbol{\varphi} \in \boldsymbol{V}$ that

$$\begin{array}{ccccccc} (\boldsymbol{e}_k, P_k\boldsymbol{\varphi}) & = & (\boldsymbol{e}_k, \boldsymbol{\varphi}) & + & (\boldsymbol{e}_k, P_k\boldsymbol{\varphi} - \boldsymbol{\varphi}) & \overset{k\to\infty}{\longrightarrow} & (\boldsymbol{e}, \boldsymbol{\varphi}), \\ (\boldsymbol{a}, P_k\boldsymbol{\varphi}) & = & (\boldsymbol{a}, \boldsymbol{\varphi}) & + & (\boldsymbol{a}, P_k\boldsymbol{\varphi} - \boldsymbol{\varphi}) & \overset{k\to\infty}{\longrightarrow} & (\boldsymbol{a}, \boldsymbol{\varphi}) \end{array}$$

and

$$\begin{array}{rcl} |(\nabla \times \boldsymbol{h}_l, \boldsymbol{\varphi} - P_k\boldsymbol{\varphi})| & \leq & \|\nabla \times \boldsymbol{h}_l\|_{\boldsymbol{V}^*} \|\boldsymbol{\varphi} - P_k\boldsymbol{\varphi}\|_{\boldsymbol{V}} \\ & \leq & C(\tau) \|\boldsymbol{\varphi} - P_k\boldsymbol{\varphi}\| \\ & \overset{k\to\infty}{\longrightarrow} & 0 \qquad \text{for any } l. \end{array}$$

Therefore we can pass to the limit in (8.8a) for $k, l \to \infty$ to obtain (8.5a), which can be written as follows

$$(\boldsymbol{e}, \boldsymbol{\varphi}) - (\boldsymbol{a}, \boldsymbol{\varphi}) = \tau (\nabla \times \boldsymbol{h}, \boldsymbol{\varphi}).$$

The left-hand side can be seen as a bounded linear functional on $\mathbf{L}_2(\Omega)$ because of $\boldsymbol{e}, \boldsymbol{a} \in \mathbf{L}_2(\Omega)$. Hence, using a density argument and the Hahn-Banach theorem, see Appendix, we conclude that $\nabla \times \boldsymbol{h} \in \mathbf{L}_2(\Omega)$. This implies $\boldsymbol{h} \in \boldsymbol{W}$.

Analogously we can also proceed in (8.8b) to arrive at (8.5b), which can be written as

$$(\boldsymbol{h}, \boldsymbol{\psi}) - (\boldsymbol{b}, \boldsymbol{\psi}) = -\tau \left(\nabla \times \boldsymbol{e}, \boldsymbol{\psi}\right),$$

where $\nabla \times \boldsymbol{e} \in \boldsymbol{W}^*$.
Due to the fact that $\boldsymbol{h}, \boldsymbol{b} \in \mathbf{L}_2(\Omega)$, we analogously deduce that $\nabla \times \boldsymbol{e} \in \mathbf{L}_2(\Omega)$. Further, $\boldsymbol{E}_0 \times \boldsymbol{\nu} \in \mathbf{L}_2\left(\Sigma\right)$ together with (8.3) yield $\boldsymbol{e} \times \boldsymbol{\nu} \in \mathbf{L}_2\left(\Sigma\right)$, i.e. $\boldsymbol{e} \in \boldsymbol{V}$, which concludes the proof. □

8.2 A priori estimates

The next step is to derive suitable a priori estimates for $\boldsymbol{e}_i\,, \boldsymbol{h}_i\,; i \in \mathbb{N}$. They are obtained in the following lemmas.

We start with some preparatory work concerning integral inequalities. To prove the first lemma it is essential to know that when an integral kernel a satisfies

$$(-1)^j\, a^{(j)}(t) \geq 0 \qquad \forall t > 0\,; \quad j = 0, 1, 2\,; \quad a' \neq 0,$$

this implies the strong positiveness of the kernel a – see Staffans [85] – i.e.,

$$\int_0^T \int_0^t a(t-s)\Phi(s)\Phi(t)\ \mathrm{d}s\ \mathrm{d}t \geq 0 \qquad \forall T > 0\,, \quad \Phi \in C([0,T])\,. \tag{8.13}$$

Inspired by the continuous case, we show that an inequality similar to (8.13) holds true in a discrete form. Denoting $b_j = a(t_{j+1})$ for $j \in \{0, 1, \dots\}$, one can easily check that $\{b_j\}_{j=0}^{\infty} \in l_\infty$ is positive, convex and then (see Zygmund [101])

$$\frac{b_0}{2} + \sum_{j=1}^{\infty} b_j \cos(j\Theta) \geq 0 \quad \forall \Theta \in \mathbb{R}\,.$$

Hence, applying McLean-Thomée [63, Lemma 4.1], we get

$$B_k(\phi) = \sum_{i=1}^{k} \sum_{j=1}^{i} b_{i-j}\phi^j\phi^i \geq 0 \quad \forall \phi = (\phi^1, \dots, \phi^k) \in \mathbb{R}^k\,,\ k \geq 1\,.$$

This can be rewritten as follows

$$\tau^2 \sum_{i=1}^{k} \sum_{j=1}^{i} a(t_{i-j+1}) \phi^j \phi^i \geq 0 \qquad \forall \phi = (\phi^1, \ldots, \phi^k) \in \mathbb{R}^k \,,\, k \geq 1 \,. \tag{8.14}$$

Remark 8.1 *The non-negativity of the term $B_k(\phi)$ can be proved using the Fourier transform (denoted by $\hat{}$), so that, e.g.*

$$\hat{b}(\theta) = \sum_{j=0}^{\infty} b_j e^{ij\theta} \,.$$

Using Parseval's theorem, we have, by simple calculation, with $\phi^j = 0$ for $j \notin 1, \ldots, k$,

$$B_k(\phi) = \frac{1}{2\pi} \int_0^{2\pi} \hat{b}(\theta) |\hat{\phi}(\theta)|^2 \mathrm{d}\theta = \frac{1}{2\pi} \int_0^{2\pi} \Re\, \hat{b}(\theta) |\hat{\phi}(\theta)|^2 \mathrm{d}\theta \,,$$

where the latter equality follows since $B_k(\phi)$ is real-valued. As $\hat{b} = \Re\, \hat{b} = \sum_{j=0}^{\infty} b_j \cos(j\Theta) \geq 0$, this yields the result.

Lemma 8.2 *Let the assumptions of Lemma 8.1 be fulfilled. Then there exists a positive constant C such that for all $k \in \mathbb{N}$ and any sufficiently small $\tau > 0$ it holds*

$$\|\boldsymbol{e}_k\|^2 + \sum_{i=1}^{k} \|\boldsymbol{e}_i - \boldsymbol{e}_{i-1}\|^2 + \|\boldsymbol{h}_k\|^2 + \sum_{i=1}^{k} \|\boldsymbol{h}_i - \boldsymbol{h}_{i-1}\|^2 + \tau \sum_{i=1}^{k} \|\boldsymbol{h}_i \times \boldsymbol{\nu}\|_\Sigma^2 \leq C.$$

Proof: By setting $\boldsymbol{\varphi} = \boldsymbol{e}_i$, $\boldsymbol{\psi} = \boldsymbol{h}_i$ in (8.2), one can sum both equations and obtain

$$(\delta \boldsymbol{e}_i, \boldsymbol{e}_i) + (\delta \boldsymbol{h}_i, \boldsymbol{h}_i) - (\boldsymbol{h}_i, \boldsymbol{e}_i \times \boldsymbol{\nu})_\Sigma = 0 \,.$$

By multiplying with τ and summing for $i = 1, \ldots, k$ we have

$$\sum_{i=1}^{k} \tau\, (\delta \boldsymbol{e}_i, \boldsymbol{e}_i) + \sum_{i=1}^{k} \tau\, (\delta \boldsymbol{h}_i, \boldsymbol{h}_i) - \sum_{i=1}^{k} \tau\, (\boldsymbol{h}_i, \boldsymbol{e}_i \times \boldsymbol{\nu})_\Sigma = 0 \,.$$

Using Abel's summation for the first two terms, we deduce

$$\|\boldsymbol{e}_k\|^2 + \sum_{i=1}^{k} \|\boldsymbol{e}_i - \boldsymbol{e}_{i-1}\|^2 + \|\boldsymbol{h}_k\|^2 + \sum_{i=1}^{k} \|\boldsymbol{h}_i - \boldsymbol{h}_{i-1}\|^2 - 2\sum_{i=1}^{k} \tau\,(\boldsymbol{h}_i, \boldsymbol{e}_i \times \boldsymbol{\nu})_\Sigma = \|\boldsymbol{e}_0\|^2 + \|\boldsymbol{h}_0\|^2 \ . \tag{8.15}$$

Next we set expansion of the boundary term (8.3) into (8.15) and obtain

$$\begin{aligned}\|\boldsymbol{e}_k\|^2 + \sum_{i=1}^{k} \|\boldsymbol{e}_i - \boldsymbol{e}_{i-1}\|^2 + \|\boldsymbol{h}_k\|^2 + \sum_{i=1}^{k} \|\boldsymbol{h}_i - \boldsymbol{h}_{i-1}\|^2 + 2\tau \sum_{i=1}^{k} \|\boldsymbol{h}_i \times \boldsymbol{\nu}\|_\Sigma^2 \\ -2\tau \sum_{i=1}^{k} \big(\boldsymbol{h}_i, (1-\tau\alpha)^{-i}[\boldsymbol{e}_0 \times \boldsymbol{\nu} - \boldsymbol{h}_0 \times \boldsymbol{\nu} \times \boldsymbol{\nu}]\big)_\Sigma \\ +2(\alpha-\beta)\tau^2 \int_\Sigma \sum_{i=1}^{k} \sum_{j=1}^{i} (1-\tau\alpha)^{j-i-1} (\boldsymbol{h}_i \times \boldsymbol{\nu}) \cdot (\boldsymbol{h}_j \times \boldsymbol{\nu}) \\ = \|\boldsymbol{e}_0\|^2 + \|\boldsymbol{h}_0\|^2 \ .\end{aligned}$$

The third boundary term is nonnegative because of (8.14). We apply Young's inequality to the second boundary term, yielding

$$\begin{aligned}\|\boldsymbol{e}_k\|^2 + \sum_{i=1}^{k} \|\boldsymbol{e}_i - \boldsymbol{e}_{i-1}\|^2 + \|\boldsymbol{h}_k\|^2 + \sum_{i=1}^{k} \|\boldsymbol{h}_i - \boldsymbol{h}_{i-1}\|^2 + \tau \sum_{i=1}^{k} \|\boldsymbol{h}_i \times \boldsymbol{\nu}\|_\Sigma^2 \\ \le C\left(\|\boldsymbol{e}_0\|^2 + \|\boldsymbol{h}_0\|^2 + \|\boldsymbol{e}_0 \times \boldsymbol{\nu}\|_\Sigma^2 + \|\boldsymbol{h}_0 \times \boldsymbol{\nu}\|_\Sigma^2\right),\end{aligned}$$

which concludes the proof. □

Lemma 8.3 *Let the assumptions of Lemma 8.1 be fulfilled. Moreover assume* $\nabla \cdot \boldsymbol{E}_0 \in \mathbf{L}_2(\Omega)$. *Then* $\nabla \cdot \boldsymbol{e}_i = \nabla \cdot \boldsymbol{E}_0$ *in* $\mathbf{L}_2(\Omega)$ *for any* $i = 1, \ldots, n$.

Proof: The existence of $\boldsymbol{e}_i$ and $\boldsymbol{h}_i$ follows from Lemma 8.1.
Let us set $\boldsymbol{\varphi} = \nabla\Phi$ into (8.2a) for any $\Phi \in C_0^\infty(\overline{\Omega})$. Using Green's formula for the second term and due to the fact that $\nabla \times \nabla\Phi = 0$, we recursively obtain

$$(\boldsymbol{e}_i, \nabla\Phi) = (\boldsymbol{E}_0, \nabla\Phi) \ .$$

Applying integration by parts, we have

$$(\nabla \cdot \boldsymbol{e}_i, \Phi) = (\nabla \cdot \boldsymbol{E}_0, \Phi) \, .$$

The last equality is valid for all $\Phi \in C_0^\infty(\overline{\Omega})$. According to the assumption on $\nabla \cdot \boldsymbol{E}_0$, the right-hand side of the last identity can be seen as a bounded linear functional on $\mathbf{L}_2(\Omega)$. The density of $C_0^\infty(\overline{\Omega})$ in $\mathbf{L}_2(\Omega)$ together with the Hahn-Banach theorem conclude the proof. □

Remark 8.2 *Note that according to Lemma 8.3 the following implication is valid:*

$$\nabla \cdot \boldsymbol{E}_0 = 0 \qquad \Longrightarrow \qquad \nabla \cdot \boldsymbol{e}_i = 0, \qquad \forall i \in \mathbb{N}.$$

For the next lemma we need the following compatibility condition[1]

$$\begin{aligned} &(\partial_t \boldsymbol{E}(0), \boldsymbol{\varphi}) - (\nabla \times \boldsymbol{H}_0, \boldsymbol{\varphi}) = 0, \\ &(\partial_t \boldsymbol{H}(0), \boldsymbol{\psi}) + (\nabla \times \boldsymbol{\psi}, \boldsymbol{E}_0) - (\boldsymbol{\psi}, \boldsymbol{E}_0 \times \boldsymbol{\nu})_\Sigma = 0 \end{aligned} \tag{8.16}$$

for any $\boldsymbol{\varphi} \in \boldsymbol{V}, \boldsymbol{\psi} \in \boldsymbol{W}$.

The compatibility condition (8.16) is satisfied for smoother initial data, namely for $\boldsymbol{E}_0 \in \boldsymbol{V}$ and $\boldsymbol{H}_0 \in \boldsymbol{W}$. Then Green's theorem can be applied to (8.16). We define

$$\delta \boldsymbol{e}_0 := \partial_t \boldsymbol{E}(0) := \nabla \times \boldsymbol{H}_0, \qquad \delta h_0 := \partial_t \boldsymbol{H}(0) := -\nabla \times \boldsymbol{E}_0 \,.$$

Lemma 8.4 *Assume (7.5), $\boldsymbol{E}_0 \in \boldsymbol{V}$ and $\boldsymbol{H}_0 \in \boldsymbol{W}$. Then there exists a positive constant C such that*

$$\begin{aligned} \|\delta \boldsymbol{e}_k\|^2 + \sum_{i=1}^k \|\delta \boldsymbol{e}_i - \delta \boldsymbol{e}_{i-1}\|^2 + \|\delta \boldsymbol{h}_k\|^2 + \sum_{i=1}^k \|\delta \boldsymbol{h}_i - \delta \boldsymbol{h}_{i-1}\|^2 \\ + \tau \sum_{i=1}^k \|\delta \boldsymbol{h}_i \times \boldsymbol{\nu}\|_\Sigma^2 \le C \end{aligned}$$

holds for all $k \in \mathbb{N}$.

Proof: We subtract (8.2) for $i = i-1$ from (8.2), then we substitute $\boldsymbol{\varphi} = \delta \boldsymbol{e}_i$, $\boldsymbol{\psi} = \delta \boldsymbol{h}_i$. For $i = 0$ we use the compatibility condition

$$\begin{aligned} &(\delta \boldsymbol{e}_i - \delta \boldsymbol{e}_{i-1}, \delta \boldsymbol{e}_i) - (\nabla \times (\boldsymbol{h}_i - \boldsymbol{h}_{i-1}), \delta \boldsymbol{e}_i) = 0, \\ &(\delta \boldsymbol{h}_i - \delta \boldsymbol{h}_{i-1}, \delta \boldsymbol{h}_i) + (\nabla \times \delta \boldsymbol{h}_i, \boldsymbol{e}_i - \boldsymbol{e}_{i-1}) - (\delta \boldsymbol{h}_i, (\boldsymbol{e}_i - \boldsymbol{e}_{i-1}) \times \boldsymbol{\nu})_\Sigma = 0. \end{aligned}$$

[1] Compatibility between the boundary data and the initial condition, stating that the Maxwell equations (8.1) are satisfied at the time $t = 0$.

Adding both equations together and summing the result again for $i = 1, \dots, k$, we have

$$\sum_{i=1}^{k} (\delta \boldsymbol{e}_i - \delta \boldsymbol{e}_{i-1}, \delta \boldsymbol{e}_i) + \sum_{i=1}^{k} (\delta \boldsymbol{h}_i - \delta \boldsymbol{h}_{i-1}, \delta \boldsymbol{h}_i) = \sum_{i=1}^{k} (\delta \boldsymbol{h}_i, (\boldsymbol{e}_i - \boldsymbol{e}_{i-1}) \times \boldsymbol{\nu})_\Sigma \,.$$

Applying Abel's summation on the left, we deduce

$$\begin{aligned} &\|\delta \boldsymbol{e}_k\|^2 + \sum_{i=1}^{k} \|\delta \boldsymbol{e}_i - \delta \boldsymbol{e}_{i-1}\|^2 + \|\delta \boldsymbol{h}_k\|^2 + \sum_{i=1}^{k} \|\delta \boldsymbol{h}_i - \delta \boldsymbol{h}_{i-1}\|^2 \\ &= \|\delta \boldsymbol{e}_0\|^2 + \|\delta \boldsymbol{h}_0\|^2 + 2\tau \sum_{i=1}^{k} (\delta \boldsymbol{h}_i, \delta \boldsymbol{e}_i \times \boldsymbol{\nu})_\Sigma \,. \end{aligned}$$

Putting together the discrete boundary condition (8.2c) and the expansion (8.3), we obtain

$$\begin{aligned} &\|\delta \boldsymbol{e}_k\|^2 + \sum_{i=1}^{k} \|\delta \boldsymbol{e}_i - \delta \boldsymbol{e}_{i-1}\|^2 + \|\delta \boldsymbol{h}_k\|^2 + \sum_{i=1}^{k} \|\delta \boldsymbol{h}_i - \delta \boldsymbol{h}_{i-1}\|^2 + 2\tau \sum_{i=1}^{k} \|\delta \boldsymbol{h}_i \times \boldsymbol{\nu}\|_\Sigma^2 \\ &= \|\delta \boldsymbol{e}_0\|^2 + \|\delta \boldsymbol{h}_0\|^2 + 2\tau \sum_{i=1}^{k} \big(\delta \boldsymbol{h}_i, \alpha(1-\tau\alpha)^{-i}(\boldsymbol{e}_0 \times \boldsymbol{\nu} - \boldsymbol{h}_0 \times \boldsymbol{\nu} \times \boldsymbol{\nu})\big)_\Sigma \\ &+2\tau \sum_{i=1}^{k} \left(\delta \boldsymbol{h}_i, \alpha \left[(\alpha - \beta) \sum_{j=1}^{i} \tau (1-\tau\alpha)^{j-i-1} \boldsymbol{h}_j \times \boldsymbol{\nu} \times \boldsymbol{\nu} + \boldsymbol{h}_i \times \boldsymbol{\nu} \times \boldsymbol{\nu} \right] - \beta \boldsymbol{h}_i \times \boldsymbol{\nu} \times \boldsymbol{\nu} \right)_\Sigma . \end{aligned}$$

Applying Young's and Hölder's inequalities and Lemma 8.2 on each boundary term on the right-hand side, we get in a straightforward way ($\varepsilon > 0$)

$$\begin{aligned} &\|\delta \boldsymbol{e}_k\|^2 + \sum_{i=1}^{k} \|\delta \boldsymbol{e}_i - \delta \boldsymbol{e}_{i-1}\|^2 + \|\delta \boldsymbol{h}_k\|^2 + \sum_{i=1}^{k} \|\delta \boldsymbol{h}_i - \delta \boldsymbol{h}_{i-1}\|^2 \\ &\qquad + (2-\varepsilon)\tau \sum_{i=1}^{k} \|\delta \boldsymbol{h}_i \times \boldsymbol{\nu}\|_\Sigma^2 \le C_\varepsilon . \end{aligned}$$

Choosing a sufficiently small but positive ε concludes the proof. □

Lemma 8.5 *Let the conditions of Lemma 8.4 be fulfilled. Then*

$$\|\nabla \times \boldsymbol{h}_i\| + \|\nabla \times \boldsymbol{e}_i\| \le C$$

for all $i \in \mathbb{N}$.

Proof: The statement of the lemma follows from the density of $(C_0^\infty(\overline{\Omega}))^3$ in $\mathbf{L}_2(\Omega)$, Lemma 8.4, the Hahn-Banach theorem and (8.2) – see also the similar consideration at the end of the proof of Lemma 8.1. □

Lemma 8.6 *Let the conditions of Lemma 8.4 be fulfilled. Then*

$$\|\boldsymbol{h}_i \times \boldsymbol{\nu}\|_\Sigma + \|\boldsymbol{e}_i \times \boldsymbol{\nu}\|_\Sigma + \tau \sum_{i=1}^{k} \|\delta \boldsymbol{e}_i \times \boldsymbol{\nu}\|_\Sigma^2 \leq C$$

for all $i \in \mathbb{N}$.

Proof: The assertion concerning $\boldsymbol{h}_i \times \boldsymbol{\nu}$ follows from Lemma 8.4 and

$$\boldsymbol{h}_i \times \boldsymbol{\nu} = \boldsymbol{h}_0 \times \boldsymbol{\nu} + \tau \sum_{j=1}^{i} \delta \boldsymbol{h}_j \times \boldsymbol{\nu}.$$

Using (8.3) we deduce that

$$\begin{aligned}
\|\boldsymbol{e}_i \times \boldsymbol{\nu}\|_\Sigma &\leq \|\boldsymbol{h}_i \times \boldsymbol{\nu} \times \boldsymbol{\nu}\|_\Sigma + \left\|(1-\tau\alpha)^{-i}\right\|_{L_\infty(\Sigma)} \|\boldsymbol{e}_0 \times \boldsymbol{\nu} - \boldsymbol{h}_0 \times \boldsymbol{\nu} \times \boldsymbol{\nu}\|_\Sigma \\
&\quad + \|\alpha - \beta\|_{L_\infty(\Sigma)} \tau \sum_{j=1}^{i} \left\|(1-\tau\alpha)^{j-i-1}\right\|_{L_\infty(\Sigma)} \|\boldsymbol{h}_j \times \boldsymbol{\nu} \times \boldsymbol{\nu}\|_\Sigma \\
&\leq C \left(1 + \tau \sum_{j=1}^{i} \left\|(1-\tau\alpha)^{j-i-1}\right\|_{L_\infty(\Sigma)}\right) \\
&\leq C.
\end{aligned}$$

The relation $\tau \sum_{i=1}^{k} \|\delta \boldsymbol{e}_i \times \boldsymbol{\nu}\|_\Sigma^2 \leq C$ can be readily obtained from (8.2c). □

8.3 Error estimates

We introduce continuous piecewise linear in time vector fields $\boldsymbol{e}_\tau$, $\boldsymbol{h}_\tau$ (τ is the time step) given by

$$\begin{aligned}
\boldsymbol{e}_\tau(0) &= \boldsymbol{E}_0, \\
\boldsymbol{e}_\tau(t) &= \boldsymbol{e}_{i-1} + (t - t_{i-1})\delta \boldsymbol{e}_i \qquad \text{for } t \in (t_{i-1}, t_i], \qquad i \in \mathbb{N}
\end{aligned}$$

and

$$\begin{aligned}
\boldsymbol{h}_\tau(0) &= \boldsymbol{H}_0, \\
\boldsymbol{h}_\tau(t) &= \boldsymbol{h}_{i-1} + (t - t_{i-1})\delta \boldsymbol{h}_i \qquad \text{for } t \in (t_{i-1}, t_i], \qquad i \in \mathbb{N}.
\end{aligned}$$

Next, we define step vector fields $\overline{\boldsymbol{e}}_\tau$, $\overline{\boldsymbol{h}}_\tau$

$$\begin{aligned}
\overline{\boldsymbol{e}}_\tau(0) &= \boldsymbol{E}_0, \qquad \overline{\boldsymbol{e}}_\tau(t) = \boldsymbol{e}_i, \\
\overline{\boldsymbol{h}}_\tau(0) &= \boldsymbol{H}_0, \qquad \overline{\boldsymbol{h}}_\tau(t) = \boldsymbol{h}_i \qquad \text{for } t \in (t_{i-1}, t_i], \qquad i \in \mathbb{N}.
\end{aligned}$$

Using the new notation we rewrite (8.2) into a more suitable form for our purposes

$$\begin{aligned}
&(\partial_t \boldsymbol{e}_\tau, \boldsymbol{\varphi}) - \left(\nabla \times \overline{\boldsymbol{h}}_\tau, \boldsymbol{\varphi}\right) = 0, \\
&(\partial_t \boldsymbol{h}_\tau, \boldsymbol{\psi}) + (\overline{\boldsymbol{e}}_\tau, \nabla \times \boldsymbol{\psi}) - (\boldsymbol{\psi}, \overline{\boldsymbol{e}}_\tau \times \boldsymbol{\nu})_\Sigma = 0, \\
&(\partial_t \boldsymbol{e}_\tau \times \boldsymbol{\nu} - \partial_t \boldsymbol{h}_\tau \times \boldsymbol{\nu} \times \boldsymbol{\nu}, \boldsymbol{\xi})_\Sigma = \left(\alpha \overline{\boldsymbol{e}}_\tau \times \boldsymbol{\nu} - \beta \overline{\boldsymbol{h}}_\tau \times \boldsymbol{\nu} \times \boldsymbol{\nu}, \boldsymbol{\xi}\right)_\Sigma,
\end{aligned} \tag{8.17}$$

which holds for any $\boldsymbol{\varphi} \in \boldsymbol{V},\ \boldsymbol{\psi} \in \boldsymbol{W},\ \boldsymbol{\xi} \in \mathbf{L}_2(\Sigma)$.

Now we have the following lemma.

Lemma 8.7 *Let the conditions of Lemma 8.4 be fulfilled. Assume $T > 0$. Then $\boldsymbol{e}_\tau$ and $\boldsymbol{h}_\tau$ are Cauchy sequences in $C([0,T], \mathbf{L}_2(\Omega))$ and $\boldsymbol{h}_\tau \times \boldsymbol{\nu}$ is a Cauchy sequence in $L_2([0,T], \mathbf{L}_2(\Sigma))$.*

Proof: We subtract the first two lines of (8.17) for $\tau = \mu$ from (8.17) and get

$$\begin{aligned}
&(\partial_t(\boldsymbol{e}_\tau - \boldsymbol{e}_\mu), \boldsymbol{\varphi}) - \left(\nabla \times (\overline{\boldsymbol{h}}_\tau - \overline{\boldsymbol{h}}_\mu), \boldsymbol{\varphi}\right) = 0, \\
&(\partial_t(\boldsymbol{h}_\tau - \boldsymbol{h}_\mu), \boldsymbol{\psi}) + (\overline{\boldsymbol{e}}_\tau - \overline{\boldsymbol{e}}_\mu, \nabla \times \boldsymbol{\psi}) - (\boldsymbol{\psi}, (\overline{\boldsymbol{e}}_\tau - \overline{\boldsymbol{e}}_\mu) \times \boldsymbol{\nu})_\Sigma = 0.
\end{aligned}$$

Further we set $\boldsymbol{\varphi} = \overline{\boldsymbol{e}}_\tau - \overline{\boldsymbol{e}}_\mu$, $\boldsymbol{\psi} = \overline{\boldsymbol{h}}_\tau - \overline{\boldsymbol{h}}_\mu$, sum both equations and integrate over $(0, \zeta)$ for any $\zeta > 0$. We obtain

$$\begin{aligned}
&\frac{1}{2}\left\|\boldsymbol{e}_\tau(\zeta) - \boldsymbol{e}_\mu(\zeta)\right\|^2 + \frac{1}{2}\left\|\boldsymbol{h}_\tau(\zeta) - \boldsymbol{h}_\mu(\zeta)\right\|^2 - \int_0^\zeta \left(\overline{\boldsymbol{h}}_\tau - \overline{\boldsymbol{h}}_\mu, (\overline{\boldsymbol{e}}_\tau - \overline{\boldsymbol{e}}_\mu) \times \boldsymbol{\nu}\right)_\Sigma \\
&= \int_0^\zeta (\partial_t(\boldsymbol{e}_\tau - \boldsymbol{e}_\mu), \boldsymbol{e}_\tau - \overline{\boldsymbol{e}}_\tau + \overline{\boldsymbol{e}}_\mu - \boldsymbol{e}_\mu) + \int_0^\zeta \left(\partial_t(\boldsymbol{h}_\tau - \boldsymbol{h}_\mu), \boldsymbol{h}_\tau - \overline{\boldsymbol{h}}_\tau + \overline{\boldsymbol{h}}_\mu - \boldsymbol{h}_\mu\right).
\end{aligned} \tag{8.18}$$

For the first term on right-hand side we deduce using the Hölder inequality and Lemma 8.2

$$\begin{aligned}
&\left|\int_0^\zeta (\partial_t(\boldsymbol{e}_\tau - \boldsymbol{e}_\mu), \boldsymbol{e}_\tau - \overline{\boldsymbol{e}}_\tau + \overline{\boldsymbol{e}}_\mu - \boldsymbol{e}_\mu)\right| \\
&\le \sqrt{\int_0^\zeta \left\|\partial_t(\boldsymbol{e}_\tau - \boldsymbol{e}_\mu)\right\|^2} \sqrt{\int_0^\zeta \left\|\boldsymbol{e}_\tau - \overline{\boldsymbol{e}}_\tau + \overline{\boldsymbol{e}}_\mu - \boldsymbol{e}_\mu\right\|^2} \\
&\le C \sqrt{\int_0^\zeta \left\|\partial_t \boldsymbol{e}_\tau\right\|^2 + \left\|\partial_t \boldsymbol{e}_\mu\right\|^2} \sqrt{\int_0^\zeta \tau^2 \left\|\partial_t \boldsymbol{e}_\tau\right\|^2 + \mu^2 \left\|\partial_t \boldsymbol{e}_\mu\right\|^2} \\
&\le C(\tau + \mu).
\end{aligned} \tag{8.19}$$

The second term on the right is estimated in the same way, i.e.

$$\left| \int_0^\zeta \left(\partial_t(\boldsymbol{h}_\tau - \boldsymbol{h}_\mu), \boldsymbol{h}_\tau - \overline{\boldsymbol{h}}_\tau + \overline{\boldsymbol{h}}_\mu - \boldsymbol{h}_\mu\right) \right| \leq C(\tau + \mu). \tag{8.20}$$

According to the mean-value theorem we have for $t > s$ and some $\theta \in (s, t)$

$$\left|(1 - t\alpha)^{-i} - (1 - s\alpha)^{-i}\right| = \left|\alpha i(1 - \theta\alpha)^{-i-1}(t - s)\right| \leq C(1 - s\alpha)^{-i-1}|t - s|. \tag{8.21}$$

By using the standard algebraic inequality

$$e = \lim_{x \to 0} \left(\frac{\frac{1}{x}}{\frac{1}{x} - 1} \right)^{\frac{1}{x}} < \left(\frac{\frac{1}{x}}{\frac{1}{x} - 1} \right)^{\frac{1}{x}+1},$$

the following estimation can be obtained

$$\begin{aligned} |e^{\alpha\tau i} - (1 - \tau\alpha)^{-i}| &< \left(\left(\frac{\frac{1}{\alpha\tau}}{\frac{1}{\alpha\tau} - 1} \right)^{\frac{1}{\alpha\tau}+1} \right)^{\alpha\tau i} - \left(\left(\frac{\frac{1}{\alpha\tau}}{\frac{1}{\alpha\tau} - 1} \right)^{\frac{1}{\alpha\tau}} \right)^{\alpha\tau i} \\ &= \left(\left(\frac{\frac{1}{\alpha\tau}}{\frac{1}{\alpha\tau} - 1} \right)^{\alpha\tau i} \right)^{\frac{1}{\alpha\tau}+1} - \left(\left(\frac{\frac{1}{\alpha\tau}}{\frac{1}{\alpha\tau} - 1} \right)^{\alpha\tau i} \right)^{\frac{1}{\alpha\tau}} \\ &= \left(\left(\frac{\frac{1}{\alpha\tau}}{\frac{1}{\alpha\tau} - 1} \right)^{\alpha\tau i} \right)^{\frac{1}{\alpha\tau}} \left[\frac{\frac{1}{\alpha\tau}}{\frac{1}{\alpha\tau} - 1} - 1 \right] \\ &= e^{\alpha\tau i} \frac{\alpha\tau}{1 - \alpha\tau} \\ &\leq C\tau\,. \end{aligned} \tag{8.22}$$

The latter inequality is valid for any bounded α and $\tau \to 0$.
In virtue of (8.3) we have for $t \in (t_{i-1}, t_i]$

$$\begin{aligned} \overline{\boldsymbol{e}}_\tau(t) \times \boldsymbol{\nu} &= \overline{\boldsymbol{h}}_\tau(t) \times \boldsymbol{\nu} \times \boldsymbol{\nu} + e^{\alpha t}\left(\boldsymbol{e}_0 \times \boldsymbol{\nu} - \boldsymbol{h}_0 \times \boldsymbol{\nu} \times \boldsymbol{\nu}\right) \\ &\quad + (\alpha - \beta) \int_0^t e^{\alpha(t-s)} \overline{\boldsymbol{h}}_\tau(s) \times \boldsymbol{\nu} \times \boldsymbol{\nu} \, \mathrm{d}s \\ &\quad + \left[(1 - \tau\alpha)^{-i} - e^{\alpha t}\right]\left(\boldsymbol{e}_0 \times \boldsymbol{\nu} - \boldsymbol{h}_0 \times \boldsymbol{\nu} \times \boldsymbol{\nu}\right) \\ &\quad + (\alpha - \beta) \sum_{j=1}^{i} \int_{t_{j-1}}^{t_j} \left[(1 - \tau\alpha)^{j-i-1} - e^{\alpha(t-s)}\right] \boldsymbol{h}_{j_\tau}(s) \times \boldsymbol{\nu} \times \boldsymbol{\nu} \, \mathrm{d}s \\ &\quad + (\alpha - \beta) \int_t^{t_i} e^{\alpha(t-s)} \overline{\boldsymbol{h}}_\tau(s) \times \boldsymbol{\nu} \times \boldsymbol{\nu} \, \mathrm{d}s. \end{aligned} \tag{8.23}$$

A similar interpretation holds true for $\overline{\boldsymbol{e}}_\mu(t) \times \boldsymbol{\nu}$ with $t \in (t_{k-1}, t_k]$.

As far as we are familiar with the relation for $\overline{\boldsymbol{e}}_\mu(t)\times\boldsymbol{\nu}$ and $\overline{\boldsymbol{e}}_\tau(t)\times\boldsymbol{\nu}$, the last term on the left in (8.18) can be written as a sum of the following subintegrals:

$$
\begin{aligned}
&-\int_0^\zeta \left(\overline{\boldsymbol{h}}_\tau-\overline{\boldsymbol{h}}_\mu,(\overline{\boldsymbol{e}}_\tau-\overline{\boldsymbol{e}}_\mu)\times\boldsymbol{\nu}\right)_\Sigma\\
&\quad=\int_0^\zeta \left((\overline{\boldsymbol{h}}_\tau-\overline{\boldsymbol{h}}_\mu)\times\boldsymbol{\nu},(\overline{\boldsymbol{h}}_\tau-\overline{\boldsymbol{h}}_\mu)\times\boldsymbol{\nu}\right)_\Sigma\\
&\quad+\int_0^\zeta \left((\overline{\boldsymbol{h}}_\tau-\overline{\boldsymbol{h}}_\mu)\times\boldsymbol{\nu},(\alpha-\beta)\int_0^t e^{\alpha(t-s)}\left(\overline{\boldsymbol{h}}_\tau(s)-\overline{\boldsymbol{h}}_\mu(s)\right)\times\boldsymbol{\nu}\,\mathrm{d}s\right)_\Sigma\\
&\quad-\int_0^\zeta \left((\overline{\boldsymbol{h}}_\tau-\overline{\boldsymbol{h}}_\mu)\times\boldsymbol{\nu},\left[(1-\mu\alpha)^{-k}-(1-\tau\alpha)^{-i}\right](\boldsymbol{e}_0-\boldsymbol{h}_0\times\boldsymbol{\nu})\right)_\Sigma\\
&\quad-\int_0^\zeta \left((\overline{\boldsymbol{h}}_\tau-\overline{\boldsymbol{h}}_\mu)\times\boldsymbol{\nu},(\alpha-\beta)\sum_{j=1}^{i}\int_{t_{j-1}}^{t_j}\left[e^{\alpha(t-s)}-(1-\tau\alpha)^{j-i-1}\right]\boldsymbol{h}_{j_\tau}(s)\times\boldsymbol{\nu}\,\mathrm{d}s\right)_\Sigma\\
&\quad-\int_0^\zeta \left((\overline{\boldsymbol{h}}_\tau-\overline{\boldsymbol{h}}_\mu)\times\boldsymbol{\nu},(\alpha-\beta)\sum_{j=1}^{k}\int_{t_{j-1}}^{t_j}\left[(1-\mu\alpha)^{j-k-1}-e^{\alpha(t-s)}\right]\boldsymbol{h}_{j_\mu}(s)\times\boldsymbol{\nu}\,\mathrm{d}s\right)_\Sigma\\
&\quad-\int_0^\zeta \left((\overline{\boldsymbol{h}}_\tau-\overline{\boldsymbol{h}}_\mu)\times\boldsymbol{\nu},(\beta-\alpha)\int_t^{t_i} e^{\alpha(t-s)}\overline{\boldsymbol{h}}_\tau(s)\times\boldsymbol{\nu}\,\mathrm{d}s\right)_\Sigma\\
&\quad-\int_0^\zeta \left((\overline{\boldsymbol{h}}_\tau-\overline{\boldsymbol{h}}_\mu)\times\boldsymbol{\nu},(\alpha-\beta)\int_t^{t_k} e^{\alpha(t-s)}\overline{\boldsymbol{h}}_\mu(s)\times\boldsymbol{\nu}\,\mathrm{d}s\right)_\Sigma\\
&\quad=I_1+I_2-I_3-I_4-I_5-I_6-I_7.
\end{aligned}
$$

The first integral is obvious. The second one will be treated later. Let us begin with the third one by applying Young's inequality:

$$
\begin{aligned}
I_3=&\int_0^\zeta \left((\overline{\boldsymbol{h}}_\tau-\overline{\boldsymbol{h}}_\mu)\times\boldsymbol{\nu},\left[(1-\mu\alpha)^{-k}-(1-\tau\alpha)^{-i}\right](\boldsymbol{e}_0-\boldsymbol{h}_0\times\boldsymbol{\nu})\right)_\Sigma\\
&\le\varepsilon\int_0^\zeta \left\|(\overline{\boldsymbol{h}}_\tau-\overline{\boldsymbol{h}}_\mu)\times\boldsymbol{\nu}\right\|_\Sigma^2+C_\varepsilon\int_0^\zeta \left\|(1-\mu\alpha)^{-k}-(1-\tau\alpha)^{-i}\right\|_\Sigma^2\\
&\le\varepsilon\int_0^\zeta \left\|(\overline{\boldsymbol{h}}_\tau-\overline{\boldsymbol{h}}_\mu)\times\boldsymbol{\nu}\right\|_\Sigma^2+C_\varepsilon\int_0^\zeta \left\|(1-\mu\alpha)^{-i}-(1-\tau\alpha)^{-i}\right\|_\Sigma^2\\
&\le\varepsilon\int_0^\zeta \left\|(\overline{\boldsymbol{h}}_\tau-\overline{\boldsymbol{h}}_\mu)\times\boldsymbol{\nu}\right\|_\Sigma^2+C(\tau^2+\mu^2).
\end{aligned}
$$

The second inequality is based on the assumption that with the time step μ the time interval is more finely divided than with the time step τ. In consequence holds $i<k$. The last inequality follows from (8.21).

The integrals I_4 and I_5 have the same character. Both of them can be estimated using Young's and Hölder's inequalities together with relation (8.22). This yields

$$
\begin{aligned}
I_5 &= \int_0^\zeta \left((\overline{\boldsymbol{h}}_\tau - \overline{\boldsymbol{h}}_\mu) \times \boldsymbol{\nu}, (\alpha-\beta) \sum_{j=1}^k \int_{t_{j-1}}^{t_j} \left[(1-\mu\alpha)^{j-k-1} - e^{\alpha(t-s)} \right] \boldsymbol{h}_{j_\mu}(s) \times \boldsymbol{\nu} \, \mathrm{d}s \right)_\Sigma \\
&\leq \varepsilon \int_0^\zeta \left\| (\overline{\boldsymbol{h}}_\tau - \overline{\boldsymbol{h}}_\mu) \times \boldsymbol{\nu} \right\|_\Sigma^2 + C_\varepsilon \int_0^\zeta \left\| \sum_{j=1}^k \int_{t_{j-1}}^{t_j} \left[(1-\mu\alpha)^{j-k-1} - e^{\alpha(t-s)} \right] \boldsymbol{h}_{j_\mu}(s) \times \boldsymbol{\nu} \right\|_\Sigma^2 \\
&\leq \varepsilon \int_0^\zeta \left\| (\overline{\boldsymbol{h}}_\tau - \overline{\boldsymbol{h}}_\mu) \times \boldsymbol{\nu} \right\|_\Sigma^2 + C_\varepsilon \int_0^\zeta \sum_{j=1}^k \int_{t_{j-1}}^{t_j} \left\| (1-\mu\alpha)^{j-k-1} - e^{\alpha(t-s)} \right\|_\Sigma^2 \left\| \boldsymbol{h}_{j_\mu}(s) \times \boldsymbol{\nu} \right\|_\Sigma^2 \\
&\leq \varepsilon \int_0^\zeta \left\| (\overline{\boldsymbol{h}}_\tau - \overline{\boldsymbol{h}}_\mu) \times \boldsymbol{\nu} \right\|_\Sigma^2 + C\mu^2 .
\end{aligned}
$$

Finally, for the integrals I_6 and I_7 we have

$$
\begin{aligned}
I_7 &= \int_0^\zeta \left((\overline{\boldsymbol{h}}_\tau - \overline{\boldsymbol{h}}_\mu) \times \boldsymbol{\nu}, (\alpha-\beta) \int_t^{t_k} e^{\alpha(t-s)} \overline{\boldsymbol{h}}_\mu(s) \times \boldsymbol{\nu} \, \mathrm{d}s \right)_\Sigma \\
&\leq \varepsilon \int_0^\zeta \left\| (\overline{\boldsymbol{h}}_\tau - \overline{\boldsymbol{h}}_\mu) \times \boldsymbol{\nu} \right\|_\Sigma^2 + C_\varepsilon \int_0^\zeta \int_t^{t_k} \left\| e^{\alpha(t-s)} \overline{\boldsymbol{h}}_\mu(s) \times \boldsymbol{\nu} \right\|_\Sigma^2 \, \mathrm{d}s \\
&\leq \varepsilon \int_0^\zeta \left\| (\overline{\boldsymbol{h}}_\tau - \overline{\boldsymbol{h}}_\mu) \times \boldsymbol{\nu} \right\|_\Sigma^2 + C(\mu^2) .
\end{aligned}
$$

Therefore, using Lemma 8.6, the Cauchy and Young inequalities, we deduce that

$$
\begin{aligned}
&- \int_0^\zeta \left(\overline{\boldsymbol{h}}_\tau - \overline{\boldsymbol{h}}_\mu, (\overline{\boldsymbol{e}}_\tau - \overline{\boldsymbol{e}}_\mu) \times \boldsymbol{\nu} \right)_\Sigma \\
&\quad \geq (1-5\varepsilon) \int_0^\zeta \left\| \left(\overline{\boldsymbol{h}}_\tau - \overline{\boldsymbol{h}}_\mu \right) \times \boldsymbol{\nu} \right\|_\Sigma^2 \\
&\quad + \int_\Sigma (\alpha-\beta) \int_0^\zeta \left(\overline{\boldsymbol{h}}_\tau(t) - \overline{\boldsymbol{h}}_\mu(t) \right) \times \boldsymbol{\nu} \int_0^t e^{\alpha(t-s)} \left(\overline{\boldsymbol{h}}_\tau(s) - \overline{\boldsymbol{h}}_\mu(s) \right) \times \boldsymbol{\nu} \, \mathrm{d}s \, \mathrm{d}t \\
&\quad - C_\varepsilon \left(\tau^2 + \mu^2 \right) .
\end{aligned}
$$

Choosing a sufficiently small positive ε and involving (8.13) we obtain

$$
- \int_0^\zeta \left(\overline{\boldsymbol{h}}_\tau - \overline{\boldsymbol{h}}_\mu, (\overline{\boldsymbol{e}}_\tau - \overline{\boldsymbol{e}}_\mu) \times \boldsymbol{\nu} \right)_\Sigma \geq \frac{1}{2} \int_0^\zeta \left\| \left(\overline{\boldsymbol{h}}_\tau - \overline{\boldsymbol{h}}_\mu \right) \times \boldsymbol{\nu} \right\|_\Sigma^2 - C \left(\tau^2 + \mu^2 \right) . \tag{8.24}
$$

Finally, collecting (8.18)-(8.20) and (8.24), we deduce that

$$
\left\| \boldsymbol{e}_\tau(\zeta) - \boldsymbol{e}_\mu(\zeta) \right\|^2 + \left\| \boldsymbol{h}_\tau(\zeta) - \boldsymbol{h}_\mu(\zeta) \right\|^2 + \int_0^\zeta \left\| \left(\overline{\boldsymbol{h}}_\tau - \overline{\boldsymbol{h}}_\mu \right) \times \boldsymbol{\nu} \right\|_\Sigma^2 \leq C \left(\tau + \mu \right) ,
$$

which is valid for any $\zeta > 0$. Therefore

$$\max_{\zeta\in[0,T]} \|\boldsymbol{e}_\tau(\zeta) - \boldsymbol{e}_\mu(\zeta)\|^2 + \max_{\zeta\in[0,T]} \|\boldsymbol{h}_\tau(\zeta) - \boldsymbol{h}_\mu(\zeta)\|^2 + \int_0^T \left\|\left(\overline{\boldsymbol{h}}_\tau - \overline{\boldsymbol{h}}_\mu\right) \times \boldsymbol{\nu}\right\|_\Sigma^2 \leq C\left(\tau + \mu\right), \tag{8.25}$$

which concludes the proof. □

Theorem 8.1 *Let the conditions of Lemma 8.4 be fulfilled. Assume $T > 0$. Then there exists a solution to (8.1) in $[0, T]$.*

Proof: The assertion can be readily obtained from (8.17) by passing $\tau \to 0$ using the a priori estimates from the previous lemmas. □

Now, we are ready to derive the error estimates for the linear approximation scheme (8.2).

Theorem 8.2 *Let the conditions of Lemma 8.4 be fulfilled and assume $T > 0$. Then*

(i) $\max_{\zeta\in[0,T]} \|\boldsymbol{e}_\tau(\zeta) - \boldsymbol{E}(\zeta)\|^2 + \max_{\zeta\in[0,T]} \|\boldsymbol{h}_\tau(\zeta) - \boldsymbol{H}(\zeta)\|^2 + \int_0^T \left\|\left(\overline{\boldsymbol{h}}_\tau - \boldsymbol{H}\right) \times \boldsymbol{\nu}\right\|_\Sigma^2 \leq C\tau$

(ii) $\int_0^T \|(\overline{\boldsymbol{e}}_\tau - \boldsymbol{E}) \times \boldsymbol{\nu}\|_\Sigma^2 \leq C\tau.$

Proof:
(i) Follows directly from (8.25) by passing to the limit $\mu \to 0$.
(ii) We have $\boldsymbol{E} \times \boldsymbol{\nu}, \boldsymbol{H} \times \boldsymbol{\nu} \in C([0, T], \mathbf{L}_2(\Sigma))$ due to Lemmas 8.4 and 8.6. The sequence $\overline{\boldsymbol{h}}_\tau \times \boldsymbol{\nu}$ is convergent in the space $L_2([0, T], \mathbf{L}_2(\Sigma))$. Passing to the limit for $\tau \to 0$ in (8.23) we obtain

$$\begin{aligned} \boldsymbol{E}(t) \times \boldsymbol{\nu} &= \boldsymbol{H}(t) \times \boldsymbol{\nu} \times \boldsymbol{\nu} + e^{\alpha t}\left(\boldsymbol{e}_0 \times \boldsymbol{\nu} - \boldsymbol{h}_0 \times \boldsymbol{\nu} \times \boldsymbol{\nu}\right) \\ &\quad + (\alpha - \beta) \int_0^t e^{\alpha(t-s)} \boldsymbol{H}(s) \times \boldsymbol{\nu} \times \boldsymbol{\nu} \, \mathrm{d}s. \end{aligned} \tag{8.26}$$

We subtract (8.26) from (8.23) and we deduce in a straightforward way that

$$\int_0^T \|(\overline{\boldsymbol{e}}_\tau - \boldsymbol{E}) \times \boldsymbol{\nu}\|_\Sigma^2 \leq C\tau.$$

□

Let us note that the uniqueness of the solution to (7.4) follows from Theorem 8.2.

Remark 8.3 *Following step by step the idea from the book [37], the artificial condition for problem (7.4) would change slightly into the form*

$$\partial_t \left(\boldsymbol{E} \times \boldsymbol{\nu} - \boldsymbol{H} \times \boldsymbol{\nu} \times \boldsymbol{\nu}\right) = -\beta \boldsymbol{H} \times \boldsymbol{\nu} \times \boldsymbol{\nu} \text{ on } \Sigma \times (0, \infty) \tag{8.27}$$

with coefficient $\alpha = 0$. We can show that the problem stays stable, what is also intuitively expected. Solving the differential equation (8.27) yields

$$\boldsymbol{H} \times \boldsymbol{\nu} \times \boldsymbol{\nu}(t) = e^{\beta t} \boldsymbol{H}(0) \times \boldsymbol{\nu} \times \boldsymbol{\nu} + \int_0^t e^{\beta(t-s)} \partial_t \boldsymbol{E} \times \boldsymbol{\nu} \; ds.$$

Using this result, the variational formulation of the problem reads

$$\begin{aligned} &(\partial_t \boldsymbol{E}, \boldsymbol{\varphi}) - (\boldsymbol{H}, \nabla \times \boldsymbol{\varphi}) = -\left(e^{\beta t} \boldsymbol{H}(0) \times \boldsymbol{\nu} \times \boldsymbol{\nu} + \int_0^t e^{\beta(t-s)} \partial_t \boldsymbol{E}(s) \times \boldsymbol{\nu} \; ds, \boldsymbol{\varphi} \times \boldsymbol{\nu}\right)_\Sigma, \\ &(\partial_t \boldsymbol{H}, \boldsymbol{\psi}) + (\nabla \times \boldsymbol{E}, \boldsymbol{\psi}) = 0. \end{aligned} \tag{8.28}$$

The stability of the problem is checked by a standard technique, i.e. setting $\boldsymbol{\varphi} = \boldsymbol{E}, \boldsymbol{\psi} = \boldsymbol{H}$, summing both equations and integrating them with respect to time. We obtain

$$\begin{aligned} \frac{1}{2} \|\boldsymbol{E}(\zeta)\|^2 + \frac{1}{2} \|\boldsymbol{H}(\zeta)\|^2 + \int_0^\zeta \left(e^{\beta t} \boldsymbol{H}(0) \times \boldsymbol{\nu} \times \boldsymbol{\nu}, \boldsymbol{E} \times \boldsymbol{\nu}\right)_\Sigma \\ + \int_0^\zeta \left(\int_0^t e^{\beta(t-s)} \partial_t \boldsymbol{E}(s) \times \boldsymbol{\nu}, \boldsymbol{E}(t) \times \boldsymbol{\nu}\right)_\Sigma \\ = \frac{1}{2} \|\boldsymbol{E}(0)\|^2 + \frac{1}{2} \|\boldsymbol{H}(0)\|^2. \end{aligned}$$

Now, Green's identity is applied to the second boundary term

$$\begin{aligned} &\int_0^\zeta \left(\int_0^t e^{\beta(t-s)} \partial_t \boldsymbol{E}(s) \times \boldsymbol{\nu}, \boldsymbol{E}(t) \times \boldsymbol{\nu}\right)_\Sigma \\ &= \int_0^\zeta \left(\left[e^{\beta(t-s)} \boldsymbol{E}(s) \times \boldsymbol{\nu}\right]_0^t + \beta \int_0^t e^{\beta(t-s)} \boldsymbol{E}(s) \times \boldsymbol{\nu}, \boldsymbol{E}(t) \times \boldsymbol{\nu}\right)_\Sigma \end{aligned}$$

and finally we can write

$$\begin{aligned} \frac{1}{2} \|\boldsymbol{E}(\zeta)\|^2 + \frac{1}{2} \|\boldsymbol{H}(\zeta)\|^2 + \int_0^\zeta \left(e^{\beta t} \boldsymbol{H}_0 \times \boldsymbol{\nu} \times \boldsymbol{\nu}, \boldsymbol{E} \times \boldsymbol{\nu}\right)_\Sigma + \int_0^\zeta \|\boldsymbol{E} \times \boldsymbol{\nu}\|_\Sigma^2 \\ - \int_0^\zeta \left(e^{\beta t} \boldsymbol{E}_0 \times \boldsymbol{\nu}, \boldsymbol{E} \times \boldsymbol{\nu}\right)_\Sigma + \beta \int_0^\zeta \int_0^t \left(e^{\beta(t-s)} \boldsymbol{E}(s) \times \boldsymbol{\nu}, \boldsymbol{E}(t) \times \boldsymbol{\nu}\right)_\Sigma \\ = \frac{1}{2} \|\boldsymbol{E}(0)\|^2 + \frac{1}{2} \|\boldsymbol{H}(0)\|^2. \end{aligned}$$

Using Young's and Cauchy's inequality one obtains

$$\begin{aligned}\frac{1}{2}\left\|\boldsymbol{E}(\zeta)\right\|^2+\frac{1}{2}\left\|\boldsymbol{H}(\zeta)\right\|^2+(1-2\varepsilon-|\beta|\varepsilon)\int_0^\zeta\left\|\boldsymbol{E}\times\boldsymbol{\nu}\right\|_\Sigma^2\\ \leq\frac{1}{2}\left\|\boldsymbol{E}(0)\right\|^2+\frac{1}{2}\left\|\boldsymbol{H}(0)\right\|^2+C_\varepsilon\int_0^\zeta\left\|e^{\beta t}\right\|_\Sigma^2\\ +|\beta|\left[C_\varepsilon\int_0^\zeta\int_0^t\left\|\boldsymbol{E}(s)\times\boldsymbol{\nu}\right\|_\Sigma^2\right].\end{aligned}$$

Choosing sufficiently small ε we have

$$\left\|\boldsymbol{E}(\zeta)\right\|^2+\left\|\boldsymbol{H}(\zeta)\right\|^2+\int_0^\zeta\left\|\boldsymbol{E}\times\boldsymbol{\nu}\right\|_\Sigma^2\leq C+C\int_0^\zeta\int_0^t\left\|\boldsymbol{E}(s)\times\boldsymbol{\nu}\right\|_\Sigma^2.$$

Finally, Gronwall's lemma is applied to the boundary term on the left–hand side, yielding

$$\left\|\boldsymbol{E}(\zeta)\right\|^2+\left\|\boldsymbol{H}(\zeta)\right\|^2+\int_0^\zeta\left\|\boldsymbol{E}\times\boldsymbol{\nu}\right\|_\Sigma^2\leq C$$

and the stability of the proposed scheme is proved. Only the boundedness of the function β needs to be assumed. Thus, without loss of generality, either the absorbing boundary condition (8.27) or the BC (7.4) proposed by Barucq can be chosen for the next analysis.

8.4 Conclusions

We have studied the exterior boundary value problem with an Artificial Boundary Condition on one part of the boundary describing the propagation of electromagnetic waves through matter. We found an efficient time-discrete approximation scheme (8.2) based on the backward Euler method. A detailed analysis of the approximate solution was done and a linear dependence of the error of the presented method on the choice of the time step τ was proved.

There is still some potential future work how to improve and develop the results of this chapter. For example the discretization in space could be studied and the stability results and convergence of the approximate solution towards the exact one could be proved. In addition, one should determine the dependence of the error of this full discretized system on the size of the mesh. This was done in Chapter 6 for a different type of problem.

Furthermore, instead of a linear Artificial Boundary Condition (7.4d) a nonlinear ABC could be considered to make the problem more general and more complex.

Another challenge for future research would be an implementation of the proposed discretized scheme. The optimality of the theoretically derived error estimates and sensibility of the scheme on the method parameters should be studied on numerical experiments.

Part III

Inverse problems in low-frequency electromagnetism

Chapter 9

Problem formulation

When speaking about an inverse problem a question comes across ones mind: Inverse to what? We call two problems inverse to each other if the formulation of one problem includes the other one. From historical reasons the simpler problem, which was studied earlier is denoted as *direct*, the other one is then the *inverse* one. In practice, we naturally detect which problem we have in mind. If one wants to predict the future state of a physical system from the knowledge of the relevant parameters, material properties and physical laws, one solves the direct problem. On the other hand, to solve the inverse problem means to determine the value of some model parameters from the observed system evolution (Figure 9.1). Solving an inverse problem is not an easy task since a solution might not exist, or different parameter values can be consistent with the data (the solution is not unique), or the solution does not depend continuously on the data. This is why we consider inverse problems to be typically *ill–posed* in the sense of Jacques Hadamard, see Definition 9.1. On top of that, discovering parameters of the model may require the exploration of a huge parameter space.

Inverse problems have been widely studied in medical applications - Computerized Tomography [71], physical chemistry - time resolved fluorescence [60], high temperature superconductivity [28], heat conduction [11, 33, 68] and in other diffusion processes. To the inverse problems for Maxwell's equations is solely devoted monograph [74].

If the direct and corresponding inverse problem are linear, the standard theory for the ill–posed linear operator equation

$$\mathcal{F}x = y \tag{9.1}$$

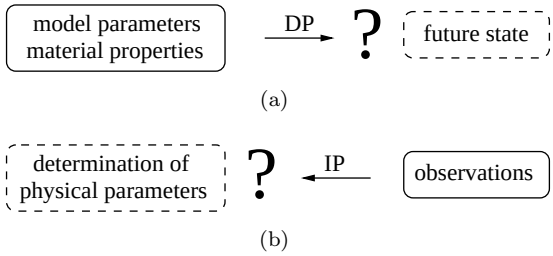

Figure 9.1: Difference between the direct (DP) and the inverse problem (IP).

is applicable. Here, $\mathcal{F}$ is a bounded linear operator between Hilbert spaces X and Y.

Definition 9.1 (Hadamard, 1932) *The problem (9.1) is said to be* well-posed *in the sense of Hadamard if the following conditions are fulfilled*

1. $\forall y \in \mathrm{Y}\ \exists x \in \mathrm{X}:\ \mathcal{F}x = y$.
2. *A solution x to the problem (9.1) is uniquely determined by the element y. In other words, the inverse $\mathcal{F}^{-1}$ of the operator $\mathcal{F}$ exists.*
3. *The solution x depends continuously on the element y. In other words, the operator $\mathcal{F}^{-1}$ is continuous.*

If at least one of these conditions is not fulfilled, the problem is said to be ill–posed *in the sense of Hadamard.*

Thus, the problem (9.1) is well–posed in the sense of Hadamard if and only if there exists a continuous inverse $\mathcal{F}^{-1}$ of the operator $\mathcal{F}$ defined on the whole space Y. A typical example of an ill-posed operator equation (9.1) is when $\mathcal{F}$ is a linear selfadjoint compact operator between Hilbert spaces, for a proof see e.g. [64, Chapter 1.2].

In general, the inverse $\mathcal{F}^{-1}$ is not defined on the whole Y. Fortunately, this condition can be bypassed by relaxing the notion of the solution. We will search for a solution in the least square sense (Definition 9.2). In general, the least square solution differs from the exact solution x to (9.1), but as the inverse problems usually involve perturbed data, they have to be regularized and hence changed anyway.

Moreover, the fulfillment of the first Hadamard's condition is closely related to the fulfillment of the third one. Following Ivanov (1978), the inverse $\mathcal{F}^{-1}$ of

a linear injective continuous operator $\mathcal{F}$ is bounded if and only if for the range $\mathcal{R}(\mathcal{F}) \subseteq \mathrm{Y}$ holds $\mathcal{R}(\mathcal{F}) = \overline{\mathcal{R}(\mathcal{F})}$. Using this result we conclude that if the range $\mathcal{R}(\mathcal{F})$ of the operator $\mathcal{F}$ is closed in Y, then inverse $\mathcal{F}^{-1}$ is continuous and thus the third Hadamard's condition is satisfied.[1]

A violation of the second Hadamard's condition is considered to be much more problematic. It might happen that there are more candidates for a solution. Then one either has to decide which one is of interest, e.g. the solution with the smallest norm defined in Definition 9.2 (this possibility is not appropriate for all applications), or to check the model for completeness. Usually this means that the available data are not sufficient to determine the solution (knowing a height of a main-mast is not sufficient to calculate captain's age) and one has to make additional measurements.

Definition 9.2 *Let $\mathcal{F} : \mathrm{X} \to \mathrm{Y}$ be a bounded linear operator. Then*

- ▷ $x \in \mathrm{X}$ *is called a* least square solution *of $\mathcal{F}x = y$ if*

$$\|\mathcal{F}x - y\| = \inf\{\|\mathcal{F}z - y\| \,;\, z \in \mathrm{X}\}. \tag{9.2}$$

- ▷ $x \in \mathrm{X}$ *is called the* best-approximate solution *of $\mathcal{F}x = y$ if x is a least square solution of $\mathcal{F}x = y$ and*

$$\|x\| = \inf\{\|z\| \,;\, z \text{ is a least square solution of } \mathcal{F}x = y\} \tag{9.3}$$

holds.

The best-approximate solution is unique. Choosing the least-square solution with a minimal norm is not always optimal. It is often desirable to replace $\|x\|$ in (9.3) by the minimization of $\|\mathcal{L}x\|$, where $\mathcal{L}$ is usually a differential operator.

The most characteristic feature of an inverse problem is the violation of the third Hadamard's condition. Even a very small perturbation of input data can cause big changes of an output. Traditional numerical methods for approximating a problem whose solution does not depend continuously on the data, become unstable. That is why *regularization methods* for the stabilization of inverse problems were invented. It started with pioneering works of A.N. Tikhonov [87–89]. One has to keep in mind that when using this regularization approach one does not solve the same problem anymore. The whole art of applying regularization methods is to find a compromise between accuracy and stability.

[1] From the closedness of the range $\mathcal{R}(\mathcal{F})$ follows the boundedness and thereby the continuity of the inverse operator $\mathcal{F}^{-1}$, $\mathcal{F}$ being linear.

For a nice overview of the classical theory of ill–posed problems and related regularization techniques we refer to the monograph [34].

This part of the thesis is devoted to the identification of the electromagnetic losses on the boundary, which are considered to be constant. This type of problem is also known as constant identification. The problem is related to the eddy current problem in low-frequency electromagnetism, derived in Section 1.2. Both, the direct and corresponding inverse problem are linear.

Chapter 10

Constant determination

This chapter is based on the article [100], the results of which were presented at the international conference ACOMEN 2008 and are summarized in the proceedings [99].

After being familiar with the problem setting and with the definition of the electromagnetic loss, the time-discretization scheme, as usually based on the backward Euler method is applied to the proposed problem. In Section 10.3 a specific side condition is introduced and used later to guarantee the uniqueness of the solution. Furthermore, we investigate the character of, let's say, a loss function. Continuity, monotonicity and an asymptotic behavior of the loss function deliver existence of the solution. In line with our good practice, the last section is devoted to numerical experiments.

10.1 Introduction and physical motivation

For a design of electromagnetic devices, an accurate evaluation of the material characteristics of the magnetic circuit, such as the electromagnetic loss P, the permeability μ and the electrical conductivity σ, is essential. The importance comes from the increasing requirements set for high performance devices. Classically, the electromagnetic losses of magnetic materials are quantified by means of a standard measurement equipment, enforcing a time dependent magnetic field to the body of the test sample. For this type of measurement equipment, one obtains the iron losses P in the ferromagnetic material under investigation starting from two sensor signals. The first signal is related to the time dependent

magnetic field $\boldsymbol{H}$ enforced at the surface of the material body while the second signal defines the time dependent magnetic flux in the material. The latter is directly related to the induced electric field $\boldsymbol{E}$ at the surface of the material body. The loss originates from the eddy currents present in the material.

The measured losses are also related to the electromagnetic fields at the surface of the body of the test sample through the pointing vector $\boldsymbol{S} = \boldsymbol{E} \times \boldsymbol{H}$. Indeed, given a surface A of the body of the material, the iron loss is

$$P = \oint_A (\boldsymbol{E} \times \boldsymbol{H}) \cdot \boldsymbol{\nu} \, \mathrm{d}s. \tag{10.1}$$

Let us derive the precise mathematical model describing this situation. Considering the quasi-static case of electromagnetic propagation at a single frequency, the time–dependent problem (1.11)–(1.14) can be reduced to the following time–harmonic Maxwell system

$$\begin{aligned} \nabla \cdot (\varepsilon \boldsymbol{E}) &= \rho, && (10.2)\\ \nabla \cdot (\mu \boldsymbol{H}) &= 0, && (10.3)\\ \nabla \times \boldsymbol{E} &= -i\omega\mu \boldsymbol{H}, && (10.4)\\ \nabla \times \boldsymbol{H} &= \boldsymbol{J}_a + \sigma \boldsymbol{E}. && (10.5) \end{aligned}$$

The fields $\boldsymbol{E}$ and $\boldsymbol{H}$ represent complex–valued amplitudes, see [65]. For the simplicity we maintain our notation from the time-dependent case. The total current density consists of the applied current density $\boldsymbol{J}_a$ and the induced current density $\sigma \boldsymbol{E}$. For ease of exposition, we set $\boldsymbol{J}_a = \boldsymbol{0}$.

Remark 10.1 *The differential system (1.11)–(1.14) is changed to the latter algebraic one (10.2)–(10.5) using Fourier transformation. The relation between the fields $\boldsymbol{E}, \boldsymbol{H}$ from time–domain and corresponding fields $\hat{\boldsymbol{E}}, \hat{\boldsymbol{H}}$ from frequency domain reads*

$$\hat{\boldsymbol{E}}(\boldsymbol{x}, \omega) = \int_{-\infty}^{\infty} \boldsymbol{E}(\boldsymbol{x}, t) e^{-i\omega t} \, dt,$$
$$\hat{\boldsymbol{H}}(\boldsymbol{x}, \omega) = \int_{-\infty}^{\infty} \boldsymbol{H}(\boldsymbol{x}, t) e^{-i\omega t} \, dt,$$

where $i = \sqrt{-1}$ and $\omega = 2\pi f > 0$ denotes the frequency of radiation of the electromagnetic waves.

A function of time is a representation of a signal with perfect time resolution, but no frequency information, while the Fourier transform of such a function yields perfect frequency resolution, but no time information. The location of the Fourier transform at a point is given by phase.

Remark 10.2 *In physics and engineering, a phase vector, or phasor, is a representation of a sine wave whose amplitude, phase and frequency are time-invariant. Phasors reduce the dependencies on parameters to three independent factors, what simplifies certain kinds of calculations. In many applications using phasors, one leaves the amplitude static and phase information combines algebraically. The term phasor therefore often refers to just two factors, phase and frequency. In older texts, it is also referred to as a sinor.*

Eliminating the electric field from the system of Maxwell's equations (10.4)–(10.5) leads to the boundary value problem in terms of the magnetic field only

$$\sigma\mu i\omega \boldsymbol{H} + \nabla \times \nabla \times \boldsymbol{H} = \boldsymbol{0}. \tag{10.6}$$

The computational problem becomes more difficult when the penetration "skin" of the conductor is narrow in comparison with its geometric dimensions. In this case, the electromagnetic fields are closely concentrated near the conductor boundaries and decay very fast in directions normal to these boundaries. These speedy spatial variations cause numerical difficulties. Fortunately, they can be circumvented by using the idea of impedance boundary condition, see Section 1.3.1. This BC is based on the local penetration of electromagnetic fields, i.e. at each boundary point, tangential components of electric and magnetic fields are related to each other.

In the frequency domain, for a frequency f, the relation between the phasors of the electric field $\boldsymbol{E}$ and the magnetic field $\boldsymbol{H}$ at the boundary of a linear conducting medium, $\boldsymbol{B} = \mu\boldsymbol{H}$, can be expressed mathematically as follows:

$$\boldsymbol{E} \times \boldsymbol{\nu} = \hat{\eta}(\boldsymbol{H} \times \boldsymbol{\nu}), \tag{10.7}$$

where $\hat{\eta}$ is the impedance matrix defined as

$$\hat{\eta} = \sqrt{\frac{\omega\mu}{\sigma_B}} e^{i\frac{\pi}{4}} \cdot \hat{\Lambda} \tag{10.8}$$

with σ_B representing the magnetic permeability on the boundary and $\hat{\Lambda}$ the rotation matrix over 90°

$$\hat{\Lambda} = \begin{pmatrix} 0 & -1 \\ 1 & 0 \end{pmatrix}.$$

After substituting the equality (10.8) in (10.7) multiplied by σ and recalling $\nabla \times \boldsymbol{H} = \sigma\boldsymbol{E}$ we arrive at

$$\nabla \times \boldsymbol{H} \times \boldsymbol{\nu} = \sqrt{\frac{i\omega\mu\sigma^2}{\sigma_B}} \boldsymbol{H} \times \boldsymbol{\nu} \times \boldsymbol{\nu}. \tag{10.9}$$

In practical applications $\sigma, \sigma_B \geq 0$ and $\mu = a - ib$. We try to build our mathematical model as simple as possible with aim to focus our attention on its inverse character. That is why we set $\mu = -i$. This substitution allows us to work with real fields from now on.

Setting $\mu = -i$ is equivalent to including a time delay of the magnetic induction $\boldsymbol{B}$ relative to the magnetic field intensity $\boldsymbol{H}$, when speaking of a linear conducting material. This delay can be due to eddy current effects or hysteresis effects. Moreover, the $\boldsymbol{BH}$ loop becomes a circle.

Note that the impedance BCs are not exact descriptions of the reality unless the skin depths are small in comparison with the geometric dimensions of the conductor.

Finally, our problem reads

$$\omega\sigma\boldsymbol{H} + \nabla \times \nabla \times \boldsymbol{H} = \mathbf{0}.$$

A direct problem of this type is usually accompanied by one of the following standard boundary conditions

$$\boldsymbol{H} \times \boldsymbol{\nu} = \boldsymbol{a} \qquad \text{or} \qquad \nabla \times \boldsymbol{H} \times \boldsymbol{\nu} = \boldsymbol{b}\,.$$

By employing relation (10.9) the physical importance of another type of the boundary condition arises, namely

$$\nabla \times \boldsymbol{H} \times \boldsymbol{\nu} = \lambda \boldsymbol{H} \times \boldsymbol{\nu} \times \boldsymbol{\nu}, \qquad \text{where } \lambda = \sqrt{\frac{\omega\sigma^2}{\sigma_B}}.$$

10.2 Problem formulation

We consider a ferromagnet occupying a bounded domain $\Omega \subset \mathbb{R}^3$ with Lipschitz continuous boundary Γ split into three complementary, non-empty and non-overlapping parts, $\Gamma = \overline{\Gamma}_{Dir} + \overline{\Gamma}_{Neu} + \overline{\Gamma}_{loss}$. The outward normal to Γ is denoted by $\boldsymbol{\nu}$. Our object of interest is to identify a coefficient λ describing the electromagnetic losses. More precisely, the following inverse eddy current problem is studied:

Problem 1. Find $(\lambda, \boldsymbol{H}_\lambda) \in (\mathbb{R}_+, \mathbf{H}(\mathbf{curl}\,;\Omega))$ such that

$$\begin{aligned} K\boldsymbol{H}_\lambda + \nabla \times \nabla \times \boldsymbol{H}_\lambda &= \mathbf{0} && \text{in } \Omega, \\ \boldsymbol{H}_\lambda \times \boldsymbol{\nu} &= \mathbf{0} && \text{on } \Gamma_{Dir}, \\ \nabla \times \boldsymbol{H}_\lambda \times \boldsymbol{\nu} &= \boldsymbol{g} \times \boldsymbol{\nu} && \text{on } \Gamma_{Neu}, \\ \nabla \times \boldsymbol{H}_\lambda \times \boldsymbol{\nu} &= \lambda(\boldsymbol{H}_\lambda \times \boldsymbol{\nu} \times \boldsymbol{\nu}) && \text{on } \Gamma_{loss} \end{aligned}$$

for a given, regular enough, source $\boldsymbol{g}$.

10.2.1 Methodology

At the first glance Problem 1 appears to be similar to the following one:

Problem 2. Find $(h, u) \in (\mathbb{R}_+, H^1(\Omega))$ such that

$$\begin{aligned} pu + \nabla \cdot (-K\nabla u) &= f && \text{in } \Omega, \\ u &= 0 && \text{on } \Gamma_{Dir}, \\ -K\nabla u \cdot \boldsymbol{\nu} &= g && \text{on } \Gamma_{Neu}, \\ -K\nabla u \cdot \boldsymbol{\nu} &= hu && \text{on } \Gamma_{in}, \end{aligned}$$

where K, p, f and g are given data and Γ_{in} denotes the inaccessible part of the boundary.

The partial differential equations in both problems are equivalent. This can be easily seen using the well-known identity

$$-\triangle \boldsymbol{H} = \nabla \times \nabla \times \boldsymbol{H} - \nabla(\nabla \cdot \boldsymbol{H})$$

and taking $\nabla \cdot \boldsymbol{B} = 0$ into account, so then $\nabla \cdot \boldsymbol{H} = 0$ as well. The difference between Problem 1 and Problem 2 lies in the regularity of the corresponding solutions and in the boundary conditions.

Many inverse problems originate from the linear steady-state elliptic boundary value Problem 2.

If one considers the heat conduction, the recovery of the convective transfer coefficient h from the overspecified data was done in [81]. The identification was based on the difference between the outside and inside temperature on Γ_{in}, in $\mathbf{L}_2(\Gamma_{in})$ sense. Slodička and Van Keer have considered the whole boundary accessible, but on the part Γ_{in} the data are not known precisely, but in an average sense only.

A very similar problem setting can be obtained from the problem of corrosion detection, see [52], where the coefficient h represents the corrosion damage. Here, the author works with a thin plate, as thick domains cause instabilities of the numerical approach. The data of the problem consist of the prescribed current flux and voltage measurements on an accessible part of the specimen's boundary. The inverse problem is to determine quantitative information about corrosion occurring on an inaccessible part of the domain.

10.3 Assumptions

As a direct consequence of the Lax–Milgram lemma, Problem 1 can have an infinite number of solutions depending on the free positive parameter λ at Γ_{loss}. Our goal is to design an additional boundary condition, which guarantees the uniqueness of a solution. As will be shown later this can be ensured by the following side condition, called iron loss boundary condition

$$0 < M = \int_{\Gamma_{loss}} |\boldsymbol{H}_\lambda \times \boldsymbol{\nu}|^2 < \lim_{\lambda \to 0_+} m(\lambda). \tag{10.10}$$

The function $m(\lambda)$ will be specified later.

We assume that

$$\begin{aligned} &0 < K_{min} \leq K \leq K_{max} \qquad \text{a.e. in } \Omega, \\ &\boldsymbol{g} \in \mathbf{L}_2(\Gamma_{Neu}). \end{aligned} \tag{10.11}$$

Then the variational formulation of Problem 1 reads

$$K(\boldsymbol{H}_\lambda, \boldsymbol{\varphi})_\Omega + (\nabla \times \boldsymbol{H}_\lambda, \nabla \times \boldsymbol{\varphi})_\Omega + (\boldsymbol{g}, \boldsymbol{\varphi} \times \boldsymbol{\nu})_{\Gamma_{Neu}} + \lambda(\boldsymbol{H}_\lambda \times \boldsymbol{\nu}, \boldsymbol{\varphi} \times \boldsymbol{\nu})_{\Gamma_{loss}} = 0 \tag{10.12}$$

for any $\boldsymbol{\varphi} \in \boldsymbol{V}$.
The space of test functions is defined by

$$\boldsymbol{V} = \{\boldsymbol{\varphi} \in \mathbf{H}(\mathbf{curl}\,;\Omega);\ \boldsymbol{\varphi} \times \boldsymbol{\nu} = \mathbf{0} \text{ on } \Gamma_{Dir}\}.$$

This is a natural choice for Problem 1. $\boldsymbol{V}$ is a reflexive Banach space endowed with the standard norm $\|\cdot\|_{\mathbf{H}(\mathbf{curl}\,;\Omega)}$.

Now the question is where the information about the electromagnetic loss P defined by (10.1) is hidden within the latter formulation. Analyzing the boundary term, we get the following equality

$$(\nabla \times \boldsymbol{H}_\lambda, \boldsymbol{\varphi} \times \boldsymbol{\nu})_{\Gamma_{loss}} = \lambda(\boldsymbol{H}_\lambda \times \boldsymbol{\nu}, \boldsymbol{\varphi} \times \boldsymbol{\nu})_{\Gamma_{loss}}.$$

Setting $\boldsymbol{\varphi} = \boldsymbol{H}_\lambda$ and recalling that $\nabla \times \boldsymbol{H} = \boldsymbol{E}$ yields

$$(\boldsymbol{E}, \boldsymbol{H}_\lambda \times \boldsymbol{\nu})_{\Gamma_{loss}} = \lambda \|\boldsymbol{H}_\lambda \times \boldsymbol{\nu}\|^2_{\Gamma_{loss}}.$$

The left–hand side of the last result can be rewritten into a more suitable form

$$(\boldsymbol{E} \times \boldsymbol{H}_\lambda, \boldsymbol{\nu})_{\Gamma_{loss}} = \lambda \|\boldsymbol{H}_\lambda \times \boldsymbol{\nu}\|^2_{\Gamma_{loss}}.$$

Using (10.1) we obtain

$$P = \lambda \left\| \boldsymbol{H}_\lambda \times \nu \right\|^2_{\Gamma_{loss}},$$

describing the physical relation between the coefficient λ and the iron loss P.

In a priori estimates we need the definition of the Sobolev norm of fractional order, see also [65, p.58].

Definition 10.1 *The norm on* $\mathbf{H}^{-1/2}(\Gamma)$ *is defined as*

$$\left\| \boldsymbol{\nu} \times \boldsymbol{v} \right\|_{\mathbf{H}^{-1/2}(\Gamma)} = \sup_{\boldsymbol{g} \in \mathbf{H}^{1/2}(\Gamma)} \frac{\left| \langle \boldsymbol{\nu} \times \boldsymbol{v}, \boldsymbol{g} \rangle_\Gamma \right|}{\left\| \boldsymbol{g} \right\|_{\mathbf{H}^{1/2}(\Gamma)}}.$$

Corollary 10.1
From Definition 10.1 it follows that $\left\| \boldsymbol{\nu} \times \boldsymbol{v} \right\|_{\mathbf{H}^{-1/2}(\Gamma)} \leq C \left\| \boldsymbol{v} \right\|_{\mathbf{H}(\mathbf{curl};\Omega)}$.

10.4 A priori estimates

The first lemma gives the uniform estimate of $\boldsymbol{H}_\lambda$ in the $\mathbf{H}(\mathbf{curl};\Omega)$-norm and its trace with respect to $\lambda > 0$.

Lemma 10.1 *Let (10.11) be satisfied. Then, for a solution* $(\lambda, \boldsymbol{H}_\lambda)$ *to the Problem 1, there exists a positive constant* C *such that*

$$\left\| \boldsymbol{H}_\lambda \right\|^2_{\mathbf{H}(\mathbf{curl};\Omega)} + 2\lambda \left\| \boldsymbol{H}_\lambda \times \boldsymbol{\nu} \right\|^2_{\Gamma_{loss}} \leq C \qquad \forall \lambda > 0.$$

Proof: The assertion can be readily proved by taking $\boldsymbol{\varphi} = \boldsymbol{H}_\lambda$ in (10.12) and using the Young inequality, Definition 10.1 and its corollary. We obtain

$$\begin{aligned} K \left\| \boldsymbol{H}_\lambda \right\|^2 + \left\| \nabla \times \boldsymbol{H}_\lambda \right\|^2 + \lambda \left\| \boldsymbol{H}_\lambda \times \boldsymbol{\nu} \right\|^2_{\Gamma_{loss}} & \\ \leq \left\| \boldsymbol{g} \right\|_{\mathbf{H}^{1/2}(\Gamma_{Neu})} \cdot \left\| \boldsymbol{\nu} \times \boldsymbol{H}_\lambda \right\|_{\mathbf{H}^{-1/2}(\Gamma_{Neu})} & \\ \leq C_\varepsilon \left\| \boldsymbol{g} \right\|^2_{\mathbf{H}^{1/2}(\Gamma_{Neu})} + \varepsilon \left\| \boldsymbol{\nu} \times \boldsymbol{H}_\lambda \right\|^2_{\mathbf{H}^{-1/2}(\Gamma_{Neu})} & \\ \leq C_\varepsilon \left\| \boldsymbol{g} \right\|^2_{\mathbf{H}^{1/2}(\Gamma_{Neu})} + \varepsilon \left\| \boldsymbol{H}_\lambda \right\|^2_{\mathbf{H}(\mathbf{curl};\Omega)} & . \end{aligned}$$

Multiplying the latter inequality by 2 yields

$$(2 - \varepsilon) \left\| \boldsymbol{H}_\lambda \right\|^2_{\mathbf{H}(\mathbf{curl};\Omega)} + 2\lambda \left\| \boldsymbol{H}_\lambda \times \boldsymbol{\nu} \right\|^2_{\Gamma_{loss}} \leq C.$$

Considering sufficiently small ε concludes the proof. □

We introduce a real function $m(\lambda) : [0,\infty) \to [0,\infty)$ given by

$$m(\lambda) = \|\boldsymbol{H}_\lambda \times \boldsymbol{\nu}\|^2_{\Gamma_{loss}} \ .$$

Hence, the function $m(\lambda)$ is defined in terms of the weak solution $\boldsymbol{H}_\lambda$ of (10.12).

Let us study first the behavior of the introduced function $m(\lambda)$.

Lemma 10.2 (Continuity) *Let (10.11) be satisfied. Then the function $m(\lambda)$ is continuous on $(0,\infty)$.*

Proof: Following the definition of continuity, $\lim\limits_{\varepsilon\to 0} |m(\lambda) - m(\lambda+\varepsilon)| = 0$ needs to be shown. Thus, let us fix any $\lambda > 0$ and choose a small parameter ε satisfying $|\varepsilon| < \lambda$. Subtracting (10.12) from (10.12) for $\lambda = \lambda + \varepsilon$ one obtains

$$\begin{aligned} K(\boldsymbol{H}_{\lambda+\varepsilon} - \boldsymbol{H}_\lambda, \boldsymbol{\varphi}) + (\nabla \times (\boldsymbol{H}_{\lambda+\varepsilon} - \boldsymbol{H}_\lambda), \nabla \times \boldsymbol{\varphi}) \\ +\lambda((\boldsymbol{H}_{\lambda+\varepsilon} - \boldsymbol{H}_\lambda) \times \boldsymbol{\nu}, \boldsymbol{\varphi} \times \boldsymbol{\nu})_{\Gamma_{loss}} + \varepsilon(\boldsymbol{H}_{\lambda+\varepsilon} \times \boldsymbol{\nu}, \boldsymbol{\varphi} \times \boldsymbol{\nu})_{\Gamma_{loss}} \quad = 0\,. \end{aligned} \tag{10.13}$$

This can be written equivalently as

$$\begin{aligned} K(\boldsymbol{H}_{\lambda+\varepsilon} - \boldsymbol{H}_\lambda, \boldsymbol{\varphi}) + (\nabla \times (\boldsymbol{H}_{\lambda+\varepsilon} - \boldsymbol{H}_\lambda), \nabla \times \boldsymbol{\varphi}) \\ +(\lambda+\varepsilon)((\boldsymbol{H}_{\lambda+\varepsilon} - \boldsymbol{H}_\lambda) \times \boldsymbol{\nu}, \boldsymbol{\varphi} \times \boldsymbol{\nu})_{\Gamma_{loss}} + \varepsilon(\boldsymbol{H}_\lambda \times \boldsymbol{\nu}, \boldsymbol{\varphi} \times \boldsymbol{\nu})_{\Gamma_{loss}} \quad = 0\,. \end{aligned} \tag{10.14}$$

Summing up (10.13) and (10.14) and choosing $\boldsymbol{\varphi} = \boldsymbol{H}_{\lambda+\varepsilon} - \boldsymbol{H}_\lambda$ we obtain

$$\begin{aligned} 2K\,\|\boldsymbol{H}_{\lambda+\varepsilon} - \boldsymbol{H}_\lambda\|^2 + 2\,\|\nabla \times (\boldsymbol{H}_{\lambda+\varepsilon} - \boldsymbol{H}_\lambda)\|^2 \\ +(2\lambda+\varepsilon)\,\|(\boldsymbol{H}_{\lambda+\varepsilon} - \boldsymbol{H}_\lambda) \times \boldsymbol{\nu}\|^2_{\Gamma_{loss}} \\ +\varepsilon((\boldsymbol{H}_{\lambda+\varepsilon} + \boldsymbol{H}_\lambda) \times \boldsymbol{\nu}, (\boldsymbol{H}_{\lambda+\varepsilon} - \boldsymbol{H}_\lambda) \times \boldsymbol{\nu})_{\Gamma_{loss}} = 0\,. \end{aligned} \tag{10.15}$$

Using Lemma 10.1 for the last term on the left we deduce

$$\begin{aligned} \lim_{\varepsilon\to 0} \quad & \left|\varepsilon\left((\boldsymbol{H}_{\lambda+\varepsilon} + \boldsymbol{H}_\lambda) \times \boldsymbol{\nu}, (\boldsymbol{H}_{\lambda+\varepsilon} - \boldsymbol{H}_\lambda) \times \boldsymbol{\nu}\right)_{\Gamma_{loss}}\right| \\ & = \lim_{\varepsilon\to 0} |\varepsilon| \left|\|\boldsymbol{H}_{\lambda+\varepsilon} \times \boldsymbol{\nu}\|^2_{\Gamma_{loss}} - \|\boldsymbol{H}_\lambda \times \boldsymbol{\nu}\|^2_{\Gamma_{loss}}\right| \\ & \le \lim_{\varepsilon\to 0} C|\varepsilon| \left(\tfrac{1}{\lambda+\varepsilon} + \tfrac{1}{\lambda}\right) \\ & \le \lim_{\varepsilon\to 0} \tfrac{C|\varepsilon|}{\lambda} \\ & = 0\,. \end{aligned} \tag{10.16}$$

Thus, the absolute value of the sum of the first three terms in (10.15) tends to 0 for $\varepsilon \to 0$. From the non-negativity of each of these terms follows

$$\lim_{\varepsilon\to 0} \|\boldsymbol{H}_{\lambda+\varepsilon} - \boldsymbol{H}_\lambda\|_{\mathbf{H}(\mathbf{curl};\Omega)} = 0 \quad \text{and} \quad \lim_{\varepsilon\to 0} \|(\boldsymbol{H}_{\lambda+\varepsilon} - \boldsymbol{H}_\lambda) \times \boldsymbol{\nu}\|_{\Gamma_{loss}} = 0\,.$$

Using Cauchy's inequality, Lemma 10.1 and the last relation yields

$$\begin{aligned}
\lim_{\varepsilon\to 0} |m(\lambda+\varepsilon) - m(\lambda)| &= \lim_{\varepsilon\to 0} \left| \|\boldsymbol{H}_{\lambda+\varepsilon} \times \boldsymbol{\nu}\|^2_{\Gamma_{loss}} - \|\boldsymbol{H}_{\lambda} \times \boldsymbol{\nu}\|^2_{\Gamma_{loss}} \right| \\
&= \lim_{\varepsilon\to 0} \left| \big((\boldsymbol{H}_{\lambda+\varepsilon} + \boldsymbol{H}_{\lambda}) \times \boldsymbol{\nu}, (\boldsymbol{H}_{\lambda+\varepsilon} - \boldsymbol{H}_{\lambda}) \times \boldsymbol{\nu}\big)_{\Gamma_{loss}} \right| \\
&\leq \lim_{\varepsilon\to 0} \|(\boldsymbol{H}_{\lambda+\varepsilon} + \boldsymbol{H}_{\lambda}) \times \boldsymbol{\nu}\|_{\Gamma_{loss}} \|(\boldsymbol{H}_{\lambda+\varepsilon} - \boldsymbol{H}_{\lambda}) \times \boldsymbol{\nu}\|_{\Gamma_{loss}} \\
&\leq \frac{C}{\lambda} \lim_{\varepsilon\to 0} \|(\boldsymbol{H}_{\lambda+\varepsilon} - \boldsymbol{H}_{\lambda}) \times \boldsymbol{\nu}\|_{\Gamma_{loss}} \\
&= 0\,,
\end{aligned}$$

which proves the continuity of the function $m(\lambda)$. □

As a next step the monotonicity, more precisely the decreasing behavior of the function $m(\lambda)$ is proved.

Lemma 10.3 (Decreasing nature) *Let (10.11) be satisfied. Moreover assume $\varepsilon > 0$ and $\lambda > 0$. Then $m(\lambda+\varepsilon) \leq m(\lambda)$.*

Proof: The first three terms in formula (10.15) are nonnegative and $\varepsilon > 0$, thus, from the last term one obtains

$$m(\lambda+\varepsilon) = \|\boldsymbol{H}_{\lambda+\varepsilon} \times \boldsymbol{\nu}\|^2_{\Gamma_{loss}} \leq \|\boldsymbol{H}_{\lambda} \times \boldsymbol{\nu}\|^2_{\Gamma_{loss}} = m(\lambda)\,.$$

□

Lemma 10.4 (Asymptotic character) *Let (10.11) be satisfied. Then it holds that $\lim\limits_{\lambda\to\infty} m(\lambda) = 0$.*

Proof: Resulting from Lemma 10.1 we have

$$\lambda \|\boldsymbol{H}_{\lambda} \times \boldsymbol{\nu}\|^2_{\Gamma_{loss}} \leq C \qquad \forall \lambda > 0.$$

Thus, the statement of the lemma is directly concluded

$$\lim_{\lambda\to\infty} m(\lambda) = \lim_{\lambda\to\infty} \frac{\lambda \|\boldsymbol{H}_{\lambda} \times \boldsymbol{\nu}\|^2_{\Gamma_{loss}}}{\lambda} = 0\,.$$

□

Now, we are in a state to prove the well–posedness of Problem 1 equipped with the side condition (10.10).

Theorem 10.1 *If the assumptions (10.11) are fulfilled and $\lambda > 0$, then for any $0 < M < \lim_{\lambda \to 0_+} m(\lambda)$ there exists a unique weak solution to the inverse boundary value problem (10.12), (10.10).*

Proof: The existence of a weak solution is directly guaranteed by Lemmas 10.1-10.4. We still have to show its uniqueness.
Suppose there exist two solutions. Then one of the three following cases can occur:

(i) Let $(\lambda, \boldsymbol{H})$ and $(\widetilde{\lambda}, \boldsymbol{H})$ be two different solutions of (10.12), (10.10). Subtracting the variational equations for both solutions from each other and setting the test function $\boldsymbol{\varphi} = \boldsymbol{H}$, one gets

$$(\lambda - \widetilde{\lambda}) \, \|\boldsymbol{H} \times \boldsymbol{\nu}\|^2_{\Gamma_{loss}} = 0 \, .$$

Hence, $\|\boldsymbol{H} \times \boldsymbol{\nu}\|^2_{\Gamma_{loss}} = 0$ contradicts with $M > 0$.

(ii) Now, let $(\lambda, \boldsymbol{H})$ and $(\lambda, \widetilde{\boldsymbol{H}})$ be two solutions of (10.12), (10.10). Using the same steps as in previous case, but setting $\boldsymbol{\varphi} = \boldsymbol{H} - \widetilde{\boldsymbol{H}}$ one obtains

$$K \left\| \boldsymbol{H} - \widetilde{\boldsymbol{H}} \right\|^2 + \left\| \nabla \times (\boldsymbol{H} - \widetilde{\boldsymbol{H}}) \right\|^2 + \lambda \left\| (\boldsymbol{H} - \widetilde{\boldsymbol{H}}) \times \boldsymbol{\nu} \right\|^2_{\Gamma_{loss}} = 0 \, .$$

On account of (10.11) and of $\lambda > 0$ the last relation implies $\boldsymbol{H} = \widetilde{\boldsymbol{H}}$.

(iii) Finally let $(\lambda, \boldsymbol{H}_\lambda)$ and $(\lambda + \varepsilon, \boldsymbol{H}_{\lambda+\varepsilon})$ with $\varepsilon > 0$ and $\lambda \geq 0$ both solve (10.12), (10.10). Resulting from formula (10.15) and recalling that each solution satisfies the side condition (10.10), i.e. $\|\boldsymbol{H}_{\lambda+\varepsilon} \times \boldsymbol{\nu}\|^2_{\Gamma_{loss}} = M = \|\boldsymbol{H}_\lambda \times \boldsymbol{\nu}\|^2_{\Gamma_{loss}}$ the equation yields

$$\begin{aligned} 2K \, \|\boldsymbol{H}_{\lambda+\varepsilon} - \boldsymbol{H}_\lambda\|^2 + 2 \, \|\nabla \times (\boldsymbol{H}_{\lambda+\varepsilon} - \boldsymbol{H}_\lambda)\|^2 \\ +(2\lambda + \varepsilon) \, \|(\boldsymbol{H}_{\lambda+\varepsilon} - \boldsymbol{H}_\lambda) \times \boldsymbol{\nu}\|^2_{\Gamma_{loss}} = 0 \, . \end{aligned} \tag{10.17}$$

This gives a contradiction, because the left-hand side is strictly positive due to $\boldsymbol{H}_\lambda \neq \boldsymbol{H}_{\lambda+\varepsilon}$.
The proof is done on the basis of these three cases.

□

Remark 10.3 *Suppose $\mu = -i$ and $\sigma = \sigma_B$. Then the Problem 1 reads*

$$\begin{aligned} \lambda^2 \boldsymbol{H}_\lambda + \nabla \times \nabla \times \boldsymbol{H}_\lambda &= \mathbf{0} && \text{in } \Omega, \\ \boldsymbol{H}_\lambda \times \boldsymbol{\nu} &= \mathbf{0} && \text{on } \Gamma_{Dir}, \\ \nabla \times \boldsymbol{H}_\lambda \times \boldsymbol{\nu} &= \boldsymbol{g} \times \boldsymbol{\nu} && \text{on } \Gamma_{Neu}, \\ \nabla \times \boldsymbol{H}_\lambda \times \boldsymbol{\nu} &= \lambda(\boldsymbol{H}_\lambda \times \boldsymbol{\nu} \times \boldsymbol{\nu}) && \text{on } \Gamma_{loss} \end{aligned}$$

with $\lambda = \sqrt{\omega\sigma}$, i.e. the processes on the boundary influence the behavior of the electromagnet in the domain. This is not a common situation because the boundary conditions describing the properties of the material surrounding the computational domain should be independent on the processes acting inside of the domain. In this case, assuming convenient data, the existence of the solution is assured, while the uniqueness cannot be proved (we are not able to show the decreasing character of the iron loss function).

10.5 A numerical experiment

Let Ω be a unit cube in $\mathbb{R}^3$. The boundary Γ is split into two pieces as follows: on the bottom and the upper face of the cube the iron loss boundary condition is prescribed, on the side faces the Neumann boundary condition is considered. We apply our method to this test problem:[1]
Find $(\lambda, \boldsymbol{H}_\lambda) \in (\mathbb{R}_+, \mathbf{H}(\mathbf{curl}\,;\Omega))$ satisfying

$$\begin{aligned} \boldsymbol{H}_\lambda + \nabla \times \nabla \times \boldsymbol{H}_\lambda &= \boldsymbol{f} && \text{in } \Omega, \\ \nabla \times \boldsymbol{H}_\lambda \times \boldsymbol{\nu} &= \boldsymbol{g}_1 \times \boldsymbol{\nu} && \text{on } \Gamma_{Neu}, \\ \nabla \times \boldsymbol{H}_\lambda \times \boldsymbol{\nu} &= \lambda(\boldsymbol{H}_\lambda \times \boldsymbol{\nu} \times \boldsymbol{\nu}) + \boldsymbol{g}_2 \times \boldsymbol{\nu} && \text{on } \Gamma_{loss}, \\ \int_{\Gamma_{loss}} (\boldsymbol{H}_\lambda \times \boldsymbol{\nu})^2 &= 1.33\,, \end{aligned}$$

where the data functions $\boldsymbol{f}$, $\boldsymbol{g}_1$ and $\boldsymbol{g}_2$ are defined such that

$$\lambda = 1.24,$$

$$\mathbf{H}_\lambda = \begin{pmatrix} x_2 - x_1 \\ x_0 - x_2 \\ x_1 - x_0 \end{pmatrix}$$

is the exact solution, (see Figure 10.1).

[1] Note that the analysis stays valid also for inhomogeneous case.

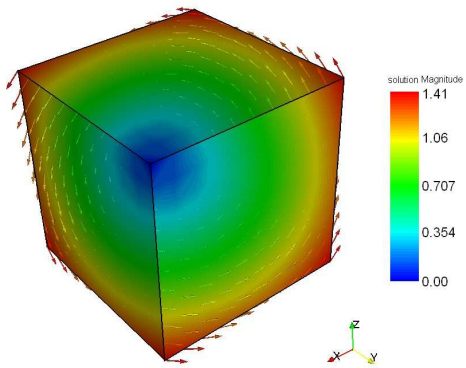

Figure 10.1: Exact solution.

Figure 10.2 shows the graph of the numerically obtained function $m(\lambda)$. For the determination of $\boldsymbol{H}_\lambda$ from the boundary value problem (10.12) for each given λ the Newton method is used, see Appendix. Thus, we solve:

$$F(\boldsymbol{H}) = 0\,.$$

Starting with an initial guess $\boldsymbol{H}_0 = \boldsymbol{0}$ we compute

$$DF(\boldsymbol{H}_m)\boldsymbol{d}_m = F(\boldsymbol{H}_m) \qquad \text{for } m > 0$$

and set

$$\boldsymbol{H}_{m+1} = \boldsymbol{H}_m - \boldsymbol{d}_m$$

until $\|\boldsymbol{d}_m\| < 1.0 \cdot 10^{-4}$. The functional $F(\boldsymbol{v})$ and its Fréchet derivative $DF(\boldsymbol{v})$ for $\boldsymbol{v} \in \mathbf{H}(\mathbf{curl}\,;\Omega)$ are defined by

$$\begin{aligned}
(F(\boldsymbol{v}), \boldsymbol{\varphi}_j) &= (\boldsymbol{v}, \boldsymbol{\varphi}_j) + (\nabla \times \boldsymbol{v}, \nabla \times \boldsymbol{\varphi}_j) + (\boldsymbol{g}_1, \boldsymbol{\varphi}_j \times \boldsymbol{\nu})_{\Gamma_{Neu}} \\
&\quad + \lambda(\boldsymbol{v} \times \boldsymbol{\nu}, \boldsymbol{\varphi}_j \times \boldsymbol{\nu})_{\Gamma_{loss}} + (\boldsymbol{g}_2, \boldsymbol{\varphi}_j \times \boldsymbol{\nu})_{\Gamma_{loss}} - (\boldsymbol{f}, \boldsymbol{\varphi}_j), \\
(DF(\boldsymbol{v})\boldsymbol{\varphi}_i, \boldsymbol{\varphi}_j) &= (\boldsymbol{\varphi}_i, \boldsymbol{\varphi}_j) + (\nabla \times \boldsymbol{\varphi}_i, \nabla \times \boldsymbol{\varphi}_j) + \lambda(\boldsymbol{\varphi}_i \times \boldsymbol{\nu}, \boldsymbol{\varphi}_j \times \boldsymbol{\nu})_{\Gamma_{loss}}\,,
\end{aligned}$$

where $\boldsymbol{\varphi}_i, \boldsymbol{\varphi}_j \in \boldsymbol{V}$.
To our numerical scheme the finite element method is applied. The computational domain is split into 384 tetrahedra (2 refinements of the basic mesh) with mesh diameter $h = \sqrt{3}/4$. There is no need to split the domain into more subdomains. Due to the linearity of our problem this "coarse mesh" is suitable enough to reach the necessary accuracy of our model. For the approximation of

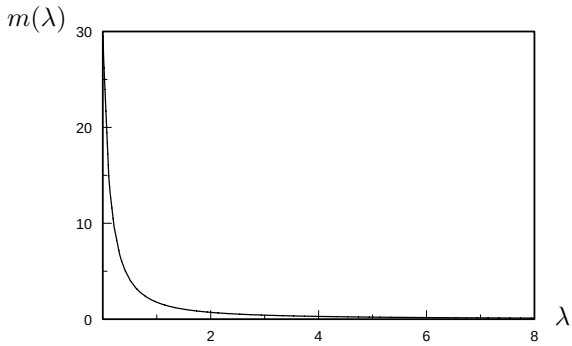

Figure 10.2: Numerically obtained graph of the iron loss function $m(\lambda)$. The behavior of the function is consistent with the theory. The three properties (continuity, monotonicity and asymptotic character) assure the existence of a unique solution for any amount of iron loss M on the boundary.

the magnetic field $\boldsymbol{H}_\lambda$ Whitney's edge elements are used, see Section 6.2.2.
The Newton method is chosen again to determinate the Robin coefficient λ for which the iron loss boundary condition is satisfied. Here, the next approximation is given by

$$\lambda_{new} = \lambda_{old} - \frac{m(\lambda)}{m'(\lambda)}\,,$$

where

$$m'(\lambda) = \frac{m(\lambda+h) - m(\lambda-h)}{2h}$$

with $h = 0.005$.
Figure 10.3 and Table 10.1 show the convergence of Newton's method. We have started with $\lambda = 0.01$ and the algorithm has stopped after five iterations with the prescribed precision $|m(\lambda) - 1.33| < 0.0001$. The following errors have been obtained for the last approximation:

$$\begin{aligned} \|\boldsymbol{H}_\lambda - \boldsymbol{H}_{\lambda app}\|_{\mathbf{L}_2(\Omega)} &= 5.920896 \cdot 10^{-09}, \\ \|\boldsymbol{H}_\lambda - \boldsymbol{H}_{\lambda app}\|_{\mathbf{H}(\mathbf{curl};\Omega)} &= 3.180161 \cdot 10^{-08}, \\ |\lambda - \lambda_{app}| &= 4.29 \cdot 10^{-4}. \end{aligned}$$

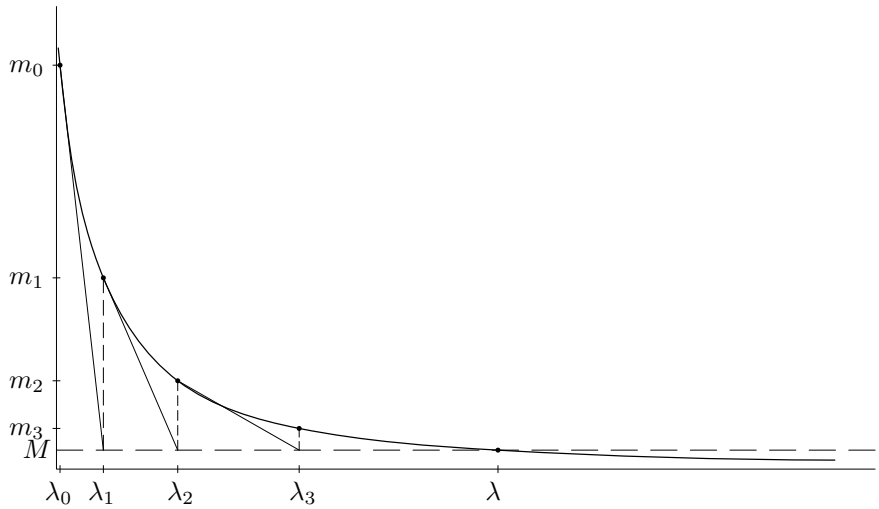

Figure 10.3: The convergence of the Newton method. The algorithm is quick and stops after five iterations.

Iter.	λ	$m(\lambda)$	error in %
1	0.010	28.379	127.47%
2	0.132	13.438	48.68%
3	0.341	6.206	14.40%
4	0.682	2.858	2.40%
5	1.240	1.330	0.00%

Table 10.1: Precision of the Newton iterations. The situation from Figure 10.3.

10.6 Conclusions

We have proved the well–posedness of the inverse recovery problem for time–harmonic evolution of electromagnetic waves. The efficiency of the numerical method has been tested by numerical experiments.

The aim of this section was to prove that the information about the iron losses on a part of the boundary is sufficient to guarantee the existence and the uniqueness of the solution. Another possible approach (that is also widely used in the literature) would be to accept the fact that the mathematical model admits more solutions. Then, however, an additional information is needed to decide which solution to choose as the right one.

A generalization of the problem of the determination of unknown information on one part of the boundary has a large potential for future study. A complex valued permeability in the form $\mu = a - ib$ should be considered which will lead to a mathematical model with more practical applications. Note that in this case one will work over the field of complex numbers. Moreover, the error analysis should be performed.

A challenge for the future research would also be to divide the boundary into an accessible and inaccessible part. On the inaccessible part the impedance BC with unknown parameter λ will be prescribed and no other information will be available. On the other hand, to compensate this lack of data we will consider the rest of the boundary overspecified.

Furthermore, one could consider the parameter λ not to be a constant but a function depending on the space or on the time variable. The latter requires then working with the time-dependent domain.

Appendix

Basic algebraic (in)equalities

Vector identities

$$\begin{aligned}
(\boldsymbol{a} \times \boldsymbol{b}) \times \boldsymbol{c} &= (\boldsymbol{c} \cdot \boldsymbol{a})\ \boldsymbol{b} - (\boldsymbol{c} \cdot \boldsymbol{b})\ \boldsymbol{a} \\
(\boldsymbol{a} \times \boldsymbol{b}) \cdot (\boldsymbol{c} \times \boldsymbol{d}) &= (\boldsymbol{a} \cdot \boldsymbol{c})\ (\boldsymbol{b} \cdot \boldsymbol{d}) - (\boldsymbol{a} \cdot \boldsymbol{d})\ (\boldsymbol{b} \cdot \boldsymbol{c}) \\
(\boldsymbol{a} \times \boldsymbol{b}) \cdot \boldsymbol{c} &= \boldsymbol{a} \cdot (\boldsymbol{b} \times \boldsymbol{c}) = \boldsymbol{b} \cdot (\boldsymbol{c} \times \boldsymbol{a})
\end{aligned}$$

Green's formula

$$(\nabla \times \boldsymbol{\varphi}, \boldsymbol{\psi})_\Omega = (\boldsymbol{\varphi}, \nabla \times \boldsymbol{\psi})_\Omega + (\boldsymbol{\nu} \times \boldsymbol{\varphi}, \boldsymbol{\psi})_{\partial\Omega}$$

Abel's summation

$$\sum_{i=1}^{m} a_i(b_i - b_{i-1}) = a_m b_m - a_0 b_0 - \sum_{i=1}^{m} b_{i-1}(a_i - a_{i-1})$$

Cauchy–Schwartz's inequality

$$(f, g) \leq \|f\|\,\|g\|$$

For the following inequalities we suppose $p, q \geq 1$ to be conjugate, i.e., $1/p + 1/q = 1$.

Hölder's inequality

$$(f, g) \leq \|f\|_p\,\|g\|_q$$

Young's inequality

$$(f, g) \leq \frac{f^p}{p} + \frac{g^q}{q}$$

Modified Young's inequality

$$(f, g) \leq \varepsilon \|f\|^2 + C_\varepsilon \|g\|^2$$

Minkowski inequality (*triangle inequality in* L_p)

$$\|f + g\|_p \leq \|f\|_p + \|q\|_p$$

Simple mathematical analysis

Theorem 10.2 (Gronwall's lemma) *Let $r(t), h(t), y(t)$ be continuous real functions defined on the interval $[a, b]$ such that $r(t), h(t) \geq 0$. Suppose that*

$$y(t) \leq h(t) + \int_a^t r(s)y(s)\mathrm{d}s \quad \text{for } a \leq t \leq b.$$

Then

$$y(t) \leq h(t) + \int_a^t h(s)r(s)e^{\int_s^t r(\tau)\mathrm{d}\tau}\mathrm{d}s$$

is valid for all $t \in [a, b]$.

Theorem 10.3 (Gronwall's lemma - discrete version) *Let $\{A_i\}, \{a_i\}$ be the sequences of nonnegative real numbers and let $q \geq 0$. Suppose*

$$a_i \leq A_i + \sum_{j=1}^{i-1} a_j q$$

holds for $i \in \mathbb{N}$. Then

$$a_i \leq A_i + e^{qi} \sum_{j=1}^{i-1} A_j q.$$

Fundamental theorem on monotone operators

Theorem 10.4 *Let $\boldsymbol{F}(\boldsymbol{x})$ be a hemicontinuous, monotone and coercive operator mapping a reflexive Banach space $\boldsymbol{X}$ into $\boldsymbol{X}^*$. Then the mapping $\boldsymbol{F} : \boldsymbol{X} \to \boldsymbol{X}^*$ is surjective, i.e., the equation $\boldsymbol{F}(\boldsymbol{x}) = \boldsymbol{v}$ has a solution for any $\boldsymbol{v} \in \boldsymbol{X}^*$.*

General functional analysis

Theorem 10.5 (Lax-Milgram lemma) *Let a be a bounded coercive bilinear functional on a Hilbert space H. Then for every bounded linear functional f on H, there exists a unique u such that*

$$a(u, \phi) = f(\phi) \tag{10.18}$$

for all $\phi \in H$.

Theorem 10.6 (Céa's lemma) *Suppose $H_h \subset H$, $h > 0$, is a family of finite-dimensional subspaces of a Hilbert space H. Suppose $a : H \times H \to \mathbb{C}$ is a bounded, coercive, sesquilinear form and $f \in H'$. Then the problem of finding $u_h \in H_h$ such that*

$$a\left(u_h, \phi_h\right) = f(\phi_h) \quad \textit{for all } \phi_h \in H_h$$

has a unique solution. If $u \in H$ is the exact solution solving (10.18) then there is a constant C independent of u, u_h and h such that

$$\|u - u_h\|_H \leq C \inf_{v_h \in H_h} \|u - v_h\|_H \,. \tag{10.19}$$

Estimate (10.19) is said to be a quasi-optimal error estimate of approximate solution.

Theorem 10.7 (Hahn-Banach theorem) *Suppose M is a subspace of a vector space X, p is a seminorm on X and f is a linear functional on M such that*

$$|f(x)| \leq p(x), \quad x \in M.$$

Then f extends to a linear functional Λ on X that satisfies

$$|\Lambda x| \leq p(x), \quad x \in X.$$

Obvious consequence of Theorem 10.7 for a normed space is:

Theorem 10.8 *If f is a continuous linear functional on a subspace M of a locally convex space X then there exists $\Lambda \in X^*$ such that $\Lambda = f$ on M.*

Newton's method

In numerical analysis, Newton's method (also known as the Newton-Raphson method) is perhaps the best known method for finding good approximation to the root of a real-valued function $f(\boldsymbol{x})$. The process of finding solution is iterative. Starting form some initial guess $\boldsymbol{x}_0$, a new estimate is found from

$$\boldsymbol{x}_{k+1} = \boldsymbol{x}_k - \frac{f(\boldsymbol{x}_k)}{Df(\boldsymbol{x}_k)}.$$

Here, $Df(\boldsymbol{x}_k)$ is the Fréchet derivative of f in $\boldsymbol{x}_k$. Newton's method converges remarkably quickly if the iteration process starts close enough to the real solution $\boldsymbol{x}^*$.

Remark 10.4 *Newton's method can also be used to find local maxima and local minima of a functional $f(\boldsymbol{x})$. In this case, new estimate is given by*

$$\boldsymbol{x}_{k+1} = \boldsymbol{x}_k - [Hf(\boldsymbol{x}_k)]^{-1}\nabla f(\boldsymbol{x}_k).$$

Symbol $Hf(\boldsymbol{x}_k)$ denotes a Hessian matrix of f in $\boldsymbol{x}_k$.

List of Figures

List of Tables

Index

Bibliography

[1] R.A. Adams. *Sobolev Spaces*. Pure and Applied Mathematics. Academic Press, New York, 1975.

[2] A. Alonso and A. Valli. Some remarks on the characterization of the space of tangential traces of H(rot,Ω) and the construction of an extension operator. *Manuscripta Mathematica*, 89:159–178, 1996.

[3] A. Alonso Rodríguez, R. Hiptmair, and A Valli. Mixed finite element approximation of eddy current problems. *IMA J. Numer. Anal.*, 24(2):255–271, 2004.

[4] F. Andreu, N. Igbida, J.M. Mazón, and J. Toledoa. Renormalized solutions for degenerate elliptic-parabolic problems with nonlinear dynamical boundary conditions and $L1$-data. *Journal of Differential Equations*, 244:2764–2803, 2008.

[5] T. S. Angell and A. Kirsch. The conductive boundary condition for Maxwell's equations. *SIAM J. Appl. Math.*, 52:1597–1610, 1992.

[6] J. M. Arrieta, P. Quittner, and A. Rodríguez-Bernal. Parabolic problems with nonlinear dynamical boundary conditions and singular initial data. *Differential and Integral Equations*, 14(12):1487–1510, 2001.

[7] H. Barucq. A new family of first-order boundary conditions for the Maxwell system: derivation, well-posedness and long -time behavior. *J. Math. Pures Appl.*, 82(1):67–88, 2002.

[8] H. Barucq, F. Delaurens, and B. Hanouzet. Method of absorbing boundary conditions: phenomena of error stabilization. *SIAM J. Numer. Anal.*, 35(3): 1113–1129, 1998.

[9] Ľ. Baňas. *On dynamical micromagnetism with magnetostriction*. UGent, 2005.

[10] J. T. Beale and S. I. Rosencrans. Acoustic boundary condition. *Bull. Amer. Math. Soc.*, 80:1276–1278, 1974.

[11] J. Beck, B. Blackwell, and C. S. Clair. *Inverse Heat Conduction.* Wiley, New York, 1985.

[12] J. P. Bérenger. A perfectly matched layer for the absorption of electromagnetic waves. *J. Comput. Phys.*, 114:185–200, 1994.

[13] J. P. Bérenger. Perfectly matched layer for the FDTD solution of wave-structure interaction problems. *IEEE Trans. Antennas Propagat.*, 44:110–117, 1996.

[14] D. M. Boore. Finite difference methods for seismic wave propagation in heterogeneous materials. *Methods of Comp. Physics(Seismology)*, 11:1–37, 1972.

[15] A. Bossavit. *Computational Electromagnetism. Variational Formulations, Complementarity, Edge Elements*, volume XVIII of *Electromagnetism.* Academic Press, Orlando, FL., 1998.

[16] A. Buffa and P. Ciarlet Jr. On traces for functional spaces related to Maxwell's equations. I: An integration by parts formula in Lipschitz polyhedra. *Math. Methods Appl. Sci.*, 24(1):9–30, 2001.

[17] A. Buffa and P. Ciarlet Jr. On traces for functional spaces related to Maxwell's equations. II: Hodge decompostions on the boundary of Lipschitz polyhedra and applications. *Math. Methods Appl. Sci.*, 24(1):31–48, 2001.

[18] A. Buffa, M. Costabel, and D. Sheen. On traces for $\mathbf{H}(\mathbf{curl}\,;\Omega)$ in Lipschitz domains. *J. Math. Anal. Appl.*, 276(2):845–876, 2002.

[19] M. Cessenat. *Mathematical Methods in Electromagnetism. Linear Theory and Applications*, volume 41 of *Series on Advances in Mathematics for Applied Sciences.* World Scientific Publishers, Singapore, 1996.

[20] Z. Chen, Q. Du, and J. Zou. Finite element methods with matching and nonmatching meshes for Maxwell equations with discontinuous coefficients. *SIAM J. Numer. Anal.*, 37:1542–70, 2000.

[21] P. G. Ciarlet. *The Finite Element Method for Elliptic Problems*, volume 4 of *Studies in Mathematics and its Applications.* North-Holland, Amsterdam, 1978.

[22] P. Ciarlet Jr. Augmented formulations for solving Maxwell equations. *Comput. Methods Appl. Mech. Eng.*, 194(2-5):559–586, 2005.

[23] P. Ciarlet Jr. and E. Jamelot. Continuous Galerkin methods for solving Maxwell equations in 3D geometries. In *Proceedings of ENUMATH05*, pages 547–554, Santiago de Compostela, Spain, 2006. Springer-Verlag.

[24] I. Cimrák. *On the Landau-Lifshitz equation of ferromagnetism.* UGent, 2005.

[25] G. M. Coclite, A. Favini, G. R. Goldstein, J. A. Goldstein, and S. Romanelli. Continuous dependence on the boundary conditions for the Wentzell laplacian. *Semigroup Forum*, 77:101–108, 2008.

[26] G. M. Coclite, G. R. Goldstein, and J. A. Goldstein. Stability of parabolic problems with nonlinear Wentzell boundary conditions. *Journal of Differential Equations*, 246:2434–2447, 2009.

[27] F. Conrad and Ö. Morgül. On the stabilization of a flexible beam with a tip mass. *SIAM J. Control Optim.*, 36(6):1962–1986, 1998.

[28] C. E. Creffield, E. G. Klepfish, E. R. Pike, and S. Sarkar. Spectral weight functions for the half-filled Hubbord model: a singular value decomposition approach. *Phys. Rev. Lett.*, 75:517–520, 1995.

[29] N. Dunford and J.T. Schwartz. *Linear Operators*, volume I. Wiley-Interscience, 1958.

[30] M. Eller, J. E. Lagnese, and S. Nicaise. Stabilization of heterogeneous Maxwell's equations by linear or nonlinear boundary feedbacks. *Electronic Journal of Differential Equations*, 2002(21):1–26, 2002.

[31] M. Eller, J. E. Lagnese, and S. Nicaise. Decay rates for solutions of a Maxwell system with non linear boundary damping. *Computational and Applied Mathematics*, 21(1):135–165, 2002.

[32] T. Elvius and A. Sundström. Computationally efficient schemes and boundary conditions for a fine mesh barotropic model based on the shallow water equations. *Tellus*, 25:132–156, 1973.

[33] H. W. Engl and W. Rundell. *Inverse Problems in Diffusion Processes*. SIAM, Philadelphia, 1995.

[34] H. W. Engl, M. Hanke, and A. Neubauer. *Regularization of Inverse Problems*, volume 375 of *Mathematics and its Applications*. Kluwer Academic Publishers, Dordrecht, 1996.

[35] B. Engquist and A. Majda. Absorbing boundary conditions for the numerical simulation of waves. *Math. Comp.*, 31(139):629–651, 1977.

[36] L.C. Evans. *Weak Convergence Methods for Nonlinear Partial Differential Equations*, volume 74 of *Conference Board of the Mathematical Sciences. Regional Conference Series in Mathematics*. American Mathematical Society, Providence, RI, 1990.

[37] M. Fabrizio and A. Morro. *Electromagnetism of Continuous Media. Mathematical Modelling and Applications.* Oxford University Press, Oxford, 2003.

[38] M. Fabrizio and A. Morro. A boundary condition with memory in electromagnetism. *Arch. Rational Mech. Anal.*, 136:359–381, 1996.

[39] A. Favini, G. R. Goldstein, J. A. Goldstein, and S. Romanelli. The heat equation with generalized Wentzell boundary condition. *Journal of evolution equations*, 2:1–19, 2002.

[40] P. Fernandes and M. Raffetto. Existence, uniqueness and finite element approximation of the solution of time-harmonic electromagnetic boundary value problems involving metamaterials. *COMPEL*, 24(4):1450–1469, 2005.

[41] H. Gajewski, K. Gröger, and K. Zacharias. *Nichtlineare Operatorgleichungen und Operatordifferentialgleichungen*, volume 38 of *Mathematische Lehrbücher und Monographien. II. Abteilung.* Akademie-Verlag, Berlin, 1974.

[42] V. Girault and P.A. Raviart. *Finite Element Methods for Navier-Stokes Equations.* Springer Verlag, Berlin, 1986.

[43] G. R. Goldstein. Derivation and physical interpretation of general boundary conditions. *Adv. Diferential Equations*, 11(4):457–480, 2006.

[44] M. J. Grote. Non-reflecting boundary conditions for electromagnetic scattering. *Int. J. Numer. Modell.*, 13:397–416, 2000.

[45] M. J. Grote and J. B. Keller. Nonreflecting boundary conditions for Maxwell's equation. *J. Comput. Phys.*, 139:327–342, 1998.

[46] B. Guo and CH.-Z. Xu. On the spectrum-determined growth condition of a vibration cable with a tip mass. *IEEE Trans. Automat. Control*, 45(1):89–93, 2000.

[47] P. Halmos. *Introduction to Hilbert Space and the Theory of Spectral Multiplicity.* Chelsea Pub. Co, 1957.

[48] P. Halmos. *A Hilbert Space Problem Book.* Springer-Verlag, 1982.

[49] K. Hameyer and R. Belmans. *Numerical Modelling and Design of Electrical Machines and Devices.* WIT Press, Southampton, UK, 2001.

[50] R. Hiptmair. Analysis of multilevel methods for eddy current problems. *Math. Comput.*, 72(243):1281–1303, 2003.

[51] R. Hiptmair. Symmetric coupling for eddy current problems. *SIAM J. Numer. Anal.*, 40:41–65, 2002.

[52] G. Inglese. An inverse problem in corrosion detection. *Inverse Problems*, 13(4): 977–994, 1997.

[53] E. Janíková. *On numerical methods for diffusion of electric fields in type-II superconductors.* UGent, 2008.

[54] E. Janíková and M. Slodička. A robust linearization scheme for nonlinear diffusion in type-II superconductors. *Applied Mathematical Modelling*, 32(10):1933–1940, 2007.

[55] J. Kačur. *Method of Rothe in Evolution Equations*, volume 80 of *Teubner-Texte zur Mathematik [Teubner Texts in Mathematics].* BSB B. G. Teubner Verlag, Leipzig, 1985.

[56] K. R. Kelly, R. M. Alford, S. Treitel, and R. W. Ward. Applications of finite difference methods to exploration seismology. In *Proceedings Roy. Irish Acad. Conf. on Numerical Analysis*, pages 57–76, London and New York, 1974. Academic Press.

[57] I. Kossaczký. A recursive approach to local mesh refinement in two and three dimensions. *J. Comput. Appl. Math.*, 55:275–288, 1994.

[58] R. Kress. Uniqueness in inverse obstacle scattering for electromagnetic waves. In *Proceedings of the URSI General Assembly 2002*, Maastricht, 2002.

[59] A. Kufner, O. John, and S. Fuk. *Function Spaces.* Springer Science & Business, New York, 1977. ISBN 9028600159.

[60] G. Landl, T. Langthaler, H. W. Engl, and H. F. Kauffmann. Distribution of event times in time-resolved fluorescence: the exponential series approach - algorithm, regularization, analysis. *J. Comput. Phys.*, 95:1–28, 1991.

[61] B. Lazzari and R. Nibbi. Variational principles in electromagnetism. *IMA J. Appl. Math.*, 65(1):45–95, 2000.

[62] I. Mayergoyz. *Nonlinear Diffusion of Electromagnetic Fields with Applications to Eddy Current and Superconductivity.* Academic Press, San Diego, 1998.

[63] W. McLean and V. Thomée. Numerical solution of an evolution equation with a positive type memory term. *J. Australian Math. Soc.*, 35:23–70, 1993. Ser. B.

[64] V. Melicher. *Parameter identification in low–frequency electromagnetism and in micromagnetism.* UGent, 2007.

[65] P. Monk. *Finite Element Methods for Maxwell's Equations.* Numerical Mathematics and Scientific Computation. Oxford University Press, Oxford, 2003.

[66] C. Müller. *Foundation of the Mathematical Theory of Electromagnetic Waves.* Springer, Berlin, 1969.

[67] G. Mur. Absorbing boundary conditions for the finite-difference approximation of the time-domain electromagnetic-field equation. *IEEE Trans. Electromag. Compatibility*, 23:377–382, 1981.

[68] D. A. Murio. *The Mollification Method and the Numerical Solution of Ill-posed Problems.* Wiley, New York, 1993.

[69] J. Nečas. *Les Mèthodes Directes en Thèorie des Equations Elliptiques.* Masson, Paris, 1967.

[70] S. Nicaise and C. Pignotti. Boundary stabilization of Maxwell's equations with space-time variable coefficients. *ESAIM: Control, Optimisation and Calculus of Variations*, 9:563–578, 2003.

[71] J. Radon. *Über die Bestimmung von Funktionen durch ihre Integralwerte längs gewisser Mannigfaltigkeiten*, volume 2. Verlag d. Österr. Akad. d. Wiss., Basel, 1987.

[72] P. J. Roache. *Computational Fluid Dynamics.* Hermosa Press, Albuquerque, N. M., 1972.

[73] J. F. Rodrigues, V. A. Solonnikov, and F. Yi. On a parabolic system with time derivative in the boundary conditions and related free boundary problems. *Mathematische Annalen*, 315:61–95, 1999.

[74] V. G. Romanov and S. I. Kabanikhin. *Inverse Problems for Maxwell's Equations.* VSP, Utrecht, 1994.

[75] W. Rudin. *Functional Analysis.* McGraw-Hill Science, 1991.

[76] M. N. O. Sadiku. *Numerical Techniques in Electromagnetics.* CRC Press LLC, Boca Raton, 2001.

[77] A. Schmidt and K. G. Siebert. *ALBERT: An adaptive hierarchical finite element toolbox.* Freiburg, 2000. http://www.mathematik.uni-freiburg.de/IAM/Research/projectsdz/albert.

[78] R. P. Silvester and R. L. Ferrari. *Finite Element Methods for Electrical Engineers.* Cambridge University Press, Cambridge, 1996. 3rd edn.

[79] J. C. Slater and N. H. Frank. *Electromagnetism.* International series in pure and applied physics. McGraw-Hill Book Company, New York, 1947.

[80] M. Slodička and J. Buša Jr. Error estimates for the time discretization for nonlinear Maxwell's equations. *J. Comp. Math.*, 26:677–688, 2008.

[81] M. Slodička and R. Van Keer. Determination of the convective transfer coefficient in elliptic problems from a nonstandard boundary condition. In J. Maryška, M. Tůma, and J. Šembera, editors, *Simulation, Modelling, and Numerical Analysis*, pages 13–20, Liberec, 2000. Technical University of Liberec.

[82] M. Slodička and V. Zemanová. Error estimate for the time-discretization of a Maxwell system accompanied with the first order boundary condition. In G. Akrivis and E. Gallopoulos, editors, *NumAn 2008 Book of Proceedings*, pages 183–186, 2008.

[83] M. Slodička and V. Zemanová. Time discretization scheme for quasi-static Maxwell's equations with a non-linear boundary condition. *Journal of Computational and Applied Mathematics*, 216:514–522, 2008.

[84] M. Slodička and V. Zemanová. Error estimate for the time-discretization of a Maxwell system accompanied with the first order boundary condition. *Applied Numerical Mathematics.* submitted.

[85] O.J Staffans. An inequality for positive definite Volterra kernels. *Proc. American Math. Society*, 58:205–210, 1976.

[86] M. E. Taylor. *Pseudodifferential Operators.* Princeton Mathematical Series, 34. Princeton University Press, Princeton, New Jersey, 1981.

[87] A. N. Tikhonov. The stability of inverse problems. *Doklady Akad. Nauk SSSR*, 39(5):195–198, 1943. in Russian.

[88] A. N. Tikhonov. Solution of incorrectly formulated problems and the regularization method. *Doklady Akad. Nauk SSSR*, 151(3):501–504, 1963. in Russian.

[89] A. N. Tikhonov. Regularization of incorrectly posed problems. *Doklady Akad. Nauk SSSR*, 153(1):49–52, 1963. in Russian.

[90] C. Timofte. Homogenizations results for parabolic problems with dynamical boundary contidions. *Romanian Reports in Physics*, 56(2):131–140, 2004.

[91] M.M. Vajnberg. *Variational Method and Method of Monotone Operators in the Theory of Nonlinear Equations.* John Wiley & Sons, New York, 1973.

[92] J. L. Vázquez and E. Vitillaro. Heat equation with dynamical boundary conditions of reactive type. *Communications in Partial Differential Equations*, 33: 561–612, 2008.

[93] J. L. Vázquez and E. Vitillaro. Wave equation with second-order non-standard dynamical boundary conditions. *Mathematical Models and Methods in Applied Sciences*, 18(12):2019–2054, 2008.

[94] M. Warma. Wentzell-Robin boundary conditions on C[0,1]. *Semigroup Forum*, 66:162–170, 2003.

[95] J. P. Webb and V. N. Kanellopoulos. Absorbing boundary conditions for the finite element solution of the vector wave equation. *IEEE Microwave and Opt. Technol. Lett.*, 2:370–372, 1989.

[96] H. Whitney. *Geometric Integration Theory.* Princeton University Press, 1957.

[97] V. Zemanová and M. Slodička. Full discretization scheme for linearized quasi-static Maxwell's equations with a non-linear boundary condition. In T. Simos, G. Psyhoyios, and Ch. Tsitouras, editors, *Numerical Analysis and Applied Mathematics*, pages 621–624, Melville, New York, 2008. American Institute of Physics.

[98] V. Zemanová and M. Slodička. Quasi-static Maxwell's equations with a dissipative non-linear boundary condition: Full discretization. *Journal of Mathematical Analysis and Applications.* submitted.

[99] V. Zemanová, M. Slodička, and L. Dupré. Determination of a material constant in the impedance boundary condition for electromagnetic field. In *Fourth International Conference on Advanced Computational Methods in Engineering*, Liège, Belgium, 2008.

[100] V. Zemanová, M. Slodička, and L. Dupré. Determination of a material constant in the impedance boundary condition for electromagnetic field. *Journal of Computational and Applied Mathematics*, 2009. doi:10.1016/j.cam.2009.08.064.

[101] A. Zygmund. *Trigonometric Series I.* Cambridge University Press, Cambridge, 1959.